Technical Report Documentation Page

1. Report No.	2. Government Accession No.	3. Recipient's Catalog No.
FHWA/TX-92+1169-3		

4. Title and Subtitle	5. Report Date
DEVELOPMENT OF LOAD TRANSFER COEFFICIENTS FOR USE WITH THE AASHTO GUIDE FOR DESIGN OF RIGID PAVEMENTS BASED ON FIELD MEASUREMENTS	February 1992
	6. Performing Organization Code
7. Author(s) Chao Wei, B. Frank McCullough, W. Ronald Hudson, and Kenneth Hankins	8. Performing Organization Report No. Research Report 1169-3
9. Performing Organization Name and Address Center for Transportation Research The University of Texas at Austin Austin, Texas 78712-1075	10. Work Unit No. (TRAIS)
	11. Contract or Grant No. Research Study 3-8-88/1-1169
12. Sponsoring Agency Name and Address Texas Department of Transportation Transportation Planning Division P. O. Box 5051 Austin, Texas 78763-5051	13. Type of Report and Period Covered Interim
	14. Sponsoring Agency Code

15. Supplementary Notes

Study conducted in cooperation with the U. S. Department of Transportation, Federal Highway Administration

Research Study Title: "Concrete Pavement Design Update"

16. Abstract

A rational procedure was developed for estimating load transfer coefficients for use with the AASHTO guide for the design of continuously reinforced concrete pavements (CRCP) based on field deflection measurements. Load transfer coefficients for design of CRCP in Texas were determined using the information available in the rigid pavement database stored at the Center for Transportation Research, The University of Texas at Austin. An evaluation of structural conditions of CRCP sections in the rigid pavement database was performed to assess the ability of in-service CRCP in Texas to transfer load at transverse cracks. A finite-element analysis of CRCP using the ILLI-SLAB program was conducted to identify critical stress positions in CRCP. In addition, a conceptual model for estimating load transfer coefficients for jointed concrete pavements from deflection measurements is presented.

17. Key Words	18. Distribution Statement
rigid pavement, continuously reinforced concrete pavement (CRCP), structural evaluation, deflection, load transfer, load transfer coefficient, J-factor, thickness	No restrictions. This document is available to the public through the National Technical Information Service, Springfield, Virginia 22161.

19. Security Classif. (of this report)	20. Security Classif. (of this page)	21. No. of Pages	22. Price
Unclassified	Unclassified	102	

DEVELOPMENT OF LOAD TRANSFER COEFFICIENTS FOR USE WITH THE AASHTO GUIDE FOR DESIGN OF RIGID PAVEMENTS BASED ON FIELD MEASUREMENTS

by

Chao Wei
B. Frank McCullough
W. Ronald Hudson
Kenneth Hankins

Research Report 1169-3

Concrete Pavement Design Update
Research Project 3-8-88/1-1169

conducted for

Texas Department of Transportation

in cooperation with the

U.S. Department of Transportation
Federal Highway Administration

by the

CENTER FOR TRANSPORTATION RESEARCH
Bureau of Engineering Research
THE UNIVERSITY OF TEXAS AT AUSTIN

February 1992

NOT INTENDED FOR CONSTRUCTION, BIDDING OR PERMIT PURPOSES

B. Frank McCullough, P.E. (Texas No. 19914)
W. Ronald Hudson, P.E. (Texas No. 16821)
Study Supervisors

PREFACE

Research Report 1169-3, "Development of Load Transfer Coefficients for Use with the AASHTO Guide for Design of Rigid Pavements Based on Field Measurements," is the third report for Research Project 3-8-88/1-1169, "Concrete Pavement Design Update," conducted by the Center for Transportation Research, The University of Texas at Austin. The study is part of the Cooperative Highway Research Program sponsored by the Texas Department of Transportation (TxDOT) and the Federal Highway Administration (FHWA).

The purpose of this report is to present a rational procedure for estimating (1) load transfer coefficients for use with the AASHTO guide to rigid pavement design based on field deflection measurements, and (2) the derived load transfer coefficients for the design of continuously reinforced concrete pavements (CRCP) in Texas. The load transfer coefficients were determined using the information available in the rigid pavement database at the Center for Transportation Research, The University of Texas at Austin.

The authors are grateful to the staff of the Center for Transportation Research for their technical assistance and support, with special thanks extended to Mr. Terry Dossey for his assistance with the computer system. We would also like to thank the Texas Department of Transportation for their sponsorship of, and assistance with, this project.

Chao Wei
B. Frank McCullough
W. Ronald Hudson
Kenneth Hankins

LIST OF REPORTS

Research Report 1169-1, "A Study of Drainage Coefficients for Concrete Pavements in Texas," by Venkatakrisna Shyam, Humberto Castedo, W. Ronald Hudson, and B. Frank McCullough, discusses the efforts to determine coefficients of drainage for concrete pavements with three subbase types and a range of rainfall conditions. May 1989.

Research Report 1169-2, "Mechanistic Analysis of Continuously Reinforced Concrete Pavements Considering Material Characteristics, Variability, and Fatigue," by Mooncheol Won, Kenneth Hankins, and B. Frank McCullough, presents a mechanistic model for estimating continuously reinforced concrete (CRC) pavement life in terms of frequency of punchouts. This model was incorporated in computer program CRCP-5, which is described in detail. The model uses the stochastic nature of the material properties and the fatigue behavior of pavement concrete for predicting the extent and time of occurrence of punchouts in CRC pavements. April 1990.

Research Report 1169-3, "Development of Load Transfer Coefficients for Use with the AASHTO Guide for Design of Rigid Pavements Based on Field Measurements," by Chao Wei, B. Frank McCullough, W. Ronald Hudson, and Kenneth Hankins, presents a rational procedure for estimating (1) load transfer coefficients for use with the AASHTO guide to rigid pavement design based on field deflection measurements, and (2) the derived load transfer coefficients for the design of continuously reinforced concrete pavements (CRCP) in Texas using the information available in the rigid pavement database at the Center for Transportation Research, The University of Texas at Austin. February 1992.

ABSTRACT

A rational procedure was developed for estimating load transfer coefficients for use with the AASHTO guide for the design of continuously reinforced concrete pavements (CRCP) based on field deflection measurements. Load transfer coefficients for design of CRCP in Texas were determined using the information available in the rigid pavement database stored at the Center for Transportation Research, The University of Texas at Austin. An evaluation of structural conditions of CRCP sections in the rigid pavement database was performed to assess the ability of in-service CRCP in Texas to transfer load at transverse cracks. A finite-element analysis of CRCP using the ILLI-SLAB program was conducted to identify critical stress positions in CRCP. In addition, a conceptual model for estimating load transfer coefficients for jointed concrete pavements from deflection measurements is presented.

KEY WORDS: rigid pavement, continuously reinforced concrete pavement, structural evaluation, deflection, load transfer, load transfer coefficient, J-factor, thickness.

SUMMARY

The main objective of this report was to develop suitable load transfer coefficients for use with the AASHTO guide for the design of continuously reinforced concrete pavement (CRCP) in Texas based on field measurements. In conjunction with this objective, an evaluation of structural conditions of CRCP sections in the rigid pavement database at the Center for Transportation Research was performed to assess the ability of in-service CRCP in Texas to transfer load across the cracks and joints. Following this evaluation, a rational procedure was developed for estimating load transfer coefficients for rigid pavements based on field deflection measurements. The field load transfer coefficients were determined using information available in the rigid pavement database. In addition, a conceptual model was developed for estimating load transfer coefficients for jointed concrete pavements.

IMPLEMENTATION STATEMENT

A rational procedure was developed for estimating load transfer coefficients for rigid pavements based on field deflection measurements. In addition, load transfer coefficients for the design of continuously reinforced concrete pavement in Texas were determined using information available in the rigid pavement database. It is recommended that the methodology developed in this study be implemented by the Texas Department of Transportation to determine suitable design values of load transfer coefficients for the design of different types of pavement. It is also recommended that the load transfer coefficient values for continuously reinforced concrete pavement developed in this study be used as guidelines for the design of rigid pavements in Texas.

TABLE OF CONTENTS

CHAPTER 1. INTRODUCTION

1.1 BACKGROUND

The current pavement design procedure recommended by the American Association of State Highway and Transportation Officials (AASHTO) is based largely upon the findings of the AASHO (American Association of State Highway Officials) Road Test conducted in the late 1950s at Ottawa, Illinois (Ref 6). The AASHO (currently the AASHTO) Design Committee published the first Interim Pavement Design Guide in 1961 based on the results of the Road Test (Ref 12). The Interim Pavement Design Guide was later revised in 1972 and 1981 (Refs 19 and 41). In 1986, the AASHTO Design Committee published a new guide, the "AASHTO Guide for Design of Pavement Structures," and, for convenience, it is referred to in this report as the AASHTO guide (Ref 6).

During the development of the current AASHTO guide, the basic form of the AASHO Road Test rigid pavement performance equation was retained but was expanded to include additional parameters because the original Road Test was limited in scope (i.e., few materials, one subgrade, one environment, etc.). One of the features in the rigid pavement performance equation used in the AASHTO guide is the expansion of the load transfer coefficient (J-factor) to consider various rigid pavement slab configurations, including jointed concrete pavements and continuously reinforced concrete pavements (Ref 6).

The use of load transfer coefficients in rigid pavement performance equations accounts for the differences in the ability of various types of concrete pavement structures to transfer loads across joints or cracks. The load transfer coefficient is defined as the ability of a concrete pavement structure to transfer (distribute) load across such discontinuities as joints or cracks. The load transfer coefficient may be affected by many factors, including aggregate interlock, load transfer devices used in the pavement, and the presence of tied concrete shoulders.

Figure 1.1 presents the basic concept of the load transfer coefficient. If load transfer devices are not used at the joint, the deflection at the joint is likely to be higher than that associated with the use of load transfer devices. Consequently, if the same performance life is required for these two types of pavement, a thicker slab is needed for the pavement not equipped with load transfer devices at its joints. This may be accomplished in the design by using different values of load transfer coefficients in the rigid pavement performance equation. A larger load transfer coefficient would be used for pavements without load transfer devices, while a lower load transfer coefficient would be used for pavements with load transfer devices.

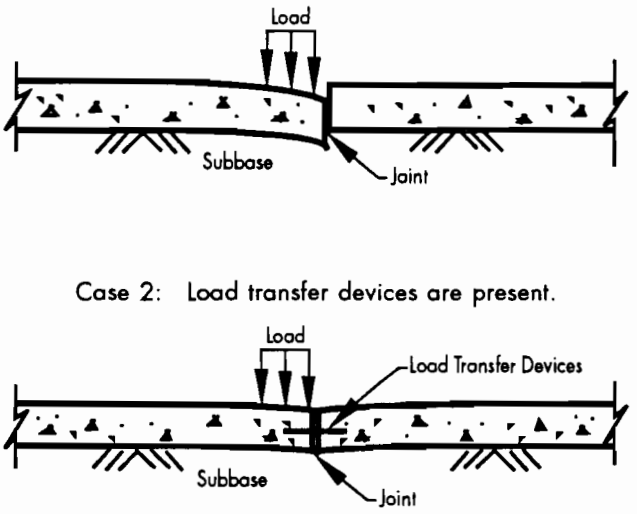

Figure 1.1 Illustration of the basic concept of load transfer coefficient

To develop suitable load transfer coefficients for use with the AASHTO guide in designing rigid pavements in Texas, the CTR study team sought to develop load transfer coefficients from measurements of in-service pavements. Since the AASHO Road Test did not include the study of continuously reinforced concrete pavements (CRCP), these pavements received priority. This report, then, documents the development of suitable load transfer coefficients for use in the design of CRCP in Texas.

1.2 OBJECTIVE OF THE STUDY

The primary objective of the study was to develop appropriate load transfer coefficients for use with the AASHTO guide for the design of continuously reinforced concrete pavements in Texas. Such coefficients were to be based on measurements of in-service pavements and incorporated into future pavement design guidelines. Specifically, the objectives of the study included the following:

(1) to assess load transfer ability of in-service CRCP using available information in the rigid pavement database (Ref 21),
(2) to develop a procedure to estimate load transfer coefficients for rigid pavements in Texas based on field measurements,
(3) to apply the developed procedure to obtain load transfer coefficients from measurements of in-service CRCP in Texas, and
(4) to recommend load transfer coefficients for the design of CRCP in Texas.

1.3 SCOPE OF THE STUDY AND ORGANIZATION

The overall approach to the research task, along with a general outline of the study activities, is shown in Figure 1.2. The approach is primarily based on information obtained from Research Project 472, "Rigid Pavement Data Base," and from Research Project 460, "Assessment of Load Transfer Across Joints or Cracks in Rigid Pavements Using the Falling Weight Deflectometer," both sponsored by the Texas Department of Transportation and the Federal Highway Administration (Refs 21 and 25).

The first chapter presents the background, objectives of the research, and scope of the study. Chapter 2 summarizes a literature review that recounts the evolution of the load transfer coefficient for rigid pavements. Chapter 3 presents an assessment of the load transfer ability of rigid pavements (with emphasis on in-service CRC pavements) using information available in the rigid pavement database (Refs 21 and 32).

Chapter 4 describes the development of a rational model (J-factor model) for estimating the load transfer coefficient for continuously reinforced concrete pavements based on field measurements. A conceptual model for estimating the load transfer coefficient for jointed concrete pavements based on field measurements is also described.

Chapter 5 describes the application of the J-factor model to obtain load transfer coefficients for CRCP using information available in the rigid pavement database, while Chapter 6 presents the statistics of the obtained load transfer coefficients. A multiple regression analysis of coefficient values obtained was performed to identify the variables that may have an important influence on load transfer coefficients.

Chapter 7 provides a discussion of the analysis performed in Chapter 6. Load transfer coefficients for the design of CRCP in Texas are also presented. Chapter 8 outlines steps for implementing the J-factor model in order to obtain load transfer coefficients from field measurements. The implications of using the load transfer coefficients developed in this study in the design of CRCP are discussed. Finally, the summary, conclusions, and recommendations are provided in Chapter 9.

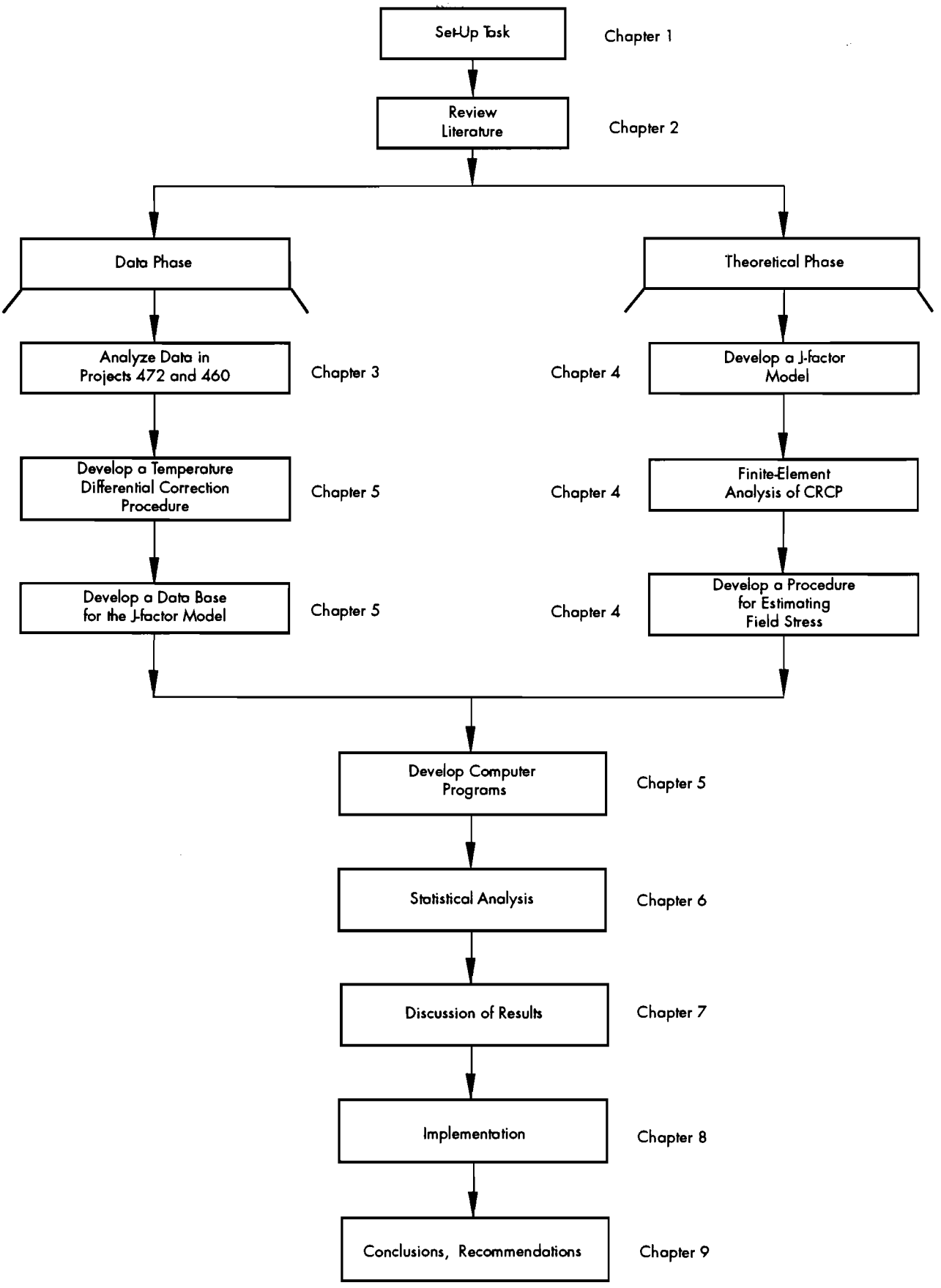

Figure 1.2 Outline of the study of load transfer coefficient

CHAPTER 2. REVIEW OF LOAD TRANSFER COEFFICIENT DEVELOPMENT

This chapter presents a review of the available literature related to load transfer coefficients. The first section discusses in particular the Spangler equation, which was used in the development of the rigid pavement performance equation to extend the AASHO Road Test conditions to other soil and concrete properties (Ref 1). A brief review of the development of the AASHO Road Test equation is then presented. The remainder of the chapter reviews recent developments of load transfer coefficients for use with the AASHTO guide.

2.1 SPANGLER EQUATION

In the mid-1930s, Spangler undertook at Iowa State College a study of corner stress conditions (Ref 2). The primary purpose of the research was to provide experimental data for verification or modification of (1) the original corner equation proposed by Goldbeck and (2) the theoretical corner equation developed by Westergaard, both of which related to the design of concrete pavement slabs.

In the Spangler study, five experimental slabs were constructed in a building basement to provide controlled conditions for testing. One slab was used primarily for the development of procedures and measuring techniques. Static loads were applied to the slabs through a circular cast-iron bearing plate, 6.72 inches in diameter. The modulus of subgrade reaction (K-value) was determined by dividing the unit load at any point on the slab by the deflection of the slab at that point. Slab maximum stresses were estimated by converting the strains, which were measured by means of optical levered extensometers.

One of the findings of Spangler's study was that the values of the maximum stresses in a free corner region of a concrete slab generally agree with stresses calculated by the Kelley corner load stress formula (Ref 3), which has the form:

$$\sigma_c = \frac{3P}{D^2}\left[1-\left(\frac{a_1}{L}\right)^{1.2}\right] \qquad (2.1)$$

where

σ_c = maximum stress due to a corner load (psi),
P = load (lb),
D = slab thickness (inch),
a_1 = $a\sqrt{2}$
a = radius of circle equal in area to load area (inch), and
L = radius of relative stiffness, inch, as defined by the following formula:

$$L = \sqrt[4]{\frac{ED^3}{12\left(1-\mu^2\right)K}} \qquad (2.2)$$

where

E = concrete modulus of elasticity (psi),
μ = Poisson's ratio for concrete, and
K = subgrade reaction (psi).

Spangler simplified the Kelley formula by removing the fractional exponent of the quantity (a_1/L) and by raising the numerical coefficient from 3.0 to 3.2. The result was the Spangler corner load formula, as shown in Equation 2.3.

$$\sigma_c = \frac{3P}{D^2}\left[1-\left(\frac{a_1}{L}\right)\right] \qquad (2.3)$$

Equation 2.3 yields essentially the same results as the stresses estimated from the Spangler test.

The Kelley corner load formula was developed primarily from the maximum stresses estimated in the Arlington tests conducted in the 1930s. The tests were made on a group of 10 concrete pavement slabs, each measuring 40 feet long by 20 feet wide and having different cross sections. The slabs were divided by a longitudinal and a transverse joint. The results of the Arlington tests showed that during the day, when the corner of the slab was warped downward and had contact with the

subgrade, there was a good correlation between the estimated stresses and those computed by the Westergaard formula (Ref 4), which is of the following form:

$$\sigma_c = \frac{3P}{D^2}\left[1-\left(\frac{a_1}{L}\right)^{0.6}\right] \qquad (2.4)$$

When the slab was warped upward, the maximum estimated stresses caused by a corner load were considerably greater than those calculated by the Westergaard corner load formula, though still highly correlated with the stresses calculated from the Kelley corner load formula (Equation 2.1). As pointed out by Kelley, Equation 2.1—while purely empirical and having no theoretical background—has the same general form as the Westergaard formula. It is important to mention that the development of the Kelley corner formula was based on the estimated maximum stresses in the test pavement slabs exposed to normal fluctuations of temperature and moisture. In other words, if particular temperature or environmental conditions differ from those associated with the Arlington tests, the results might not be the same as those calculated by the formula.

In the early 1920s, Westergaard developed his corner load formula purely from theoretical considerations based on classic linear elastic theory with an important assumption made for the subgrade simulation. He assumed that the subgrade reaction is vertical and proportional to the deflection of the slab. A comparison of the stresses calculated from the Westergaard and Kelley formulas shows that the Kelley formula yields stresses that are about 20 to 50 percent greater than those given by the Westergaard formula. Figure 2.1 shows the plots of the stresses calculated from the above three corner load formulas considering variations in slab thickness, modulus of subgrade reaction, and concrete modulus of elasticity. As seen from these figures, the difference in stress between Kelley's and Spangler's formulas are very small; however, the difference in stress between Westergaard's and Kelley's, and also between Westergaard's and Spangler's, formulas are quite large.

The above review of the evolution of the Spangler equation reveals that the Spangler corner load formula is also purely empirical. It was based on results conducted on experimental slabs in a basement room not affected by outside environmental changes (hence the environmental conditions differed from those of the Arlington tests). Thus, the agreement between the Kelley and Spangler formula does not guarantee that the Spangler formula can yield the same values if the environment and the pavement structures differ from those of the test conditions.

2.2 AASHO ROAD TEST EQUATION

The AASHO Road Test equation discussed here is the rigid pavement performance equation for the design of concrete pavement structures developed from the AASHO Road Test data (Ref 1).

The AASHO Road Test, sponsored by the American Association of State Highway Officials and other highway agencies, was conducted on a specially constructed section of highway near Ottawa, Illinois, between 1958 and 1961. One of the objectives of the AASHO Road Test was to determine the significant relationships between the number of repetitive applications of specified axle loads of varying magnitude and arrangement and the performance of different thicknesses of uniformly designed and constructed pavements (Ref 5). While both flexible and rigid pavement structures were investigated, only jointed rigid pavements are reviewed in this report.

A study of the serviceability trends of pavement sections at the AASHO Road Test demonstrated that serviceability loss was proportional to a power function of the number of axle load applications (Ref 1), which can be expressed as:

$$p = C_0 - (C_0 - C_1)(W/\rho)^{\beta} \qquad (2.5)$$

where

$C_1 < p \le C_0$,
p = serviceability at a given time,
C_0 = initial serviceability value,
C_1 = serviceability level (1.5) at which test sections were removed from test,
W = weighted (the number of seasonal load applications multiplied by a seasonal weighting function) traffic factor,
ρ = a function of design and load variables that denotes the expected number of axle load applications to a serviceability index of 1.5, and
β = a function of design and load variables that influences the shape of the p vs W serviceability curve.

Rearrangement of Equation 2.5 gives:

$$\log\left(\frac{C_0 - p}{C_0 - C_1}\right) = \beta(\log W - \log\rho) \qquad (2.6)$$

For convenience, the left side of Equation 2.6 can be termed as G, which gives:

$$G = \log\left(\frac{C_0 - p}{C_0 - C_1}\right) \tag{2.7}$$

Substituting into Equation 2.6 from Equation 2.7 gives:

$$G = \beta(\log W - \log \rho) \tag{2.8}$$

Using the values for the AASHO Road Test conditions for rigid pavements, along with an 18-kip single axle, Equation 2.8 may be expressed as follows:

$$\log W_{18} = 7.35\log(D+1) - 0.06 + G/\beta_{18} \tag{2.9}$$

where

W_{18} = total equivalent 18-kip single axle load applications,
D = thickness of rigid slab (inches),

$$\beta_{18} = 1.00 + 1.624 \times 10^7 / (D+1)^{8.46}, \tag{2.10}$$

for equivalent 18-kip single axle load applications, and

$$\rho_{18} = 0.87533(D+1)^{7.35}, \tag{2.11}$$

for equivalent 18-kip single axle load applications.

Since Equation 2.9 includes only two variables—slab thickness and the total number of load applications—its applicability is limited. Furthermore, Equation 2.9 was derived by holding the following factors constant:

(1) concrete modulus of elasticity, E_c;
(2) concrete modulus of rupture, S_c;
(3) modulus of subgrade reaction, k;
(4) environmental conditions;
(5) 2-year life span; and
(6) load transfer characteristics.

To apply the relationship between load application and thickness (as defined in Equation 2.9) to the structural design of rigid pavements in physical environments differing from those which existed during the Road Test, a modification was made by an AASHO Subcommittee on Design to incorporate those factors that were not evaluated by the Road Test.

A comparison was made between the strains actually measured on the Road Test pavement slabs and the corner stresses calculated in the theoretical formulas of Westergaard, Spangler, and Pickett. The absolute values of the estimated stresses differ from those calculated, but both the Westergaard and Spangler formulas for corner load stresses do an excellent job of linearizing the Road Test measurements. Because of its simplicity, the Spangler formula was selected for use in extending the AASHO Road Test to other conditions (Ref 1).

The Spangler formula used by the AASHO subcommittee is in the following form:

$$\sigma_c = \frac{JP}{D^2}\left[1 - \left(\frac{a_1}{L}\right)\right] \tag{2.12}$$

where

J = a coefficient depending upon load transfer characteristics (3.2 for protected corner conditions).

In order to simplify the work without damaging the theory, μ is fixed at 0.20, and a_1 is taken as 10 inches (the average for Road Test loads) in the Spangler equation for the regression analysis. The J-term cancels out for protected corner conditions for the jointed concrete pavements at the AASHO Road Test.

It was found by the AASHO subcommittee that a linear relationship exists between log W and the ratio of modulus of rupture at the AASHO Road Test to stresses calculated by the Spangler equation. This relationship can be mathematically defined as follows:

$$\log W = a + b \log F \tag{2.13}$$

where

a = constant,
b = 4.22 – 0.32p for 18-kip single axle load for p ranging from 1.5 to 2.5, (2.14)
W = number of applications of a given load to a given terminal serviceability,
F = S_c/σ,
S_c = concrete modulus of rupture, and
σ = stress calculated from Equation 2.12.

Differentiating Equation 2.13 gives:

$$d(\log W) = (b)d \log F \tag{2.15}$$

Then the difference in life (expressed in load applications) between a rigid pavement with given physical properties described by F, and one with modified physical properties described by F′ could be expressed:

$$\log W' - \log W = b(\log F' - \log F) \tag{2.15a}$$

W′ = number of load applications required to reach a given terminal serviceability p for a pavement similar to the Road Test pavements but with different physical properties as described by F′, and

F′ = the S_c/σ ratio for the properties other than at the Road Test.

Rearranging terms gives:

$$\log W' = \log W + b(\log F' - \log F) \qquad (2.16)$$

If W is calculated in terms of 18-kip single axle loads, the following relationship can be obtained by inserting Equation 2.14 into Equation 2.16:

$$\log W' = \log W_{18} + (4.22 - 0.32p)(\log F' - \log F) \qquad (2.17)$$

From Equation 2.17, the life of a pavement with given physical properties as defined by F′ (which are different from the physical properties associated with the Road Test) can then be predicted.

Equation 2.17 can be further simplified into the following design equation, referred to as the AASHO Road Test equation, by substituting the values for the physical constants that represent the Road Test conditions:

$$\log W' = 7.35\log(D+1) - 0.06 + \frac{G}{1+\frac{1.624\times 10^7}{(D+1)^{8.46}}}$$

$$+(4.22-0.32p)\log\left(\left(\frac{S_c'}{215.63\,J}\right)\left(\frac{D^{0.75}-1.132}{D^{0.75}-\frac{18.42}{Z^{0.25}}}\right)\right) \qquad (2.18)$$

where

S_c' = concrete modulus of rupture differing from the Road Test,

Z = E/K, and

J = 3.2 for the AASHO Road Test conditions.

It should be noted that the relationship defined in Equations 2.17 and 2.18 contains the following two important assumptions, which were made at the Road Test (Ref 1):

(1) The variation in pavement life (W) for different loads at the same level of S_c/σ is accounted for by the basic Road Test equation and is covered in the AASHO design procedure by traffic equivalence factors.

(2) Any change in the S_c/σ resulting from changes in the physical constants E, K, D, and S_c will have the same effect on W′ as varying slab thickness. This relationship is defined by Equation 2.13.

From the above review of the development of the AASHO Road Test equation, two important points can be made. One is that the relationship defined by Equation 2.13 is based on the jointed concrete pavements investigated at the Road Test. The use of this relationship for the design of CRC pavements needs further investigation, since it is a different type of pavement. The other point is that the J-term was introduced in assumption (2). A J-term of 3.2 (from the Spangler equation) for the AASHO Road Test equation does not indicate a free corner loading condition; instead, it represents a regression coefficient used in obtaining the relationship as defined by Equation 2.13. In fact, all the joints at the Road Test were provided with load transfer devices. In other words, there were no actual free corners existing in the Road Test's jointed concrete pavements.

Load transfer across the joints was not included as a variable in the Road Test study. As a result, the load transfer coefficient value for design of other pavement types cannot be studied with the Road Test data.

2.3 LOAD TRANSFER COEFFICIENTS FOR RIGID PAVEMENTS

This section reviews more recent developments in load transfer coefficients for rigid pavements. The review is organized in terms of two types of rigid pavement: (1) jointed concrete pavements (JCP), and (2) continuously reinforced concrete pavements (CRCP).

2.3.1 Load Transfer Coefficients for Jointed Concrete Pavements

In the AASHTO guide, the load transfer coefficient for jointed concrete pavements can be classified into four groups in terms of:

(1) plain jointed pavement (PJP), or jointed reinforced concrete pavement (JRCP), with some type of load transfer device (such as a dowel bar) at the joints;

(2) jointed pavements without load transfer devices at the joints;

(3) PJP or JRCP with load transfer devices having a tied portland cement concrete (PCC)

shoulder; and
(4) jointed pavements without load transfer devices but having a tied PCC shoulder.

Table 2.1 shows the values of load transfer coefficients recommended in the AASHTO guide for the four pavement groups. Pavement group 1 basically represents the AASHO Road Test conditions. A load transfer coefficient value of 3.2 for the thickness design of this group of pavements is still used. No change has been made regarding the use of load transfer coefficients for this pavement group since the Road Test. Load transfer coefficients for the other three groups are found only in the 1986 AASHTO guide.

Table 2.1 Recommended load transfer coefficients for jointed concrete pavements (Ref 6)

Pavement Group	Load Transfer Type	Load Transfer Coefficient
1	Load transfer devices at the joints	3.2
2	No load transfer devices at the joints	3.8 - 4.4
3	Load transfer devices at the joints with a tied PCC shoulder	2.5 - 3.1
4	No load transfer devices at the joint but with a tied PCC shoulder	3.6 - 4.2

The development of load transfer coefficients for groups 2, 3, and 4 was based on a mechanistic analysis using a discrete element program (Ref 7). No field data were used for the development. Table 2.2 shows the load transfer coefficient values derived for the four types of jointed concrete pavement.

2.3.2 Load Transfer Coefficients for CRC Pavements

Load transfer coefficients for the design of CRC pavements are more difficult to obtain, since a CRC pavement type was not included in the Road Test study. The first use of load transfer coefficients for the design of CRC pavements using the AASHO Road Test equation can be found in a paper by Hudson and McCullough (Ref 9). Seeking to extend the AASHO Road Test equation to CRC pavements, this paper recommended 2.2 for the load transfer coefficient value. This value seems to be based on experience, since no source for this value was given. Using 2.2 as the load transfer coefficient in the design of CRC pavements results in a reduction of about 2 inches in thickness as compared to jointed pavements at the Road Test (load transfer coefficient of 3.2).

Table 2.2 Load transfer coefficients for jointed concrete pavements derived from a mechanistic analysis (Ref 7)

Pavement Group	Load Transfer Type	Load Transfer Coefficient
1	Load transfer devices at the joints	3.2
2	No load transfer devices at the joints	3.9 - 4.8
3	Load transfer devices at the joints with a tied PCC shoulder	2.7 - 3.0
4	No load transfer devices at the joint but with a tied PCC shoulder	3.6 - 4.0

The use of a 2.2 value in the design of CRC pavements was later supported by a statewide deflection study of CRC pavements in Texas (Ref 10). This study showed that the deflections in 10-inch jointed concrete pavements were almost the same as those in 8-inch CRC pavements. A new value for load transfer coefficients in CRC pavements was developed based on the results (Ref 11).

In Reference 11, the load transfer coefficient for CRC pavement is defined as follows:

$$J_c = J_j \times \frac{A}{B} \tag{2.19}$$

where

J_c = load transfer coefficient for CRC pavement,
J_j = load transfer coefficient for jointed pavement = 3.2,
A = percent difference in deflection at cracks and at midway between cracks for CRC pavement, and
B = percent difference in deflection between joints and midway for jointed pavement.

Based on the results of the statewide deflection study of rigid pavements in Texas, the following load transfer coefficient value was obtained:

$$J_c = 3.2 \times \frac{12.87}{17.66} = 2.33 \tag{2.20}$$

As pointed out in Reference 11, this value was based only on 8-inch CRC pavements. Therefore, the validity and application of this value to other thicknesses of pavements, traffic levels, and environmental conditions is of questionable validity (Ref 16).

In the 1960s, the Illinois DOT used a thickness that was 70-80 percent of a typical jointed pavement for the design of CRC pavements (Ref 13). This design policy was once referred to as the "80-percent rule." The use of this rule also implies that a value of 2.2 for the load transfer coefficient could be considered when using the AASHO Road Test equation for the design of CRC pavements.

A load transfer coefficient of 2.2 was also found in a NCHRP report of the evaluation of the AASHTO Interim Guide for Design of Pavement Structures, published in 1972 (Ref 14). The CRC pavement design procedure published in the ACI journal in 1972 also considered the use of a load transfer coefficient of 2.2 for CRC pavement thickness design. However, no information is provided in the ACI design procedure on how to select a load transfer coefficient for design purposes, other than to suggest that the values of these coefficients may range from 2 to 3 (Ref 15).

A performance study of CRC pavements in Indiana, conducted by Asif Faiz in the mid-1970s, showed that the "80-percent rule" regarding CRC pavement thickness was ineffective in withstanding the traffic loadings on interstate highways (Ref 16). Faiz's study found that 9-inch CRC pavements have critical edge conditions with regard to stresses and deflections; thus, he suggested that CRC pavement thickness be the same as that required for an equivalent jointed concrete pavement.

However, another performance study of CRC pavements in Illinois in the late 1970s showed that the performance of 9- and 10-inch CRC pavements was superior to that of the conventional jointed concrete pavement under extremely heavy Chicago metropolitan area truck-traffic conditions (Ref 17). Furthermore, a 10-inch CRC pavement was expected to carry four times the traffic of a 10-inch jointed pavement. The study also indicated that the performance of the thinner 7-inch and 8-inch CRC pavements was poor, showing an accelerated rate of distress over time. This was probably due to the fact that thinner pavements may easily lose load transfer capability after a number of load applications. In Colly and Humphrey's study of aggregate interlock load transfer across joints, it was found that there was a significant difference in load transfer efficiency between 7- and 9-inch pavements after a number of load cycles (Ref 18). In addition, their study showed that a decrease in load magnitude significantly reduced the rate of loss of load transfer efficiency. Figure 2.2 shows their test results in terms of load transfer efficiency and load cycles for 7- and 9-inch pavements.

During the 1980s, the trend toward using a load transfer coefficient value of 3.2 increased as a result of more heavy-truck traffic on interstate highways and because of the increased use of pavement shoulders, or "off-tracking," which creates critical conditions at the pavement edge. Previous use of a load transfer coefficient of 2.2 was based on the interior loading condition, as pointed out by McCullough (Ref 53). The change toward using 3.2 for a load transfer coefficient can be found in the 1981 version of the AASHTO Interim Guide for Design of Pavement Structures (Ref 19), as well as in the ARBP (Associated Reinforced Bar Producers) manual for the design of CRC pavements (Ref 20). The ARBP manual also gives a value of 2.56 as a load transfer coefficient for the design of CRC pavements with a tied concrete shoulder.

The mechanistic derivation of a load transfer coefficient for the design of CRC pavements can be found in Volume 2 of the 1986 AASHTO Guide for the Design of Pavement Structures (Ref 7). Table 2.3 shows the values of load transfer coefficients derived from the mechanistic analysis. The load transfer coefficient values recommended in the AASHTO guide are presented in Table 2.4.

Table 2.3 Load transfer coefficients for CRC pavements obtained from mechanistic analysis (Ref 7)

Pavement Group	Load Transfer Type	Load Transfer Coefficient
1	Load transfer devices at the cracks with a tied PCC shoulder	2.3 - 2.6
2	Load transfer devices at the cracks with an AC shoulder	2.6 - 3.1

Table 2.4 Recommended load transfer coefficients for CRC pavements (Ref 6)

Pavement Group	Load Transfer Type	Load Transfer Coefficient
1	Load transfer devices at the cracks with a tied PCC shoulder	2.3 - 2.9
2	Load transfer devices at the cracks with an AC shoulder	2.9 - 3.2

A comparison between load transfer coefficients in Tables 2.3 and 2.4 reveals that some adjustments were made in the AASHTO guide. Also, it can be seen that the ranges of recommended values for load transfer coefficients are quite wide. For instance, in designing CRC pavements without a tied PCC shoulder, one can choose a value ranging from 2.3 to 2.9, which may result in a large difference in thickness. Therefore, it is necessary to develop a suitable load transfer coefficient value for the local condition if the AASHTO guide procedure is to be used.

From the previous review of the development of load transfer coefficients, it can be concluded that the concept of a load transfer coefficient is not only a problem of percent of load transfer that will transfer across the joint/crack. Rather, the concept has been expanded to consider the abilities of various pavement structures to support the traffic load under different conditions. For instance, the use of a tied PCC shoulder may reduce the load transfer coefficient value. Light traffic and reduced temperature variations may also reduce this value. Load transfer devices, aggregate interlock, subgrade reaction, and the presence of tied concrete shoulders will all have an effect on this value. Therefore, a procedure should be developed that can take into account pavement thickness, pavement geometric conditions and/or boundary conditions, subgrade, and the discontinuities in the field pavements. However, at the time of this study, a review of the available literature has shown that such a procedure is not available.

2.4 SUMMARY

In this chapter, the evolution of load transfer coefficients for rigid pavements, beginning with Hudson and McCullough's original concept, was reviewed. While a load transfer coefficient value of 2.2 was used in the 1960s, the concept of load transfer coefficient was later expanded in the 1986 AASHTO guide to consider various types of pavement structures in different conditions. A mechanistic approach was provided in Volume 2 of the 1986 AASHTO guide. However, a procedure to obtain a suitable value of load transfer coefficients for local conditions, especially a procedure based on field measurements, is not available in the AASHTO guide. The current CTR study team recommends that such a procedure—one that is sound from both a theoretical and a practical standpoint—be developed.

CHAPTER 3. ASSESSMENT OF STRUCTURAL CONDITIONS OF RIGID PAVEMENTS IN TEXAS

3.1 INTRODUCTION

To develop a suitable load transfer coefficient for the design of CRCP in Texas, an assessment of structural conditions of in-service CRCP in Texas was performed.

In Research Project 472, "Rigid Pavement Data Base," a study conducted in 1988 by the Center for Transportation Research (CTR) of The University of Texas at Austin, falling weight deflectometer (FWD) deflection measurements were taken on in-service CRC pavements across Texas and stored in the rigid pavement database at CTR (Ref 21). These FWD measurements were taken from both original CRC pavements and overlaid pavements; however, only measurements from original CRC pavements are analyzed in this report.

This chapter presents the assessment of in-service CRC pavement structural conditions using the statewide deflection measurement data and other information available in the rigid pavement database. The primary purpose of this assessment is to evaluate the abilities of in-service CRC pavements to transfer load across pavement discontinuities. The assessment includes the following conditions:

(1) load transfer at transverse cracks in CRC pavements;
(2) difference in deflections at cracks and at mid-span between cracks; and
(3) difference in deflections between the pavement edge and the interior.

In addition, variations in deflections for different loading positions are evaluated, with comparisons made between deflections from in-service CRC pavements and deflections from a test section of jointed pavement. Analytical results from the theoretical model are also compared with deflections from in-service CRC pavements and jointed pavements.

3.2 ASSESSMENT OF STRUCTURAL CONDITIONS OF IN-SERVICE CRCP

3.2.1 Brief Description of FWD Data from In-Service CRCP

The FWD measurements taken on non-overlaid CRC pavements during the summer of 1988 covered the 11 Texas districts shown in Figure 3.1. Selected pavement sections for the measurements included:

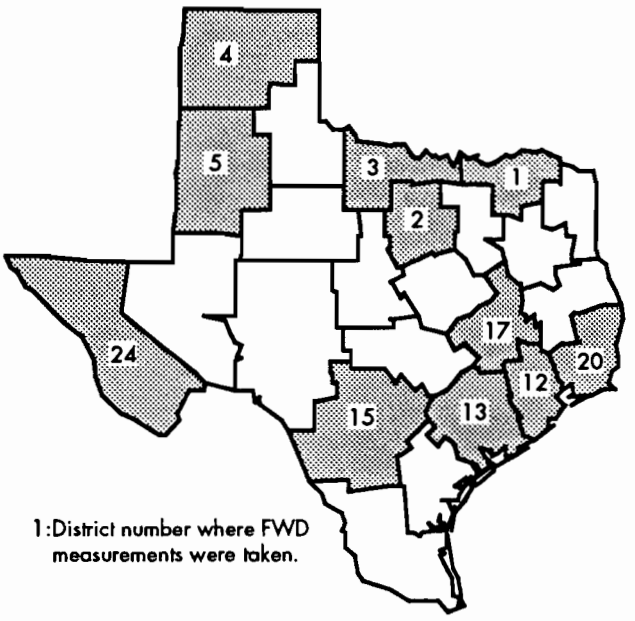

Figure 3.1 The geographical distribution of CRCP FWD measurements in Texas, displayed by districts

(1) Three slab thicknesses of CRC pavements—
- 8-inch,
- 9-inch, and
- 13-inch;

(2) Two pavement shoulder types—
- asphaltic concrete (AC) shoulder, and
- tied portland cement concrete (PCC) shoulder;

(3) Three coarse aggregate types—
- limestone (LS),
- siliceous river gravel (SRG), and
- combination of limestone and siliceous river gravel (LS/SRG or SRG/LS); and

(4) Four different subbase types—
- asphalt-stabilized (ACT),
- cement-stabilized (CT),
- lime-treated (LT), and
- crushed stone (CRS).

Each test section was 1,000 feet long and was divided into five subsections (Ref 21). A set of FWD measurements was taken in each subsection, as shown in Figure 3.2. This set of FWD measurements included two stations near the crack, one station at the crack, one station at the mid-span between the cracks, and one station in the interior. These stations were numbered stations 1 to 5, as indicated in Figure 3.2. Four sets of FWD measurements were taken at each station using four different drop heights, with peak loads ranging from about 6,000 to 17,000 pounds. (For detailed information about the deflection measurements and the rigid pavement database, see Refs 21, 22, 23, and 24.)

3.2.2 Repeatability of FWD Measurements

In the United States, the standard design axle load for pavement is 18,000 pounds, i.e., a 9,000-pound wheel load. Therefore, it would be desirable to use the deflections measured at such a wheel load level for the analysis. However, as pointed out by Weissmann (Ref 24), inconsistent results were found at low drop heights (small loads) in the deflection data collected. Thus, in order to choose suitable deflection measurements for the analysis, a repeatability check of the FWD measurements was performed.

The repeatability analysis consisted of studying a set of deflection measurements collected on 8-inch pavements with two coarse aggregates over four different subbases. Figure 3.3 shows a plot of the transformed 9-kip deflections with four drop heights for limestone pavements over four different subbases. As the figure shows, drop height 1 has lower deflections, but drop heights 2, 3, and 4 have almost the same deflections. The difference in deflections between drop heights 2, 3, and 4 can, therefore, be neglected as compared with the allowable measurement errors. A similar plot for siliceous river gravel pavements over two types of subbases is shown in Figure 3.4, where we can see that the difference in deflections between each drop height is also small. Therefore, if drop height 1 is not considered, a linear relationship exists

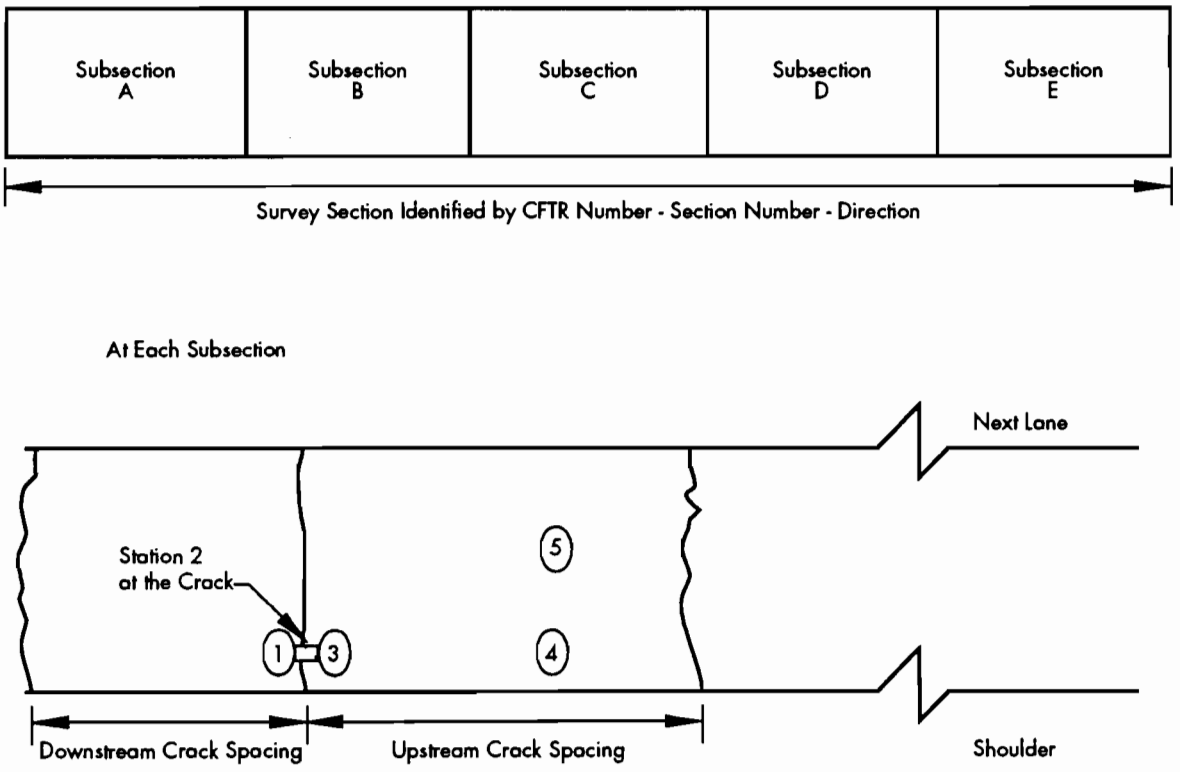

Figure 3.2 Layout for FWD measurements in a non-overlaid section (Ref 24)

between the deflection measurements and the FWD load. Similar results were also found by Owusu-Antwi (Ref 25), who indicated that the coefficient of variation in the response of the pavement for each of the drop heights decreases at higher load levels, as shown in Figure 3.5. Using deflections measured at higher load levels for structural evaluation of pavements was also recommended by Bush (Ref 26). Therefore, the deflections measured at drop height 4 were used for all the analyses undertaken in the remainder of this report. Furthermore, for the convenience of analysis, all the results in this report are based on the transformed 9-kip deflections, unless otherwise specified.

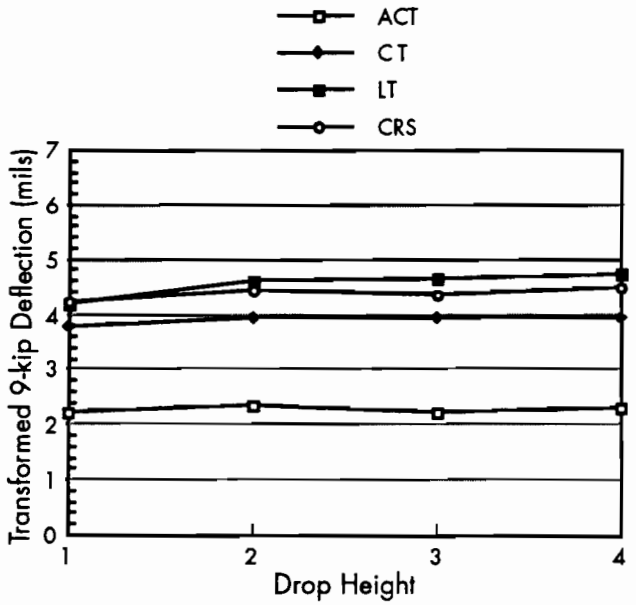

Figure 3.3 Effect of drop height on the transformed deflection for CRCP with a LS coarse aggregate

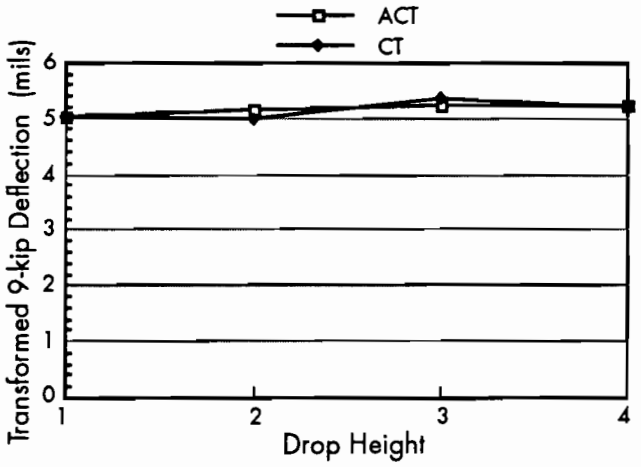

Figure 3.4 Effect of drop height on the transformed deflection for CRCP with a SRG coarse aggregate

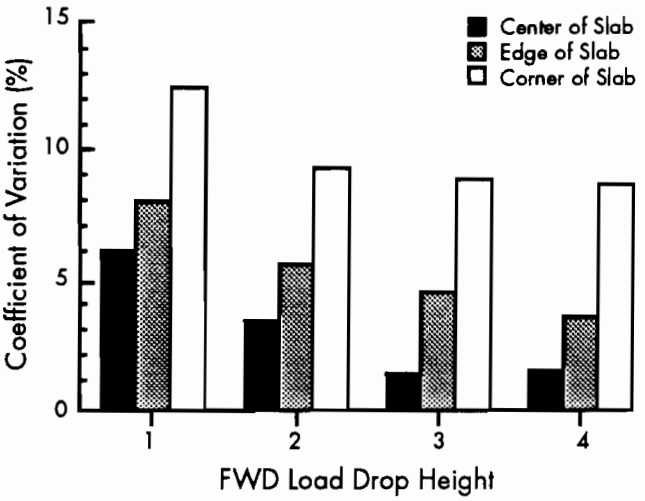

Figure 3.5 Variability in pavement response at each FWD load drop height (Ref 25)

3.2.3 *Load Transfer at Transverse Cracks in CRCP*

Continuously reinforced pavements are constructed without transverse joints; therefore, volume change stresses caused by shrinkage and temperature differentials are dissipated by the formation of transverse cracking. Longitudinal reinforced steel is used in this concrete pavement type to keep the transverse cracks tightly closed so that effective load transfer can be maintained at the cracks.

Load transfer at cracks in CRC pavement, as defined herein, is the ability of that pavement to transfer loads across transverse cracks from one slab of pavement to another. If a CRC pavement can maintain good load transfer (about 100 percent) at the cracks, it usually shows good pavement performance. However, as the load repetitions increase and the pavement ages, the load transfer at the cracks will decrease until a loss of load transfer is experienced. This loss of load transfer is one of the main causes of punchout distress in CRC pavements. Therefore, an assessment of load transfer at the cracks of in-service CRC pavements across Texas would provide valuable information regarding CRCP performance.

3.2.3.1 *Selection of a Procedure for Assessment of Load Transfer at Cracks*

The load transfer across joints in jointed pavement has been studied by many investigators (Refs 18, 25, 27, 28, and 29; a good summary of the procedures for assessment of load transfer across joints can be found in Ref 25). However, for the evaluation of load transfer across the cracks in CRCP, no universally accepted procedure is

available. In this section, three procedures for the assessment of load transfer across joints were selected for evaluation. From these three procedures, an appropriate one will be chosen for use in the assessment of load transfer at the cracks in the in-service CRC pavements.

The first procedure considered was developed by Teller and Sutherland, which is referred to as the Teller procedure (Ref 28). In this procedure, load transfer across the joint is evaluated in terms of a deflection ratio, which is defined in Equation 3.1 as

$$LTE = \frac{2W_u}{W_u + W_l} \times 100\% \qquad (3.1)$$

where

LTE = load transfer efficiency, percent;
W_u = deflection on an unloaded slab; and
W_l = deflection on an adjacent loaded slab.

The concept of this procedure is illustrated in Figure 3.6. If the deflection at an unloaded slab is zero, the LTE is equal to zero, which means that no load is transferred from the loaded slab to the adjacent unloaded slab. If the deflection at the unloaded slab is the same as that at the adjacent loaded slab, namely $W_u = W_l$, the procedure yields a value of 100 percent load transfer efficiency. This means that 50 percent of the applied load at the loaded slab is transferred across the joints to the adjacent unloaded slab. This may be considered as a perfect load transfer condition.

The second procedure assessing joint efficiency uses the following formula:

$$LTE = \frac{W_u}{W_l} \times 100\% \qquad (3.2)$$

This procedure was from Darter (Ref 6). Equation 3.2 has the same boundary condition as the Teller procedure; that is, when the unloaded slab has zero deflection, the procedure gives zero for the load transfer efficiency, and yields 100 percent load transfer efficiency if the deflections at both sides of the joints are the same. This procedure is referred to as the Darter procedure.

The third procedure considered was developed by Ricci (Ref 31) and later modified by Owusu-Antwi (Ref 25). For upstream FWD loading, as shown in Figure 3.7a, the load transfer across the joint is defined as a ratio of the deflection at sensor 2 to that at sensor 3. Mathematically, this ratio can be expressed (LTE_u) as follows:

$$LTE_u = \frac{W2}{W3} \times 100\% \qquad (3.3)$$

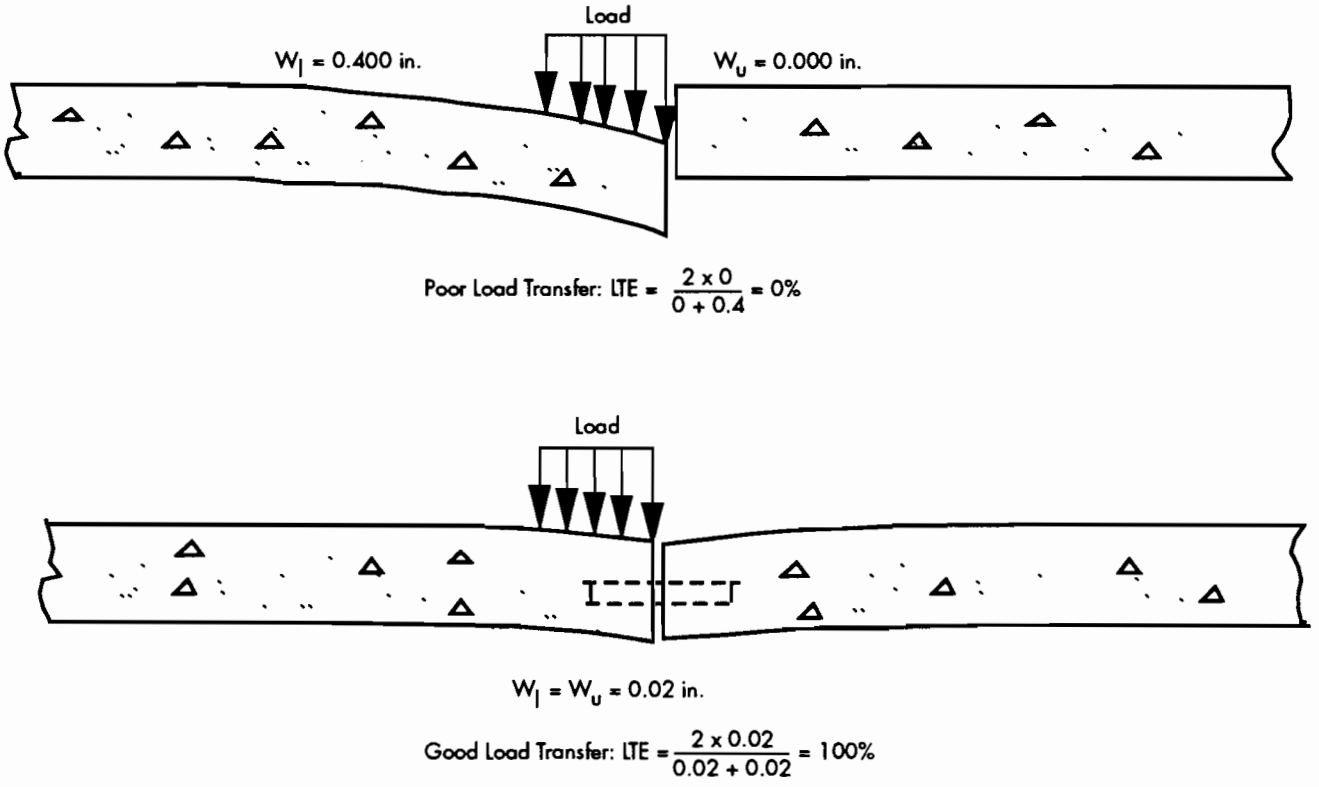

Figure 3.6 Illustration of Teller procedure for the assessment of load transfer

where

LTE_u = load transfer efficiency for upstream loading;
W2 = deflection measured at sensor 2 for upstream loading; and
W3 = deflection measured at sensor 3 for upstream loading.

For downstream FWD loading, as shown in Figure 3.7b, the load transfer across the joint is calculated in terms of the following formula:

$$LTE_d = \frac{W3}{W2} \times 100\% \qquad (3.4)$$

where

LTE_d = load transfer efficiency for downstream loading;
W2 = deflection measured at sensor 2 for downstream loading; and
W3 = deflection measured at sensor 3 for downstream loading.

In the case of full load transfer at the joint, the deflections at sensor 2 and sensor 3 will be the same; therefore, both LTE_u and LTE_d will yield a value of 100 percent load transfer efficiency. In the case of no load transfer, the deflection at sensor 2 for upstream loading and the deflection at sensor 3 for downstream loading will be zero, and the LTE_u and LTE_d will both yield zero for the load transfer efficiency. This procedure is referred to as the Ricci procedure.

An evaluation of the above procedures was performed using FWD data obtained from the study conducted by Morales-Valentin (Ref 32). These FWD data were collected on an in-service 10-inch jointed pavement on US 90 in Beaumont, Texas. Three pavement sections were selected for the measurements, but only two sections have detailed temperature measurements. These two sections are labeled as Slabs 1 and 2, respectively, as schematically shown in Figure 3.8. The layout of the test section and station numbers for data collection are also shown in the figure. Each slab includes one joint and one crack. Stations C_u (station at crack for upstream loading) and C_d (station at crack for

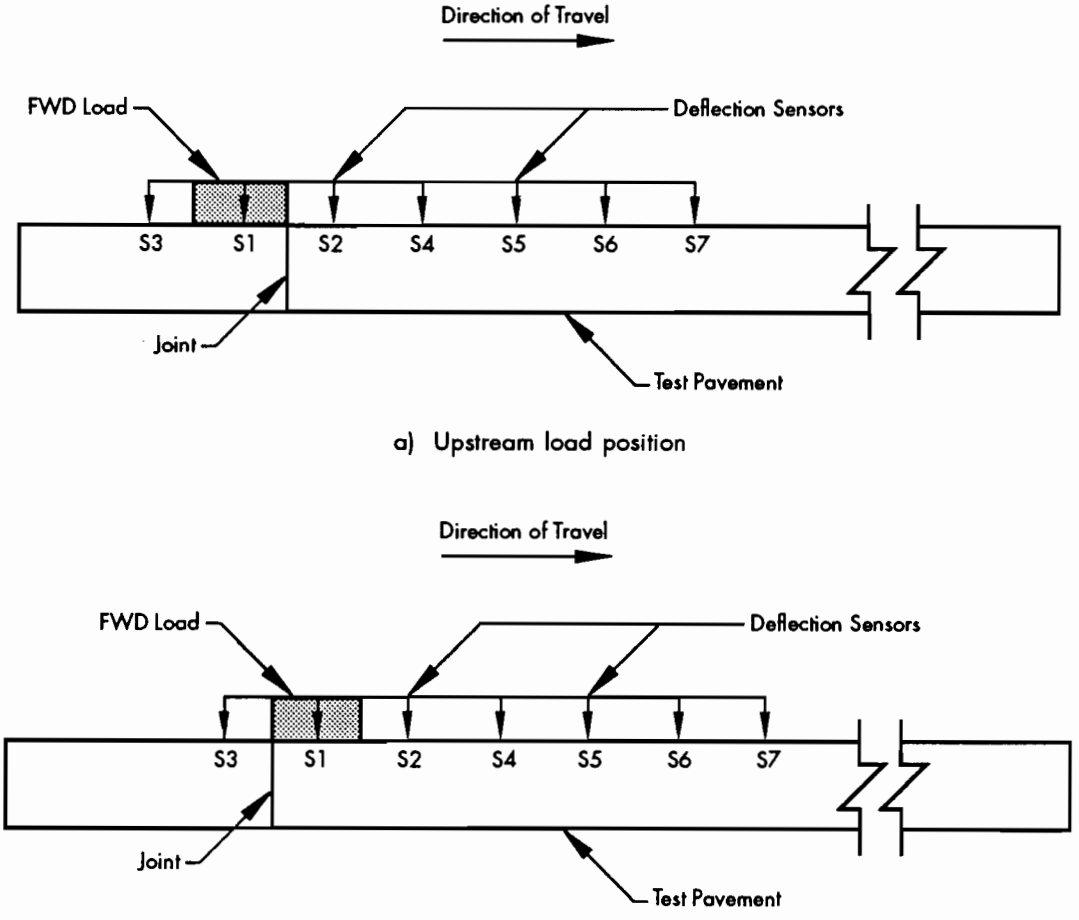

Figure 3.7 FWD load plate and deflection sensor locations (Ref 31)

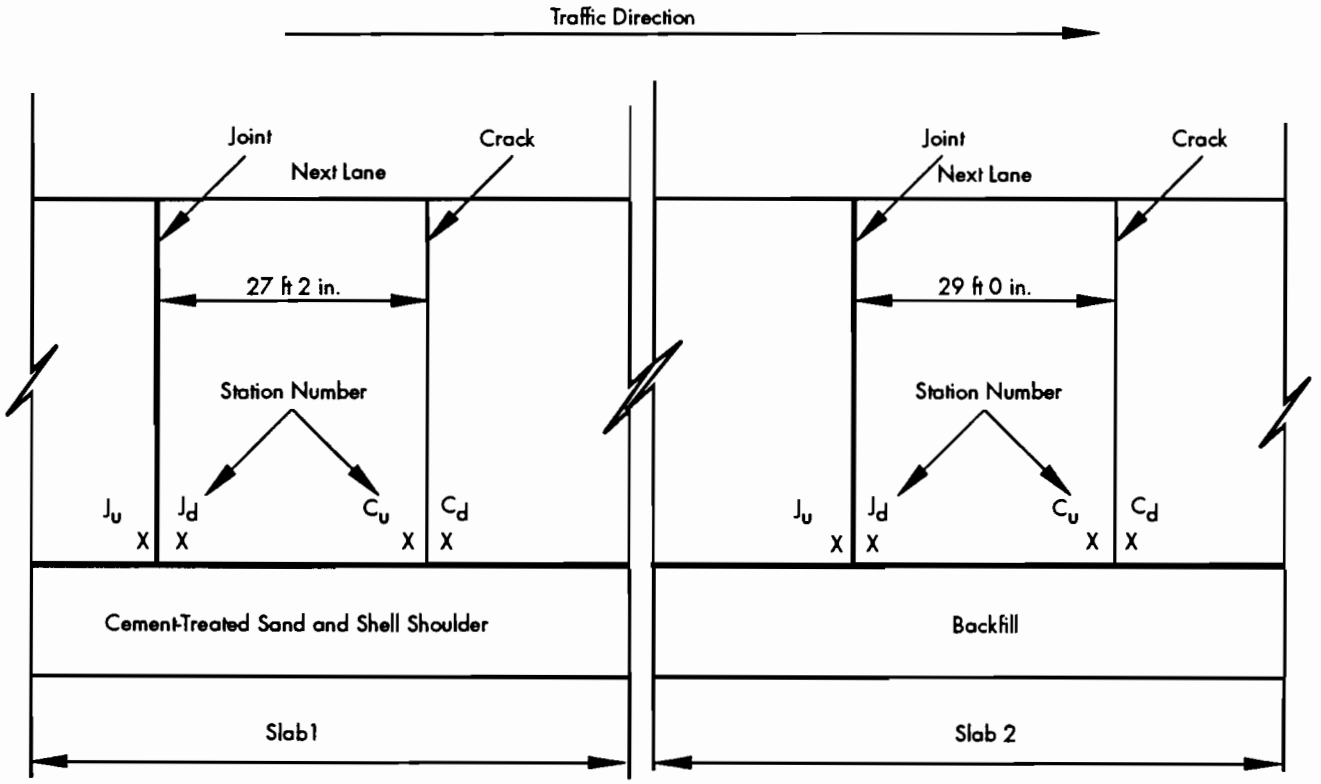

Figure 3.8 Layout of the test section and station numbers

downstream loading) are at the crack, while stations J_u and J_d are at the joint. All the measurements are near the edge. (Detailed information about the measurements on this pavement section can be found in Ref 32.)

Figures 3.9 and 3.10 show the results of the evaluation of the above three procedures for Slabs 1 and 2, respectively. As the two figures indicate, the values of load transfer efficiency given by the Teller and the Darter procedures range from 40 to 100 percent, while load transfer efficiencies from the Ricci procedure are greater than 100 percent for stations C_u and C_d in Slab 1 and for station C_d in Slab 2. A "test of reasonableness" indicates that the Ricci procedure is not useful in the assessment of load transfer, specifically for the assessment of load transfer at the cracks. For a better understanding of these three procedures, a mechanistic analysis is presented below.

As shown in Figure 3.11, only when full moment transfer is maintained at the joint or the crack are the deflections at sensor 2 and at sensor 3 the same. This is a symmetry problem. In this case, the Ricci procedure will give a value of 100 percent for the load transfer efficiency. However, if there is no moment transfer at the joint or crack, but full shear transfer is maintained, the deflection basin would look like that shown in Figure 3.12. This is also a symmetry problem. In this latter case, the deflection at sensor 3 is always greater than that at sensor 2, and the Ricci procedure will give a value of more than 100 percent for the load transfer efficiency.

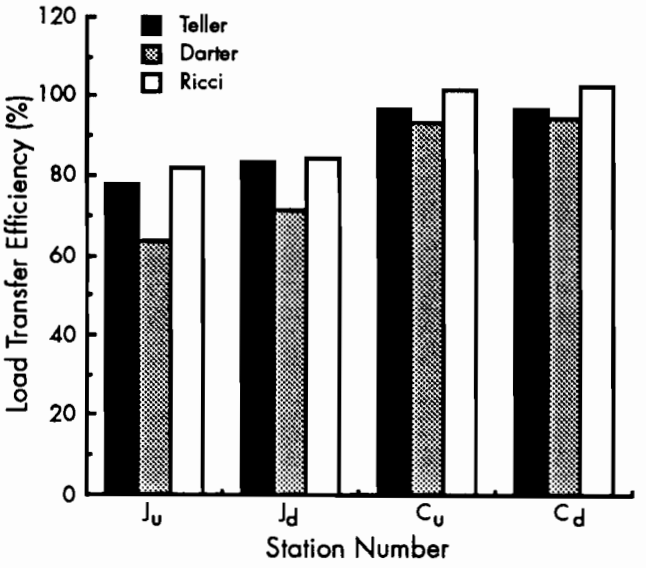

Figure 3.9 Comparison of Teller, Darter, and Ricci procedures, Slab 1

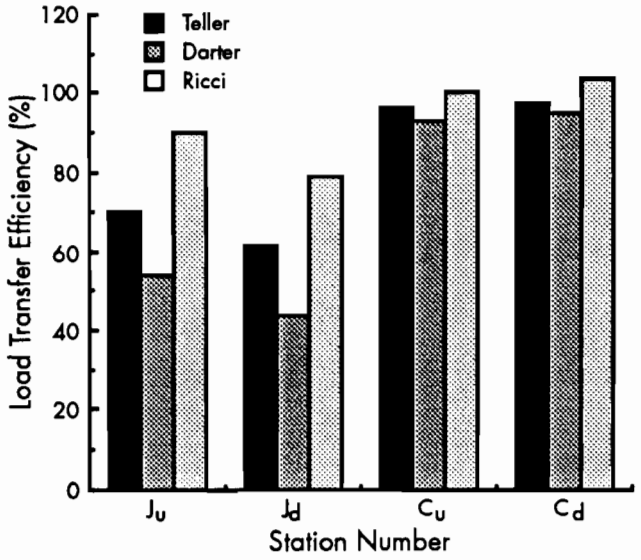

Figure 3.10 Comparison of Teller, Darter, and Ricci procedures, Slab 2

Furthermore, if we evaluate the Teller and the Darter procedures for the full moment transfer case as shown in Figure 3.11, we find that both procedures will yield a value of lower than 100 percent load transfer efficiency. This results from the fact that deflection at the adjacent unloaded slab is less than that at the loaded slab, namely, $W_u < W_l$. However, both the Teller and the Darter procedures would give a value of 100 percent load transfer efficiency for the full shear load transfer case, as shown in Figure 3.12. In the case in which neither moment transfer nor shear transfer is maintained at the joint or the crack, as shown in Figure 3.13, both the Teller and the Darter procedures yield zero value for the load transfer efficiency, as does the Ricci procedure.

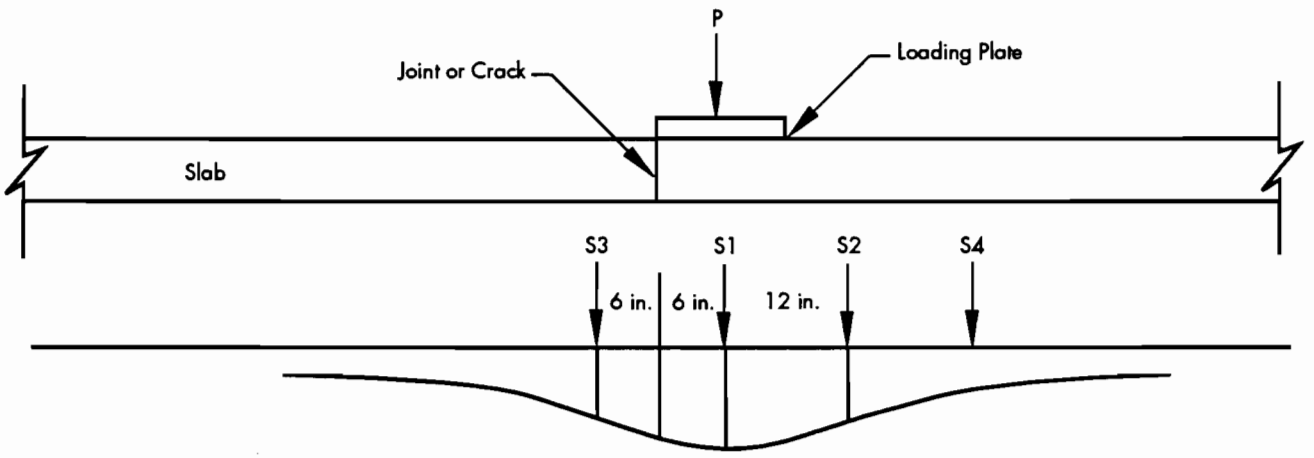

Figure 3.11 Deflection basin for the case of full moment transfer

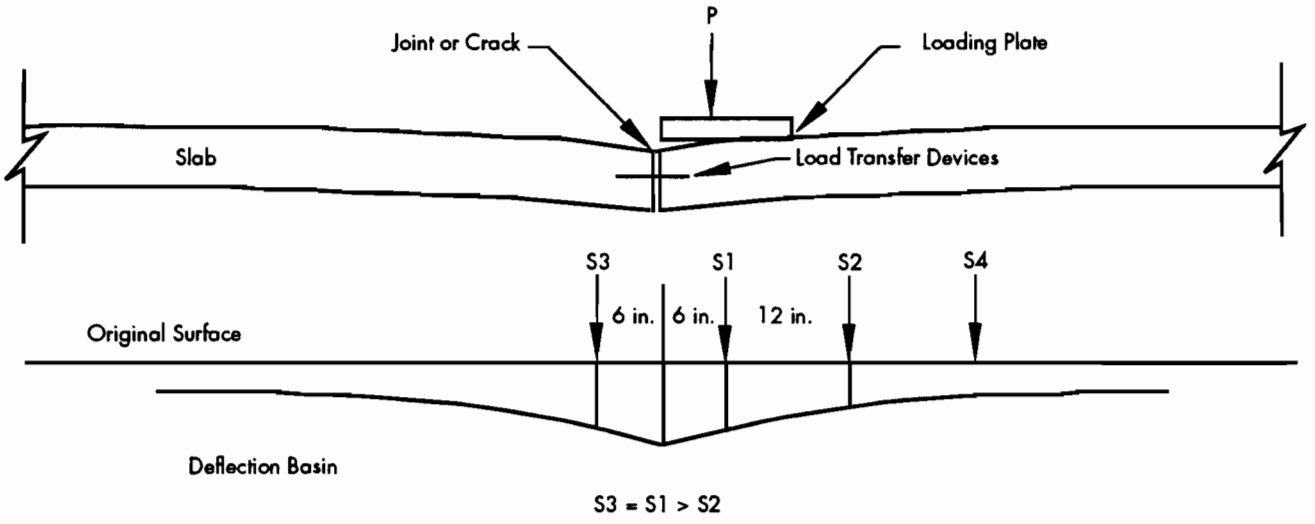

Figure 3.12 Deflection basin for the case of full shear transfer

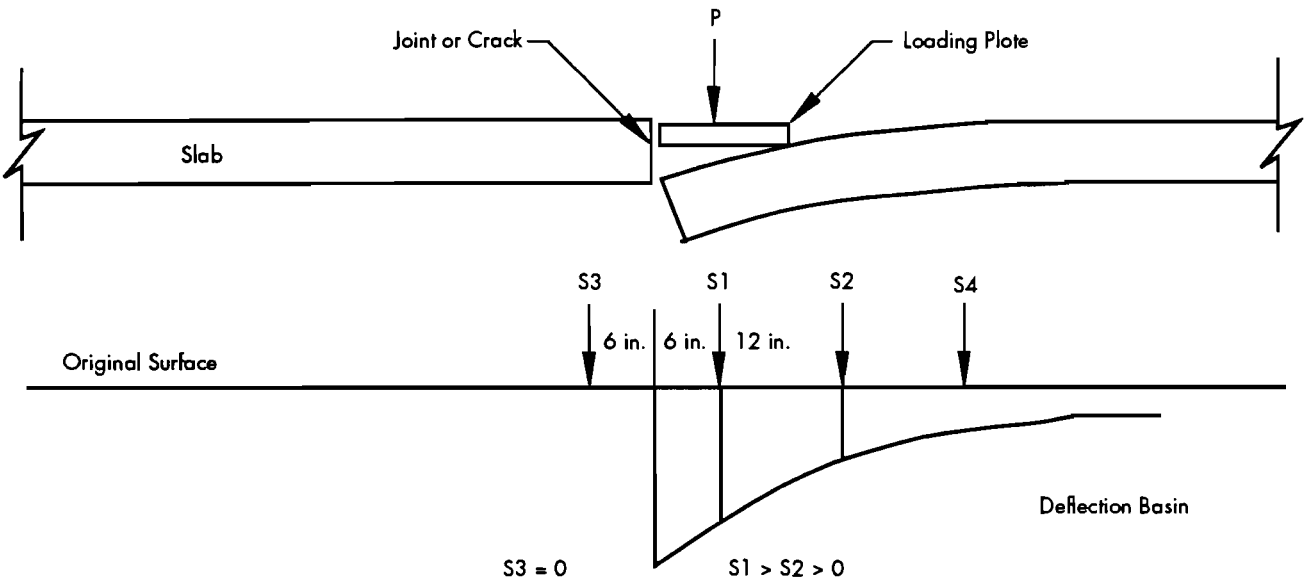

Figure 3.13 Deflection basin for the case of no load transfer

Since both the Teller and the Darter procedures meet the criteria as given by their definitions (load transfer efficiency ranges from 0 to 100 percent), further comparison of these two procedures was made. It is interesting to note that both procedures use the same measurements, but the forms for expressing the load transfer efficiency are different. Therefore, an analytical comparison was performed.

Supposing that ΔLTE is the difference in load transfer efficiency between the Teller and the Darter procedures, we can express ΔLTE as

$$\begin{aligned}\Delta LTE &= LTE_T - LTE_D = \frac{2W_u}{W_u + W_l} - \frac{W_u}{W_l} \\ &= \frac{2W_uW_l - W_uW_l - W_uW_u}{W_l(W_l + W_u)} \\ &= \frac{W_uW_l - W_uW_u}{W_l(W_l + W_u)} \\ &= \frac{W_u(W_l - W_u)}{W_l(W_l + W_u)} \\ &= LTE_D \frac{(W_l - W_u)}{(W_l + W_u)}\end{aligned} \tag{3.5}$$

where

LTE_T = LTE from Teller procedure; and
LTE_D = LTE from Darter procedure.

Since $W_l \geq W_u > 0$, $W_l - W_u \geq 0$, therefore, ΔLTE ≥ 0. Only when $W_l = W_u$, then ΔLTE = 0; or when $W_u = 0$, then ΔLTE = 0.

This information clearly indicates that the Darter procedure will always give a lower value of load transfer efficiency than the Teller procedure if $W_l \neq W_u$ or $W_u \neq 0$. Only for two extreme load transfer conditions—zero load transfer and full shear transfer—do the Teller and the Darter procedures give the same results. In other words, they have the same boundary conditions.

Considering a set of measurements as shown in Table 3.1, values from the Teller and the Darter procedures can be obtained, and an intuitive comparison between the two procedures can be made as shown in Figure 3.14. As illustrated in this figure, the Darter procedure gives a lower value for the load transfer efficiency than does the Teller procedure. A relationship between these two procedures may also be established, as shown in the figure.

Further, if the load transfer is defined in terms of the percent transfer of applied load, the following formula is applicable:

Table 3.1 Comparison of Teller and Darter procedures

Case	W_u	W_l	$W_u + W_l$	Teller LTE (%)	Darter LTE (%)
1	0.00	0.10	0.10	0	0
2	0.01	0.09	0.10	20	11
3	0.02	0.08	0.10	40	25
4	0.03	0.07	0.10	60	43
5	0.04	0.06	0.10	80	67
6	0.05	0.05	0.10	100	100

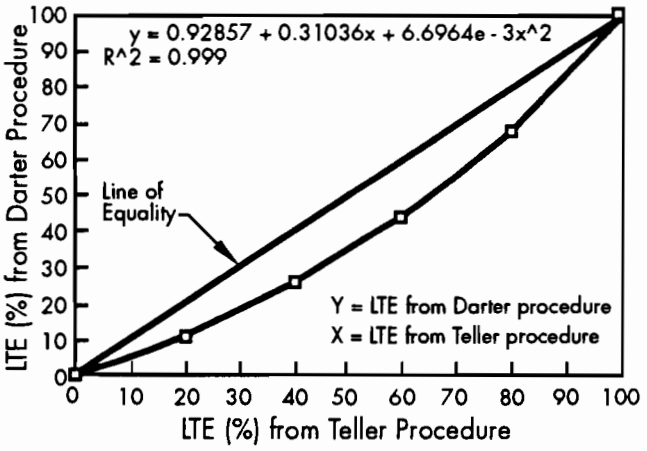

Figure 3.14 Relationship between Teller and Darter procedures

$$LTE_P = \frac{2P_u}{P} \times 100\% \qquad (3.6)$$

where

LTE_P = load transfer efficiency in terms of percentage of actual load transferred,

P_u = magnitude of load transferred from the loaded slab to the unloaded slab, and

P = total applied load at the loaded slab.

When one-half of the total applied load is transferred from the loaded slab to the unloaded slab, namely $P_u = 0.5$ P, then $LTE_P = 100$ percent. When $P_u = 0.2$ P, then $LTE_P = 40$ percent. Obviously, the value of LTEP doubles the actual percentage of total load transferred.

If it is assumed that the deflection is proportional to the applied load, the Teller procedure gives exactly the same value as Equation 3.6. From this standpoint, the Teller procedure is better for characterizing the load transfer across the joints and cracks. On the other hand, one can still use other procedures by calibrating the actual values with the calculated values from those procedures, assuming Equation 3.1 is correct. In conclusion, the Teller procedure was selected for use in this study for the evaluation of load transfer at the cracks for the in-service CRC pavements.

3.2.3.2 Temperature Differential Effect on Load Transfer Evaluation

Many studies have shown that the temperature differential has a significant effect on FWD deflection measurements, especially measurements near the edge and joints (Refs 5, 32, and 33). The temperature differential (DT) discussed here is defined as the difference between the temperature at the top and at the bottom of a pavement (Ref 32). The data collected from Slab 1 (as shown in Figure 3.8) were therefore analyzed to determine the effect of temperature differential on load transfer evaluation.

Figure 3.15 presents the plots of load transfer efficiencies (calculated from three procedures) versus temperature differential at the joint, while Figure 3.16 shows the plots at the crack. As shown in Figure 3.15, load transfer does vary at the joint with temperature differential, particularly from about -5 to +5 degrees Fahrenheit. As the temperature differential becomes greater than 5 degrees Fahrenheit, the DT effect is not significant. This result could be caused by the expansion of two pavement slabs and/or by the pavement warping downward. However, as shown in Figure 3.16, the effect of temperature differential on load transfer evaluation at the cracks is not significant. This condition could be because the cracks are held so tightly that the effect of temperature differential on load transfer evaluation is not significant. A recent study conducted by CTR confirms this to be the case (Refs 25 and 34). Therefore, the effect of temperature differential on the evaluation of load transfer at the cracks in the in-service CRC pavements was not considered.

3.2.3.3 Results of Load Transfer Evaluation at the Cracks in In-Service CRCP

The statewide FWD measurements were taken using two types of geophone configurations, termed Types A and B, as shown in Figures 3.17 and 3.18, respectively. When a Type A geophone configuration was used for deflection measurements, the load transfer efficiencies at stations 1 and 3 (refer to Figure 3.2) were averaged to represent the load transfer efficiency for the crack between stations 1 and 3.

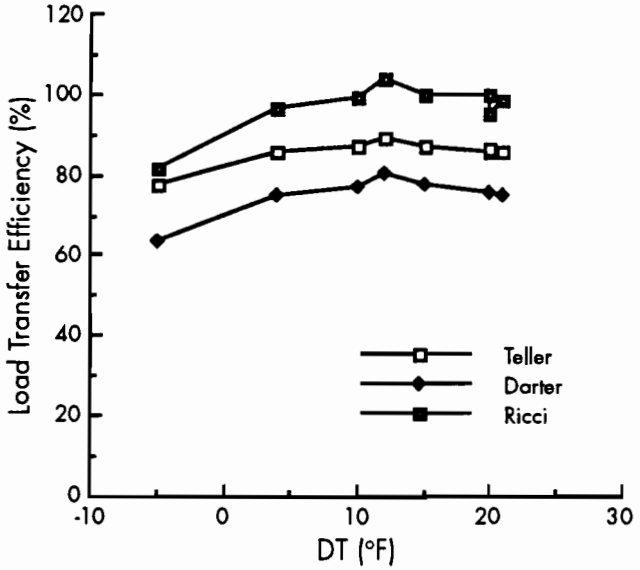

Figure 3.15a Effect of temperature differential (DT) on load transfer evaluation at station J_u, Slab 1

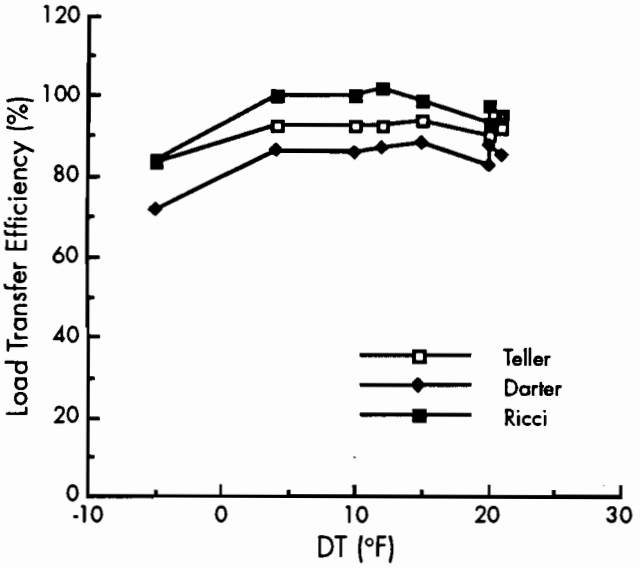

Figure 3.15b Effect of temperature differential (DT) on load transfer evaluation at station J_d, Slab 1

Suppose that X_i (i = 1, 2, 3, to n) represents the *ith* data point of load transfer efficiency; then, the mean value of n data points is calculated as

$$\overline{X} = \frac{1}{n}\sum_{i=1}^{n} x_i \tag{3.7}$$

The standard deviation is determined using the following formula:

$$STD = \sqrt{\frac{\sum_{i=1}^{n}(x_i - \overline{x})}{n-1}} \tag{3.8}$$

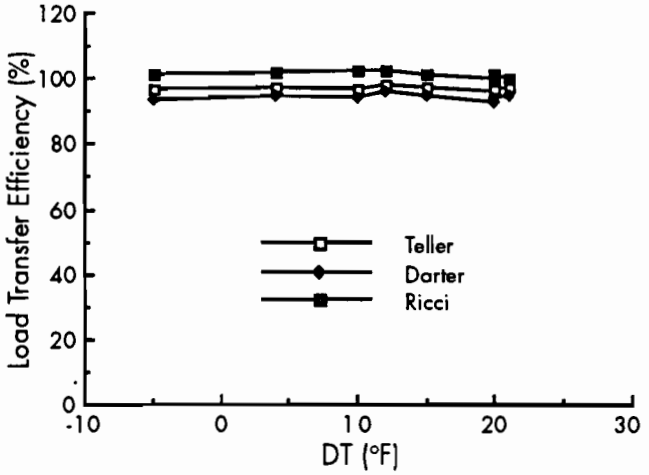

Figure 3.16a Effect of temperature differential (DT) on load transfer evaluation at station C_u, Slab 1

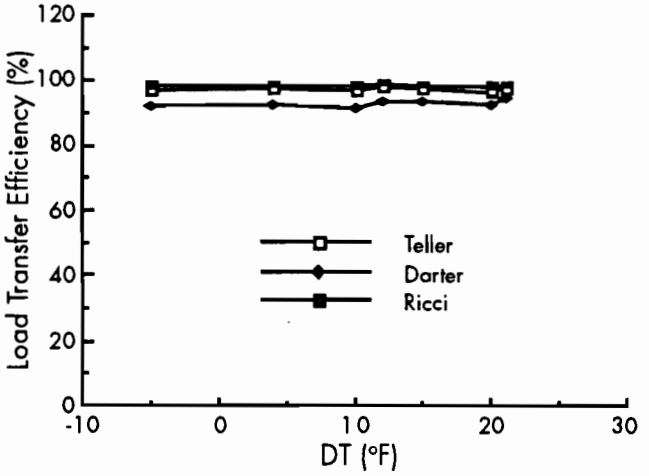

Figure 3.16b Effect of temperature differential (DT) on load transfer evaluation at station C_d, Slab 1

and the coefficient of variation is defined as

$$COV = \frac{STD}{\overline{X}} \tag{3.9}$$

The results of the evaluation of load transfer at the cracks in the in-service CRC pavements are presented in terms of groups that have three different types of thickness and two types of pavement shoulder. Figure 3.19 shows the plot of mean load transfer efficiency. Figures 3.20 and 3.21 present the plots of the standard deviation and the coefficient of variation of the load transfer efficiency, respectively. Table 3.2 shows the number of data points used for the calculation.

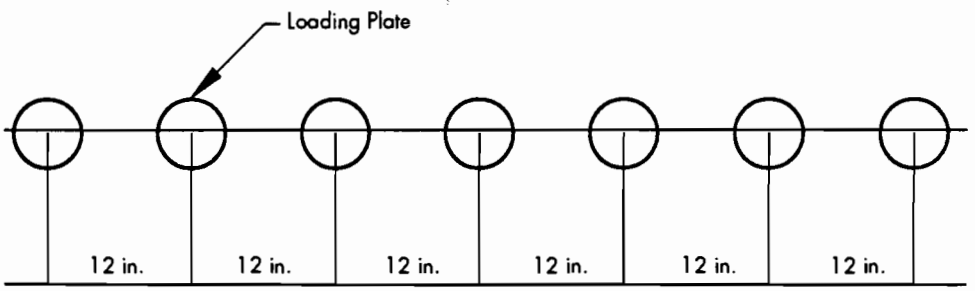

Figure 3.17 Layout of geophone configuration A (Ref 24)

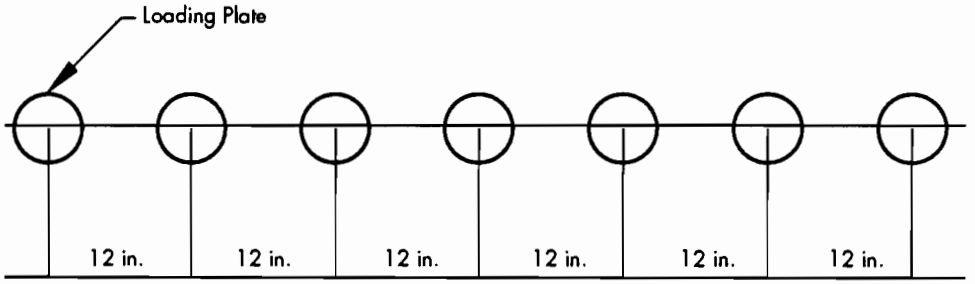

Figure 3.18 Layout of geophone configuration C (Ref 24)

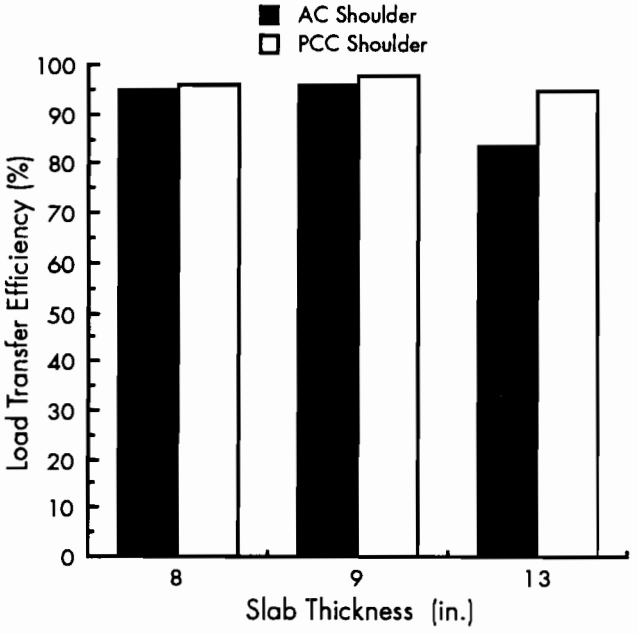

Figure 3.19 Load transfer efficiency at the cracks in CRC pavements

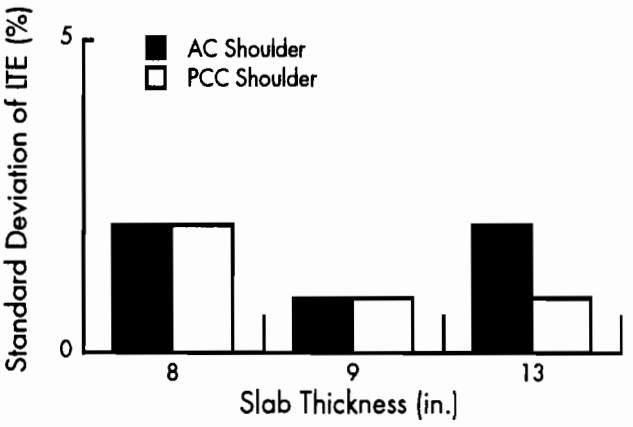

Figure 3.20 Standard deviation of LTE at the cracks in CRC pavements

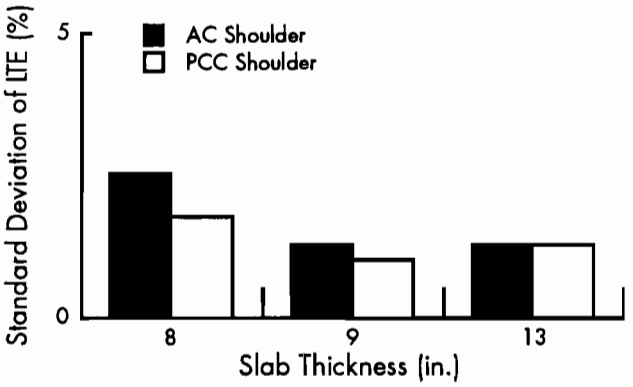

Figure 3.21 Variability of load transfer efficiency at the cracks in CRC pavements

Table 3.2 Number of data points for calculation of the LTE

Shoulder Type	AC			Tied PCC		
Slab thickness (in.)	8	9	13	8	9	13
Number of observations	408	70	5	56	15	27

As observed in Figure 3.19, the mean values of load transfer efficiency are around 95 percent for all the groups except for the 13-inch slab pavement group with an AC shoulder. In addition, the standard deviations are very small (see Figure 3.20), and the coefficients of variation of LTE are less than 5 percent (see Figure 3.21). These results indicate that the in-service CRC pavements in Texas still have very good load transfer at the cracks. The results given in Section 3.2.4 also support this conclusion.

As can also be seen from Figures 3.19 to 3.21, pavements with a tied PCC shoulder have a higher value of load transfer efficiency than those with an AC shoulder. The coefficients of variation of LTE for pavements with a tied PCC shoulder are also lower than those with an AC shoulder. This information indicates that a tied PCC shoulder assists the pavement in maintaining load transfer.

The cause of the unexpected results of load transfer efficiency for the 13-inch pavement group is not clear, but is probably a result of the small number of available sections having this thickness. It is expected that the load transfer value for the 13-inch group will be greater than for the 8-inch pavement group because greater thicknesses are believed to have better load transfer ability. Since only five data points were collected, no further conclusion can be made regarding this pavement group. Therefore, this 13-inch pavement group will not be discussed in the following analyses and conclusions in this chapter (though the results will be shown).

3.2.4 *Difference in Deflections at the Corner of the Crack and at Mid-Span between the Cracks*

Load transfer efficiencies at the cracks were evaluated in the above section. This section evaluates the difference between deflections collected at the corner (formed by the pavement edge and the crack) and those collected at the pavement edge (but mid-span between the cracks). Using Figure 3.2, this difference can be defined as follows:

$$R_{ce} = \frac{\text{Deflection at Station 3}}{\text{Deflection at Station 4}} \qquad (3.10)$$

Basically, if there is some loss of load transfer at the crack, the deflection at the crack will be greater than at the point of mid-span between the cracks. If the deflections are the same, the crack has a very good load transfer. It can then be assumed that there is no loss of load transfer at the crack. Therefore, the pavement could be treated as a continuous slab in the longitudinal direction.

Figure 3.22 presents the mean values of R_{ce} for various groups of pavements in terms of slab thickness and pavement shoulder types. As the figure shows, the mean values of R_{ce} for all the pavement groups are almost equal to 1. Therefore, these results support the conclusion of Section 3.2.3 that approximately 100 percent load transfer is maintained. The standard deviation of R_{ce} is depicted in Figure 3.23.

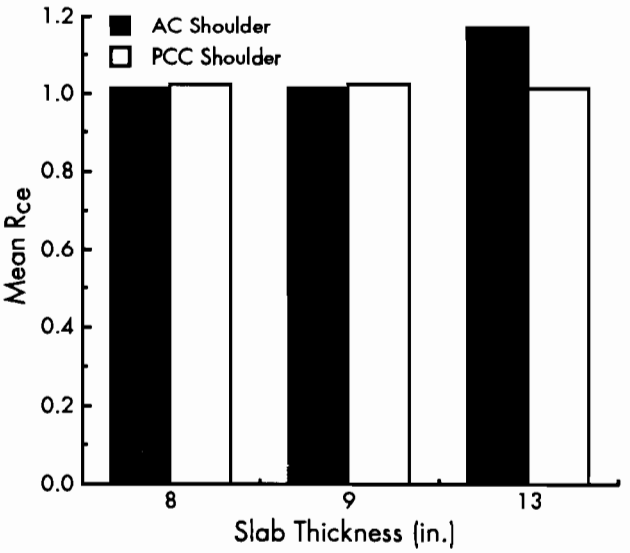

Figure 3.22 Mean value of R_{ce} for CRC pavements

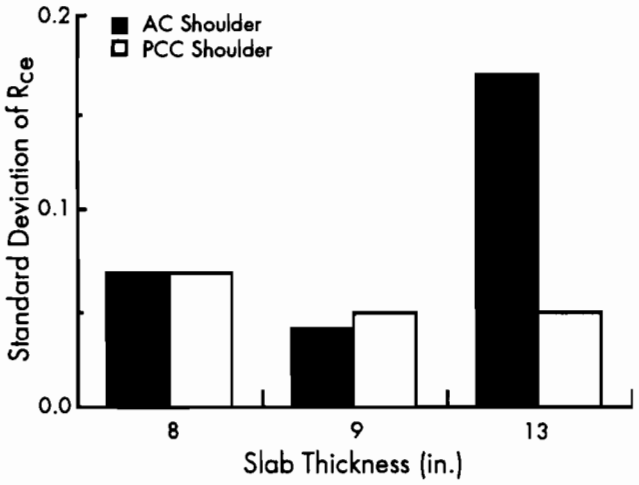

Figure 3.23 Standard deviation for R_{ce} for CRC pavements

3.2.5 *Difference in Deflections between the Pavement Edge and Interior*

The difference in deflection between the pavement edge and the interior is defined as follows:

$$R_{ei} = \frac{\text{Deflection at Station 4}}{\text{Deflection at Station 5}} \qquad (3.11)$$

For this evaluation, the effect of temperature differential on the FWD measurements was considered in that deflections at station 4 (near the edge) were corrected to a standard condition of zero temperature differential. (A detailed description of the temperature differential correction on the deflection measurements is presented in Chapter 5.)

The mean values of the deflection ratio, R_{ei}, are shown in Figure 3.24, and the standard deviations of R_{ei} are shown in Figure 3.25. As shown in Figure 3.24, the mean values of R_{ei} for pavements with an AC shoulder range from 1.2 to 1.7—higher values than for pavements with a tied PCC shoulder. These data indicate the effect of a tied PCC shoulder on reducing edge deflections. A comparison of the mean values of R_{ei} between different slab thicknesses indicates that R_{ei} decreases as slab thickness increases.

3.2.6 *Statistics of Deflections from In-Service CRCP*

The mean, the standard deviation, and the coefficient of variation of the deflections measured at stations 1, 2, 3, 4, and 5 were also determined and are presented in Table 3.3. As seen from part (a) of Table 3.3, the means of the deflections at stations 1, 2, 3, and 4 are almost the same. The maximum difference in the mean deflections between these four stations is less than 5 percent of the minimum mean deflection. This indicates that the load transfer at the cracks is very good. Obviously, the means of the deflections in the interior of the pavement are less than those near the edge and those at the corner near the cracks. However, the coefficients of variation of the interior deflections are larger, which could be due to the fact that the pavement sections studied are from different subbase and soil conditions. As expected, the means of the deflections decrease as the slab thickness increases, as do the coefficients of variation.

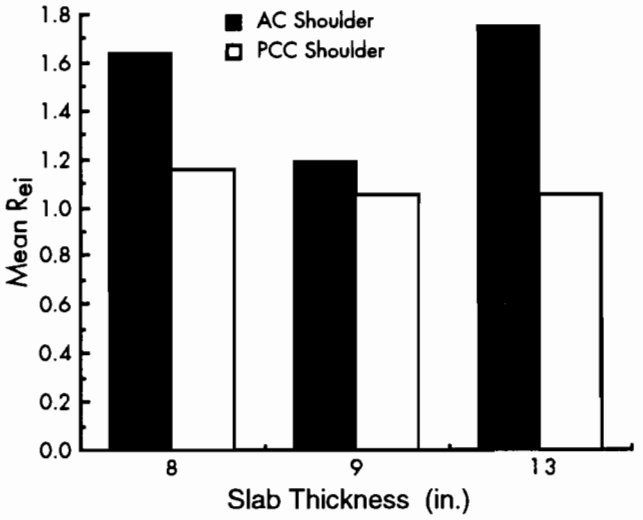

Figure 3.24 Mean value of R_{ei} for CRC pavements

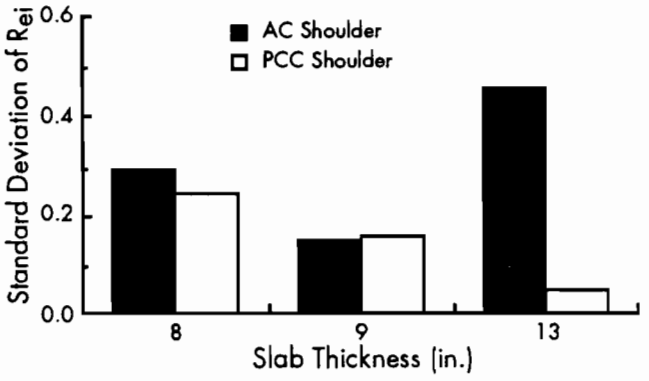

Figure 3.25 Standard deviation of R_{ei} for CRC pavements

3.3 COMPARISON OF DEFLECTIONS BETWEEN IN-SERVICE CRCP AND JCP

Jointed concrete pavement (JCP) and CRC pavement are two of the most widely used rigid pavement types in the United States. A comparison of responses (e.g., deflections) between CRC pavement and jointed concrete pavement, presented

below, will perhaps enhance our understanding of CRC pavement performance.

The jointed pavement used for comparison is a test slab of jointed pavement, which has load transfer devices at the joint. A layout of this test slab, the test paths, and its location is shown in Figure 3.26 (the data used in the comparison are from Ref 32). Only the open-joint condition was considered.

The following deflection equations for the different load positions in the test pavement were derived in terms of temperature differential from the measurements in the test slab:

(1) Interior deflection

$$W_i = 2.16 \times 10^{-0.0011DT} \quad (3.12)$$
$$R^2 = 0.69$$

(2) Edge deflection

$$W_e = 4.67 \times 10^{-0.0053DT} \quad (3.13)$$
$$R2 = 0.85$$

(3) Joint deflection

$$W_J = 5.02 \times 10^{-0.0069DT} \quad (3.14)$$
$$R^2 = 0.97$$

(4) Corner deflection

$$W_c = 13.15 \times 10^{-0.0114DT} \quad (3.15)$$
$$R^2 = 0.96$$

where

DT = temperature at the top minus temperature at the bottom of slab (°F)
Wi = deflection at the intersection of test path B and position F,
We = deflection at the intersection of test path A and position F,
W_J = deflection at the intersection of test path B and position E, and
W_c = deflection at the intersection of test path A and position E.

It is noted that Equation 3.10 has a low value of R^2, but the coefficient of DT is also very small. In other words, the effect of temperature differential on the interior deflections is very small.

With these equations available, the deflections at the standard condition of zero temperature differential can easily be obtained. The results of the deflection ratios of R_{ce}, R_{ei}, and R_{ci} (note: R_{ci} = ratio of the deflection at station 3 to that at station 5) for the jointed pavement, along with the results from the in-service CRCP, are presented in Table 3.4.

Table 3.3 Statistics of the response of CRCP

(a) Mean Deflections (mils)	Slab Thickness (in.)	Station 1	2	3	4	5
AC Shoulder	8	4.83	5.00	4.80	4.80	3.77
	9	2.73	2.77	2.73	2.72	2.66
	13	2.06	2.55	2.24	2.03	1.35
PCC Shoulder	8	5.07	5.11	5.09	5.04	4.43
	9	4.12	4.21	4.12	4.04	3.91
	13	1.45	1.50	1.45	1.44	1.37

(b) Standard Deviation (mils)	Slab Thickness (in.)	Station 1	2	3	4	5
AC Shoulder	8	1.64	2.70	1.64	1.67	1.12
	9	0.41	0.43	0.41	0.40	0.38
	13	0.59	0.75	0.61	0.57	0.21
PCC Shoulder	8	1.48	1.47	1.49	1.52	1.46
	9	0.49	0.52	0.53	0.49	0.47
	13	0.13	0.17	0.13	0.14	0.10

(c) Coefficient of Variation (%)	Slab Thickness (in.)	Station 1	2	3	4	5
AC Shoulder	8	34	54	34	35	30
	9	15	15	15	15	14
	13	29	29	27	28	15
PCC Shoulder	8	29	29	29	30	33
	9	12	12	13	12	12
	13	9	12	10	10	8

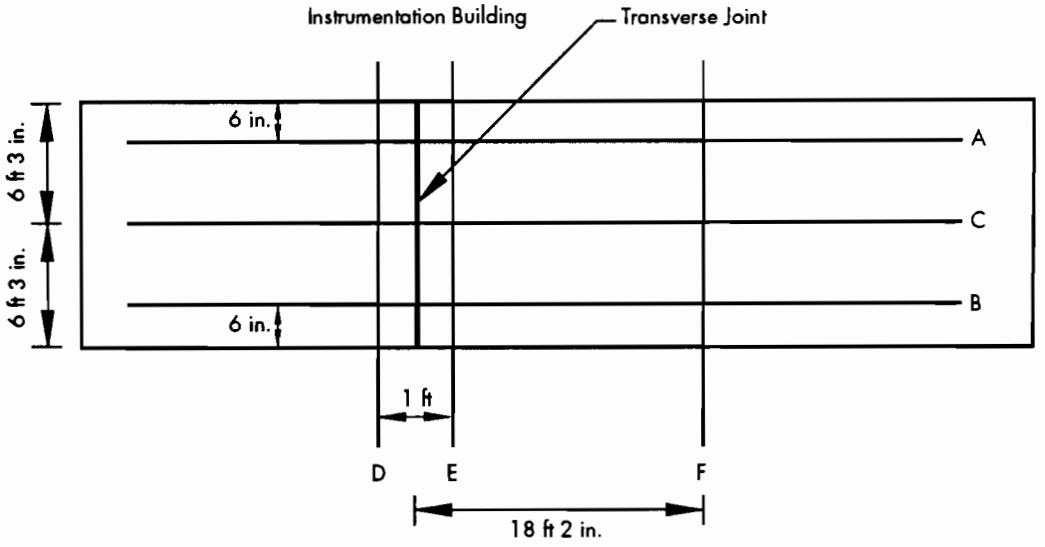

Wheel Paths: A: Side of the Slab Without Void Underneath
B: Side of the Slab With Void Underneath
C: Centerline of the Slab

Locations: D: Upstream With Respect to the Transverse Joint
E: Downstream With Respect to the Transverse Joint
F: Midspan

Figure 3.26 Layout of test pavement and test paths and locations (Ref 32)

As noted in the table, the values of these deflection ratios for the CRC pavement are much lower than those from the test slab. This evidence may indicate that CRC pavements exhibit better performance from a structural point of view. However, this comparison is based on limited data from a test slab. Further comparison of data from in-service jointed pavements with those from in-service CRC pavements is recommended.

Table 3.4 Comparison of deflections between CRCP and JCP

Shoulder Type	R_{ci}	R_{ei}	R_{ce}
CRCP (D = 8 in.	1.64	1.64	1.01
Jointed Pavement (D = 10 in.)	6.09	2.16	2.82
Percent Difference	310.0	32.0	179.0

$$\text{Percent Diff} = \frac{\text{JCP - CRCP}}{\text{CRCP}} \times 100\%$$

3.4 DEFLECTIONS FROM IN-SERVICE CRCP AND DEFLECTIONS FROM A THEORETICAL MODEL

The Westergaard plate model for a pavement was selected as the theoretical model. Specifically, the following Westergaard deflection equations (Ref 35) were used in calculating deflections to be compared to deflections from the in-service CRCP:

(1) Interior deflection

$$d_i = \frac{P}{8KL^2}\left\{1+\frac{1}{2\pi}\left[\ln\left(\frac{a}{2L}\right)+\gamma-1.25\right]\left(\frac{a}{L}\right)^2\right\} \quad (3.16)$$

(2) Edge deflection

$$d_e = \frac{P\sqrt{(2+1.2\mu)}}{ED^3K}\left[1+(0.76+0.4\mu)\left(\frac{a}{L}\right)\right] \quad (3.17)$$

(3) Corner deflection

$$d_c = \frac{P}{KL^2}\left[1.1-0.88\left(\frac{a_1}{L}\right)\right] \quad (3.18)$$

The concrete modulus of elasticity, modulus of subgrade reaction, and Poisson's ratio were fixed during the calculation of the analytical results. Table 3.5 summarizes the constant values used.

Table 3.5 Summary of the constants

Modulus of Elasticity E (psi)	Poisson's Ratio (μ)	Contact Radius a (in.)	Load P (lbs)
5,000,000	0.2	5.9	9,000

The 8-inch CRC pavement group with an AC shoulder was selected for the comparison. A variation of the interior conditions can be simulated by varying the modulus of subgrade reaction in the theoretical model. The calculated results, along with the deflection response of the in-service CRCP, are presented in Table 3.6.

Table 3.6 Response of CRCP and the calculated results from theoretical model, D=8 in. and AC shoulder

	K (pci)	R_{ci}	R_{ei}	R_{ce}	W_i (mils)
Results from theoretical model	50	7.59	3.18	2.39	10.58
	100	7.36	3.11	2.37	7.46
	200	7.11	3.04	2.34	5.25
	400	6.80	2.96	2.30	3.69
	600	6.59	2.89	2.28	3.00
	800	6.43	2.85	2.26	2.59
	1,000	6.27	2.81	2.24	2.31
CRCP response	Mean	1.64	1.64	1.01	3.77
	STD	0.30	0.30	0.07	1.12
	COV	0.18	0.18	0.07	0.30

As seen from Table 3.6, there is tremendous difference in the values of R_{ci}, R_{ce}, and R_{ce} between the field and the analytical results. If we choose the interior deflection as a reference, then the quantitative difference in these ratios can be calculated. The difference can be greater than 100 percent.

3.5 DEFLECTIONS FROM JCP AND DEFLECTIONS FROM THEORETICAL MODEL

Deflections from a test section of in-service jointed pavement (as described in Section 3.3) were compared with deflections from the theoretical model. The Westergaard deflection equations (3.16, 3.17 and 3.18) previously presented were again selected as the theoretical model. A 10-inch slab thickness, and modulus of subgrade reaction ranging from 50 to 1,000 pci, were used in the simulation of the jointed pavement. The results are shown in Table 3.7.

Taking the interior deflection as a reference, it can be seen from Table 3.7 that the differences in results between the jointed pavement and the theoretical model are not very large. It would appear that, based on these results, the Westergaard equations are better able to estimate the deflection response for jointed pavements, as would be expected.

Table 3.7 Response from jointed pavement and the results from theoretical model, D=10 in. and AC shoulder

	K (pci)	R_{ci}	R_{ei}	R_{ce}	W_i (mils)
Results from Theoretical Model	50	7.78	3.23	2.41	7.59
	100	7.58	3.17	2.39	5.35
	200	7.37	3.11	2.37	3.77
	400	7.11	3.04	2.34	2.66
	600	6.94	2.99	2.32	2.16
	800	6.79	2.95	2.30	1.87
	1,000	6.69	2.92	2.29	1.67
JCP Response	Mean	6.09	2.16	2.82	2.16

3.6 SUMMARY

This chapter has assessed the structural conditions of Texas' in-service CRC pavements in terms of (1) load transfer across the cracks, (2) difference between deflections at the corner of the crack and those at the mid-span between the cracks, and (3) difference in deflections between the interior and the edge of the pavement slab. The results show that the CRC pavements in Texas were designed very well, and that the load transfer at the cracks is about 100 percent in terms of load transfer efficiency. Furthermore, comparisons were also made of deflection responses from in-service CRC pavements, from jointed concrete pavements, and from a theoretical model. It was found that the deflection responses from CRC pavements and jointed pavements were quite different, as were the responses from in-service CRC pavements and from the theoretical model.

CHAPTER 4. DEVELOPMENT OF A J-FACTOR MODEL FOR RIGID PAVEMENTS IN TEXAS BASED ON DEFLECTION MEASUREMENTS

4.1 INTRODUCTION

As pointed out in Chapter 2, the AASHTO concept of the load transfer coefficient was expanded in the rigid pavement performance equation to consider load capabilities of various types of pavement structures. The use of the AASHTO guide procedure for the design of rigid pavements, including CRC pavements, requires determining a suitable value for a load transfer coefficient within a given range for corresponding design conditions. However, a method for determining the load transfer coefficient based on field measurements is not available in the AASHTO guide. A rational procedure to obtain the load transfer coefficient based on field measurements is therefore required.

This chapter describes the development of such a rational procedure, namely a J-factor model, for estimating a load transfer coefficient from field measurements on CRC pavements. In addition, a conceptual J-factor model for jointed pavements is presented.

4.2 DEVELOPING A GENERAL MATHEMATICAL FORM OF THE J-FACTOR MODEL

The rigid pavement performance equation in the AASHTO guide was derived from empirical information obtained at the AASHO Road Test (Ref 6). During the development of the equation, an equal ratio of strength to stress was assumed to give equal performance, as defined in Equation 2.13 in Chapter 2. For example, a pavement with less thickness (increased stress) but with an increased flexural strength would show equal performance with another pavement, so long as the ratios between strength and stress were equal. Following this premise, it may also be hypothesized that a change in edge condition or load transfer at the joints/cracks results in a different degree of stress, and, further, results in different performance if other factors are fixed.

Considering Equation 2.13 and supposing the concrete strength is fixed, let S_{LP} be the maximum stress in jointed concrete pavements at the Road Test, $\sigma_{SP\text{-}A}$ be the stress calculated from the Spangler equation for the Road Test conditions, S be the maximum stress for an in-service pavement differing in physical properties from the Road Test conditions, and $\sigma_{SP\text{-}TXJ}$ be the stress calculated from the Spangler equation with an unknown J-term for the in-service pavement. The following relationship is then straightforward, according to the above discussions. In other words, any difference in stress due to differences in pavement physical properties and load transfer ability between the Road Test conditions and other conditions, such as found in Texas, can be accounted for by changing a J-term value in the rigid pavement performance equation as follows:

$$\frac{S}{\sigma_{SP-TXJ}} = \frac{S_{LP}}{\sigma_{SP-A}} \tag{4.1}$$

where

S = maximum stress in an in-service pavement,

$\sigma_{SP\text{-}TXJ}$ = stress calculated from the Spangler equation for an in-service pavement with an unknown J-term,

$$S_{LP} = \frac{0.32P}{D^{4/3}}, \tag{4.2}$$

which is the Loop 1 stress equation (Ref 36), and

$\sigma_{SP\text{-}A}$ = stress calculated from the Spangler Equation with J = 3.2 for the AASHO Road Test conditions.

Hudson showed (Ref 36) that Loop 1 stress can be used for performance study.

Equation 4.2 can be written in the following form, with the J-term appearing:

$$\frac{S}{J[C]} = \frac{S_{LP}}{\sigma_{SP-A}} \tag{4.3}$$

where

$$[C] = \frac{P}{D^2}\left[1-\left(\frac{a_l}{L}\right)\right] \qquad (4.3a)$$

Therefore, the J-term can be expressed as follows:

$$J = \frac{S\sigma_{SP-A}}{S_{LP}[C]} \qquad (4.4)$$

By adding 3.2 to the numerator and denominator in the right side, Equation 4.4 becomes

$$J = 3.2\frac{S\sigma_{SP-A}}{S_{LP}\sigma_{SP-TX}} \qquad (4.5)$$

where

σ_{SP-TX} = stress calculated from the Spangler Equation with J = 3.2 for the in-service pavement.

Considering the difference between the method used in estimating the stress, S, and the method used in obtaining the Loop 1 stress, S_{LP}, a factor of F needs to be added to Equation 4.5 to account for this difference. This addition results in the following general mathematical form for the J-factor model:

$$J = 3.2\frac{S\sigma_{SP-A}}{S_{LP}\sigma_{SP-TX}F} \qquad (4.6)$$

The determination of the F-factor value is described in Section 4.4 of this chapter.

4.3 APPROACH TO ESTIMATING FIELD STRESSES

In the absence of efficient and economical instruments for directly measuring strains (stress) on in-service concrete pavements, we decided to estimate the field stress from deflection measurements on field concrete pavements. Specifically, the approach to estimating the stress would use the FWD measurements taken on in-service CRC pavements across Texas during the summer of 1988.

4.3.1 CRC Pavements

In designing CRC pavements, a key hypothesis asserts that, if transverse cracks are allowed to occur, they are kept tightly closed through the use of longitudinal reinforcement steel. The occurrence of cracks in CRC pavements gives rise to difficulties in determining critical stresses in the pavement. In order to find the critical stress loading position, a finite-element program called ILLI-SLAB (Refs 37 and 38) was used to perform an analysis of CRC pavement.

4.3.1.1 *Finite-Element Analysis of CRC Pavement*

A typical field section of an in-service CRC pavement was selected for the analysis. The thickness of the slab was 8 inches. The deflections measured at the edge, at the corner of the crack, and at the interior are shown in Table 4.1. Figure 4.1 depicts these three loading positions for the deflection measurements. The concrete modulus of elasticity (E-value) was $5.2x10^6$ psi. The modulus of subgrade reaction (K-value) was 295 pci. This K-value was assumed to be uniformly distributed beneath the slab. The Poisson's ratio was assumed to be 0.2. A summary of data for this field section is presented in Table 4.1.

Table 4.1 Summary of data for the field CRCP section

Slab thickness, D= 8 in.	Interior deflection, W_i = 4.23 mils
E = 5.2 x 10^6 psi	Edge deflection, W_e = 6.29 mils
K = 295 pci	Corner deflection, W_c = 6.48 mils
Poisson's ration = 0.2	Crack spacing = 5.8 ft

Note: Deflections were transformed to a load of 9,000 lbs; edge and corner deflections were corrected to a zero temperature differential condition.

Two models were used to simulate the field conditions. The first model considered the cracks while the other did not. The layout of the first simulation model (Model 1) is shown in Figure 4.1. Three slab segments were used in this simulation model. As shown in Figure 4.1, the middle slab segment was rounded up to a length of 6 feet; the other two on each side of the middle slab segments were set at 10 feet in length. The lane width was 12 feet. The middle slab segment was divided into 6 elements in the longitudinal direction. Seven elements with different sizes were used for each of the two side slabs. The 12-foot lane was divided into 12 elements. The applied load was 9,000 pounds, and the loading area was $10.46x10.46$ inches^2.

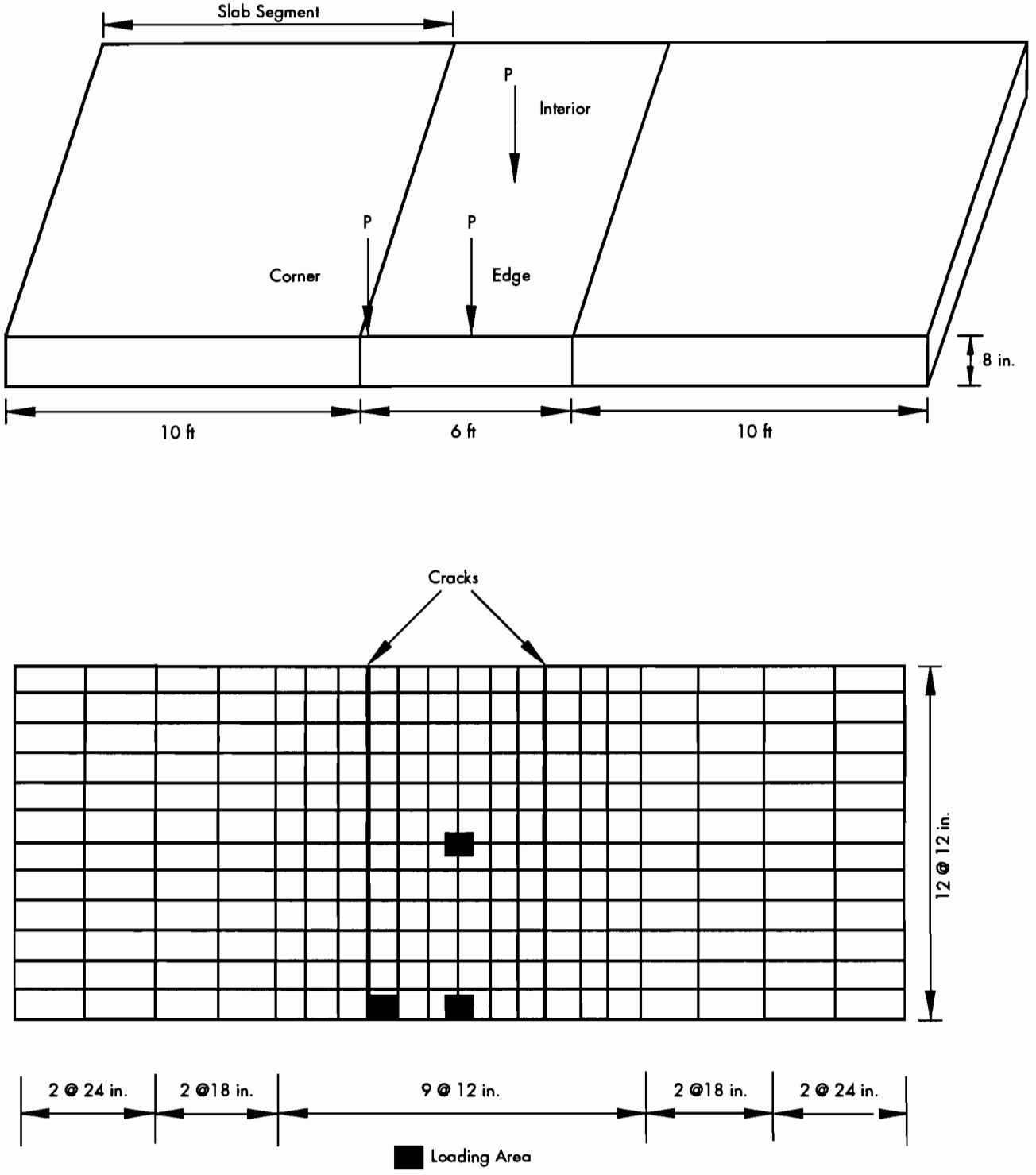

Figure 4.1 Layout of loading conditions and dimension for Model 1 and the finite-element mesh configuration used for simulation

Shear transfer was considered at the cracks. Shear transfer across the cracks was simulated through spring elements in the finite-element program. Different levels of shear transfer can be simulated by varying the spring stiffness parameter. In Model 1, five levels of shear transfer from zero (using a spring stiffness parameter of 1) to about 100 percent (using a spring stiffness parameter of 1.0×10^7) at the cracks were considered.

The results of the finite-element analysis are presented in Table 4.2. Figure 4.2 shows the plot of maximum deflection results of the finite-element analysis, while Figure 4.3 shows the plot of maximum stress results.

Table 4.2 Finite element analysis results and corresponding field data

Model	Level of Shear Transfer (spring stiffness parameter)	Loading Position					
		Interior		Edge		Corner	
		Deflection	Stress	Deflection	Stress	Deflection	Stress
1	0	5.92	226	19.36	313	37.33	241
	10^4	4.97	217	15.79	357	24.68	186
	10^5	4.51	208	13.64	381	18.90	133
	10^6	4.43	207	13.11	386	17.61	135
	10^7	4.42	207	13.03	387	17.42	138
	10^7 + dowel	4.42	207	13.03	387	17.42	138
2	Continuous Slab	4.25	200	13.02	369		
	Field Data	4.23		6.29		6.48	

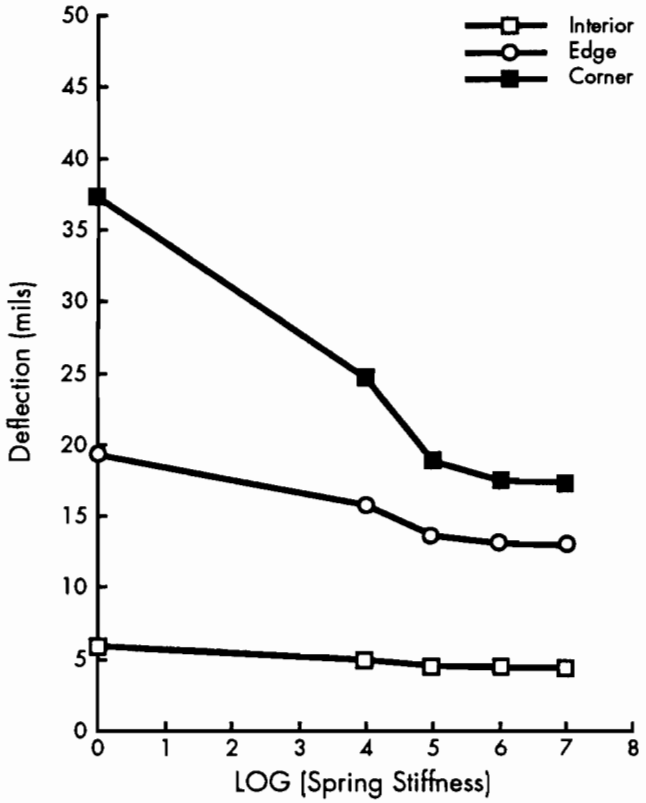

Figure 4.2 Deflections at different levels of shear transfer at the cracks for three loading positions

The second simulation model (Model 2) is a simple, continuous slab, as depicted in Figure 4.4. The thickness of the slab, the modulus of elasticity, the subgrade reaction, and the load are the same as those used in Model 1. Results of the finite-element analysis for Model 2 are also presented in Table 4.2. For the convenience of comparison, measured deflections are also included in Table 4.2.

As seen from Figure 4.2, when the spring stiffness parameter increases, deflections at the interior, at the corner of the crack, and at the edge between the cracks all decrease at varying rates. The corner deflection decreases at the fastest rate, while the interior deflection decreases at the slowest rate. For all three loading positions, when the spring stiffness parameter is greater than 1.0×10^6, there is no significant change in deflections.

It may be noted from Figure 4.2 that even when the spring stiffness parameter increases to a very large value, such as 1.0×10^7, the difference in deflections between those at the corner and those at the edge is still very large. Therefore, another strategy was sought in an attempt to reduce that difference by considering additional moment transfer at the cracks.

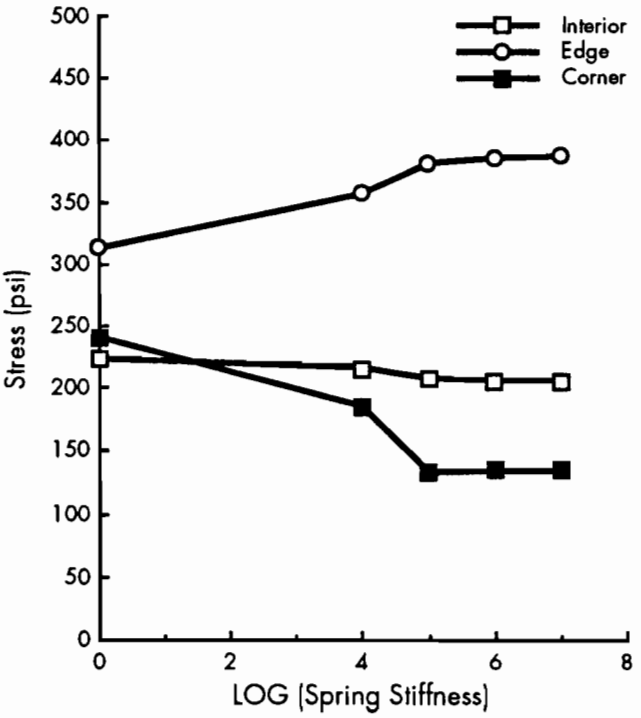

Figure 4.3 Stresses at different levels of shear transfer at the cracks for three loading positions

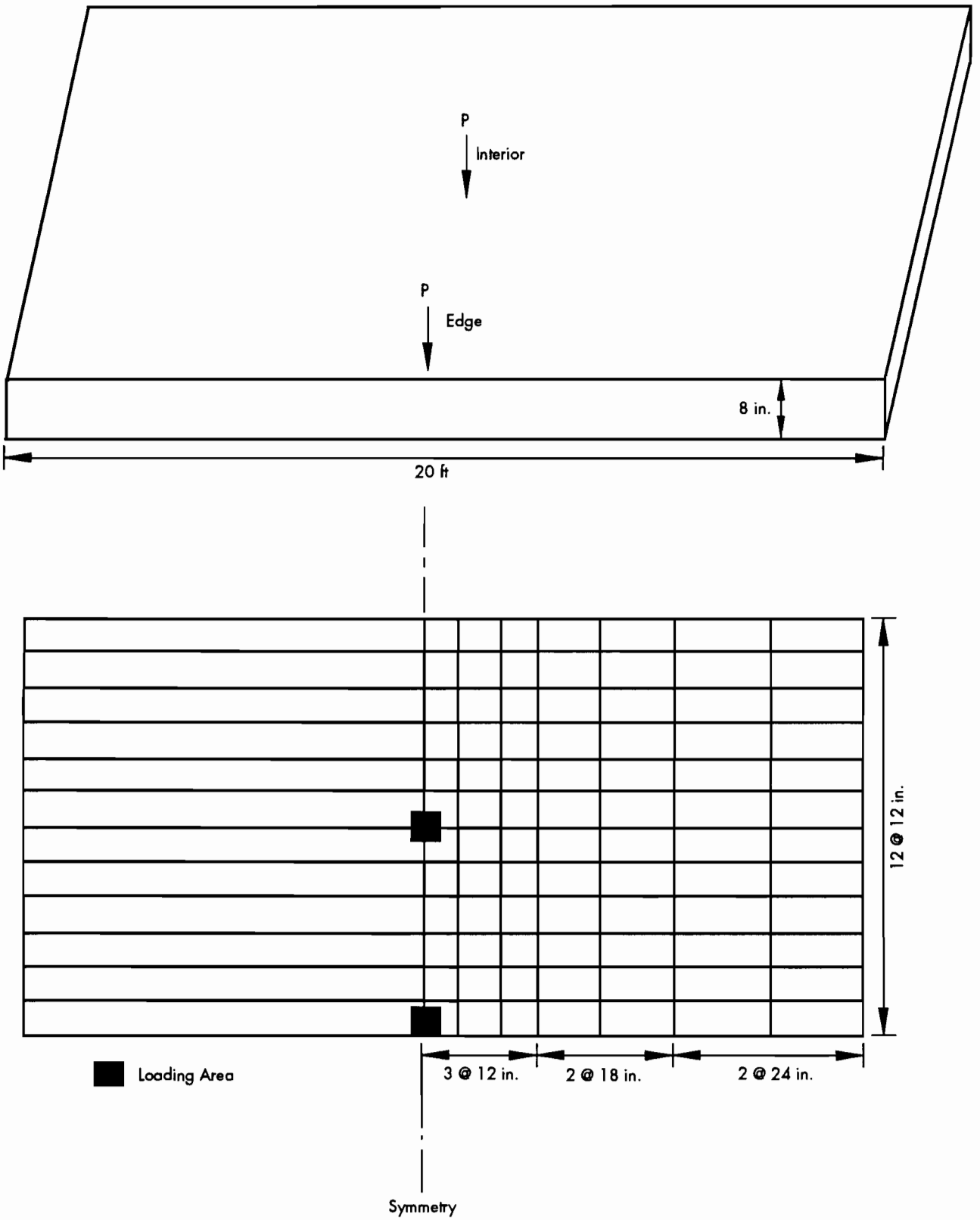

Figure 4.4 Layout of Model 2 and the finite-element mesh configuration

For the case of shear plus moment transfer at the cracks, #6 bars with 12-inch spacing were used in the simulation. The Poisson's ratio for the steel bar was 0.29, and the modulus of the steel was 2.9×10^7 psi. The spring stiffness parameter was kept at the value of 1.0×10^7. Results of the finite-element analysis are also presented in Table 4.2.

As seen from Table 4.2, the results for the case of shear plus moment transfer are the same as those having shear transfer only with a stiffness parameter value of $1.0x10^7$. This result is probably due to the finite-element program limitations.

It is important to note from Figure 4.3 that stresses at the edge between the cracks are always larger than those at the corner near the cracks and at the interior. Therefore, for CRC pavement, the critical loading position is at the edge between the cracks.

A comparison of the results from Model 1 and Model 2 in Table 4.1 indicates that, with a spring stiffness parameter of $1.0x10^7$ at the cracks, Model 1 yields the same deflection at the edge as does Model 2. Also, the stresses calculated from these two models are almost the same. For this case, the difference between the stress from Model 1 and that from Model 2 is less than 5 percent.

Based on the above results, it may be assumed that the maximum deflection or the maximum stress from the edge loading condition in a continuous pavement slab is the same as that in a pavement with the presence of cracks that have about 100 percent load transfer ability. In other words, the CRC pavements in Texas can be treated as a continuous slab in the longitudinal direction, since the results in Chapter 3 show that the load transfer efficiencies at the cracks for in-service CRC pavement in Texas are about 100 percent.

4.3.1.2 *Relationship between Field Stress and Theoretical Stress*

As noted in Table 4.2, there is a significant difference in deflections at the pavement edge between those calculated from the finite-element program and those measured in the field. Therefore, stresses calculated from a theoretical model cannot be used to represent field conditions directly. A correction for the difference between field conditions and theoretical predictions is needed before using the stress obtained from the theoretical model in calculating the J-value (load transfer coefficient).

For simplicity, a linear relationship is assumed between edge deflection and edge stress for estimating field edge stress. This relationship can be expressed as follows:

$$S_e = \frac{w_e}{d_e}\sigma_e \qquad (4.7)$$

or, it may be written as

$$S_e = R_e\ \sigma_e \qquad (4.8)$$

where

S_e = estimated edge stress in the existing concrete pavement (psi),
W_e = edge deflection measured in the existing concrete pavement (inch),
σ_e = edge stress calculated from theoretical model (psi),
d_e = edge deflection calculated from theoretical model (inch), and
$R_e = W_e/d_e$. (4.9)

The stress calculated from Equation 4.11 is assumed to be field stress, and can be used in the calculation of the J-value.

4.3.1.3 *Selection of a Theoretical Model for Calculating Stresses*

For the analysis of a simple slab that has free edge and corner conditions, two theoretical models are available. They are (1) the Westergaard slab model, and (2) the finite-element model. Finite-element models can also be used to study the effects of cracks in the pavements; however, as can be seen from the above analyses, they cannot fully simulate actual field conditions. In other words, there are still many assumptions and limitations inherent in those finite-element models. The Westergaard plate model is simple and easy to use, though it has limitations in analyzing the effects of cracks in pavement. Since the results in Section 4.3.1.1 show that the in-service CRC pavements in Texas, because they have very good load transfer at the cracks, can be treated as a continuous slab in the longitudinal direction, we decided to use the Westergaard slab model for calculating the theoretical stress. The use of the Westergaard model provides a closed form for the J-factor model, making the calculation simple. Furthermore, only the Westergaard interior and edge equations are required in the stress analysis, since no critical corner condition exists in the CRC pavement.

Following his 1926 presentation of solutions to the three loading conditions, Westergaard (Ref 4) modified and developed several different solutions to the edge, corner, and interior loading conditions in a pavement slab (Refs 27 and 39; a good summary of his solutions can be found in Ref 35). The following Westergaard interior and edge equations (Ref 35) give results similar to the finite-element analysis results:

(1) Interior loading condition

(a) Stress

$$\sigma_i = \frac{3P(1+\mu)}{2\pi D^2}\left[\ln\left(\frac{2L}{a}\right)+0.5-\gamma+\frac{\pi}{32}\left(\frac{a}{L}\right)^2\right] \quad (4.10)$$

(b) Deflection

$$d_i = \frac{P}{8KL^2}\left\{1+\frac{1}{2\pi}\left[\ln\left(\frac{a}{2L}\right)+\gamma-1.25\right]\left(\frac{a}{L}\right)^2\right\} \quad (4.11)$$

(2) Edge loading condition

(a) Stress

$$\sigma_e = \frac{3P(1+\mu)}{\pi(3+\mu)D^2}\left[\ln\left(\frac{ED^3}{100Ka^4}\right)+1.84-\frac{4\mu}{3}+\frac{(1-\mu)}{2}+1.18(1+2\mu)\left(\frac{a}{L}\right)\right] \quad (4.12)$$

(b) Deflection

$$d_e = \frac{P\sqrt{(2+1.2\mu)}}{\sqrt{(ED^3K)}}\left[1+(0.76+0.4\mu)\left(\frac{a}{L}\right)\right] \quad (4.13)$$

where

γ = 0.577, Euler's constant, and other variables are as previously defined.

Therefore, the Westergaard equations given above for interior and edge loading conditions were selected for calculating theoretical edge and interior stresses.

4.3.2 Jointed Concrete Pavements

In jointed concrete pavement design, transverse cracks occurring in the slab are not expected. Otherwise, a high percentage of longitudinal steel would be needed to keep the cracks tightly closed, preventing the development of a weak area in the pavement. Thus, jointed concrete pavements can be treated as a simple slab. Consequently, the Westergaard interior and edge equations given in the previous section can be used for calculating the theoretical stresses in jointed concrete pavements. For corner loading, the following Westergaard corner equations were selected (Ref 4).

(1) Deflection

$$d_c = \frac{P}{KL^2}\left[1.1-0.88\left(\frac{a_1}{L}\right)\right] \quad (4.14)$$

(2) Stress

$$\sigma_c = \frac{3P}{D^2}\left[1-\left(\frac{a_1}{L}\right)^{0.6}\right] \quad (4.15)$$

Similar to the estimation of field stresses for CRCP, it is assumed that a linear relationship between corner stress and corner deflection exists. In other words, if the deflection measured at the corner in an actual jointed pavement is equal to d_c (calculated from Equation 4.14), then the actual pavement stress is equal to σ_c (calculated from Equation 4.15). If the actual pavement deflection is zero, the corresponding stress becomes zero. Mathematically, this can be expressed as follows:

$$S_c = \frac{w_c}{d_c}\sigma_c \quad (4.16)$$

or

$$S_c = R_c\sigma_c \quad (4.17)$$

where

S_c = estimated corner stress in the existing pavement (psi),
W_c = corner deflection measured in the existing pavement (inch),
σ_c = corner stress calculated from Equation 4.15 (psi),
d_c = corner deflection calculated from Equation 4.14 (inch), and
$R_c = W_c/d_c$. (4.18)

The relationship defined in Equation 4.7 can be used for an estimation of the edge stress in jointed concrete pavements.

4.4 DETERMINATION OF THE F-FACTOR

In the mathematical expression of the J-factor model as defined in Equation 4.6, a factor called the F-factor was introduced to account for the difference between the method for obtaining the actual pavement stress used in this study and that used at the AASHO Road Test. Basically, the determination of the F-factor in this study is based on the interior loading condition.

In the AASHTO guide, the lowest value of the load transfer coefficient for the design of CRC pavements is 2.3. Theoretically, the interior loading represents the best condition, since the interior position of the slab has the best ability for load transfer. Also, deflections and stresses are minimum for the interior loading. Thus, a 2.3 value for

the load transfer coefficient was assigned to this loading condition. In other words, if the maximum field stress is equal to the design stress calculated from the Westergaard interior stress equation, the J-factor model will give a value of 2.3 for the load transfer coefficient. For consistency, the same F-value is also recommended for jointed concrete pavements. Such an assignment yields a value of 3.2 for the load transfer coefficient for a test slab of jointed concrete pavement at the BRC based on field deflection measurements.

4.5 FLOW CHART OF THE J-FACTOR MODEL FOR CRCP

A flowchart of the J-factor model for CRCP, depicted in Figure 4.5, was developed based on current conditions of the rigid pavement database and can be expanded to apply to other conditions of the database. In the current rigid pavement database, slab thickness (D), concrete modulus of elasticity (E), and deflections, among other parameters for CRC pavements, are available. The deflection information includes interior deflections, edge deflections, and the corresponding load (P). In addition, the radius of FWD load plate is known to be 5.9 inches. The Poisson's ratio of the concrete slab is assumed to be 0.2.

Assuming the deflection had been corrected for the effect of temperature differentials, the first step in the process of the J-factor model is the development of a database. (A more detailed description of the CRCP database development for the J-factor model is presented in the next chapter.) The interior deflections (W_i) are used first to back-calculate the modulus of subgrade reaction (K-value) using the Westergaard interior deflection equation. Once the K-values are obtained, calculations for the interior stress, edge stress, and edge deflection are straightforward. The field edge stress is obtained by multiplying the calculated edge stress by a ratio of field edge deflection (W_e) to calculated edge deflection (d_e). Finally, maximum stress between the interior stress and the estimated field edge stress is used in the calculation of the J-value using the J-factor expression as defined in Equation 4.6. The F-factor can be determined once the design information is known.

Consideration of the interior stress in the calculation of the J-value can be explained by Figure 4.6. If only the edge condition is considered, then theoretically, when edge deflection goes to zero, the ratio of edge deflection to interior deflection goes to zero. In this case, the J-value

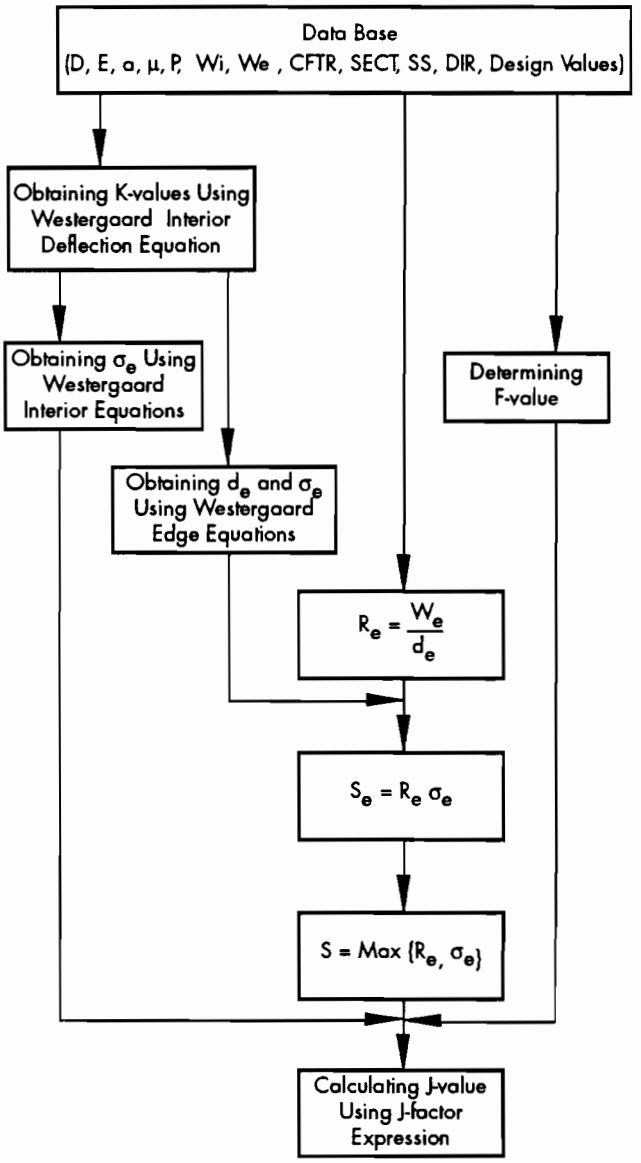

Figure 4.5 A flowchart of the J-factor model for CRCP

would also go to zero. However, this may not always be true for actual pavements, because, for example, when the pavement is thickened at the edge or is thickened as a result of non-uniformity, measured edge deflection may be very small compared with measured interior deflection, although interior stress may still be relatively large. In other words, the critical stress may be in the interior instead of at the edge. In this case, interior loading appears to be critical. The J-value is then determined by the interior condition instead of going to zero. The bold line represents predicted J-values for the pavements based on design values. A value of 3.0 for the ratio of edge deflection to interior deflection is

used to limit the upper bound J-values as a theoretical control. The ranges of J-values recommended by the AASHTO Guide are also shown in Figure 4.6. It should be realized that the J-factor model is not only a function of deflection ratio R, but is also a function of modulus of subgrade reaction, slab thickness, and concrete modulus of elasticity.

Figure 4.7 presents a plot of the obtained J-values versus the ratio of actual edge deflection to interior deflection for Texas CRC pavements in District 20. Predicted values based on design values are also plotted in the figure, as shown by the bold line. Deviations between predicted and obtained values could be caused by variations of the thickness, K-values, and/or E-values in the field.

It should also be mentioned that the above procedure does not include either the effect of daily/seasonal temperature differentials or the lateral distribution of load applications, because of the lack of actual data on these factors at the present time. It is highly recommended that such factors be included for the development of a more rational procedure.

4.6 FLOWCHART OF THE J-FACTOR MODEL FOR JCP

A conceptual flowchart of the J-factor model for jointed concrete pavements is presented in Figure 4.8. The flowchart for jointed concrete pavements is more general, compared with that for CRC pavements.

In the flowchart, four different loading conditions are considered in the J-factor model because estimated critical field stress may occur in any one of the four loading conditions. These loading positions include: (1) interior loading, (2) edge loading, (3) corner loading, and (4) transverse joint loading. Another possible critical loading position that may occur at the longitudinal joint is not considered in the flowchart, as longitudinal joint loading would not be expected to be worse than at the edge or at the transverse joint loading conditions.

The database for jointed concrete pavements includes FWD measurements for different loading conditions and includes pavement structural information, including slab thickness, coarse aggregate type, subbase treatment type, and thickness. The FWD measurements should include deflections at

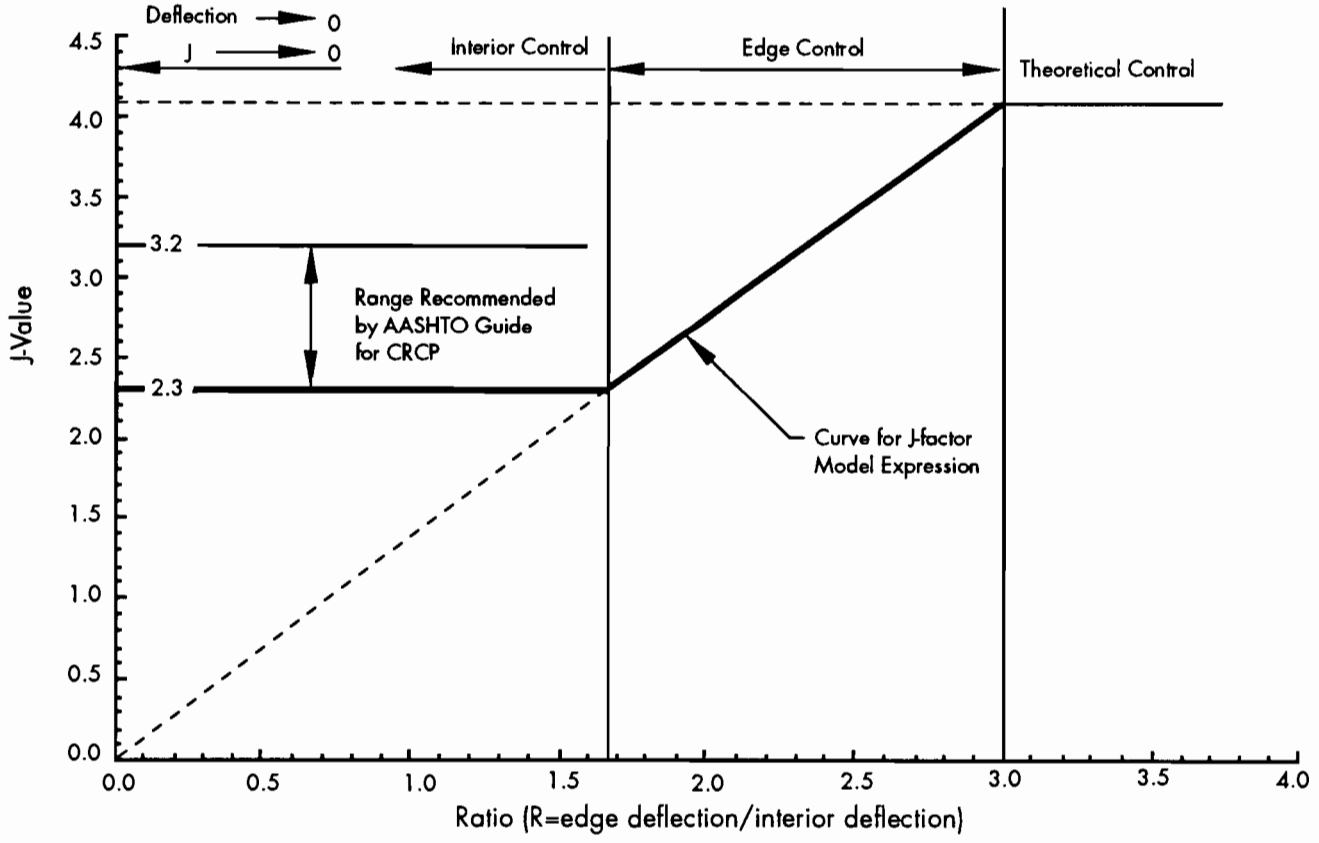

Figure 4.6 Graph of the J-factor model for CRCP

the joint (W_j), at the edge (W_e), at the corner (W_c), and at the interior (W_i). After deflection measurements are available, layer theory and other programs—such as RPEDD1 (Ref 58)—that can back-calculate pavement layer properties can be used to obtain the concrete modulus of elasticity (E-value) and the modulus of subgrade reaction (K-value). The K-value can also be determined using the Westergaard equation. The F-value can be determined once the design information is known. With E-values and K-values available, deflections (edge deflection d_e, and corner deflection d_c) and stresses (edge stress σ_e, corner stress σ_c, and interior stress σ_i) for various loading positions can be calculated using the corresponding Westergaard equations or other theoretical models. The calculated stress is then modified to represent the field stress (estimated edge stress s_e, and estimated corner stress s_c) using a ratio of measured deflections to calculated deflections. A comparison between deflections at the edge and at the transverse joint can be made to obtain the maximum deflection, WE, before estimating the field edge stress. Finally, a maximum field stress value can be selected from the estimated stresses for different loading conditions. Then the J-factor expression defined in Equation 4.6 can be used to calculate the J-value.

4.7 SUMMARY

A rational J-factor model for CRC pavements in Texas was developed in this chapter based on field deflection measurements. The assumption made at the AASHO Road Test—that an equal ratio of stress to strength gives equal performance—was the premise for the development of a mathematical form of the J-factor model (J-factor expression). A finite-element analysis of CRC pavements was performed and the results showed that the CRC pavements in Texas can be simulated as a continuous slab in the longitudinal direction. The Westergaard equations were selected as the model for calculating theoretical deflections and stresses. A linear relationship was assumed between the edge deflection and the edge stresses for an approach to estimating field edge stresses. An F-factor was introduced in the J-factor expression to account for the difference between the method used in this study to obtain field stresses and that used at the AASHO Road Test. The F-factor was determined based on the interior loading condition. Finally, a conceptual J-factor model for jointed concrete pavements was presented.

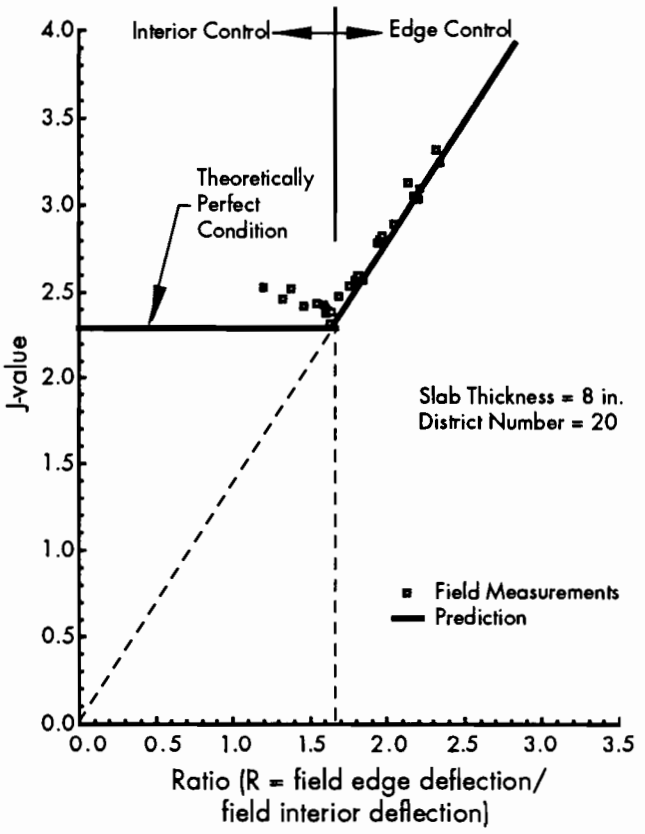

Figure 4.7 Plot of derived J-values versus deflection ratio R

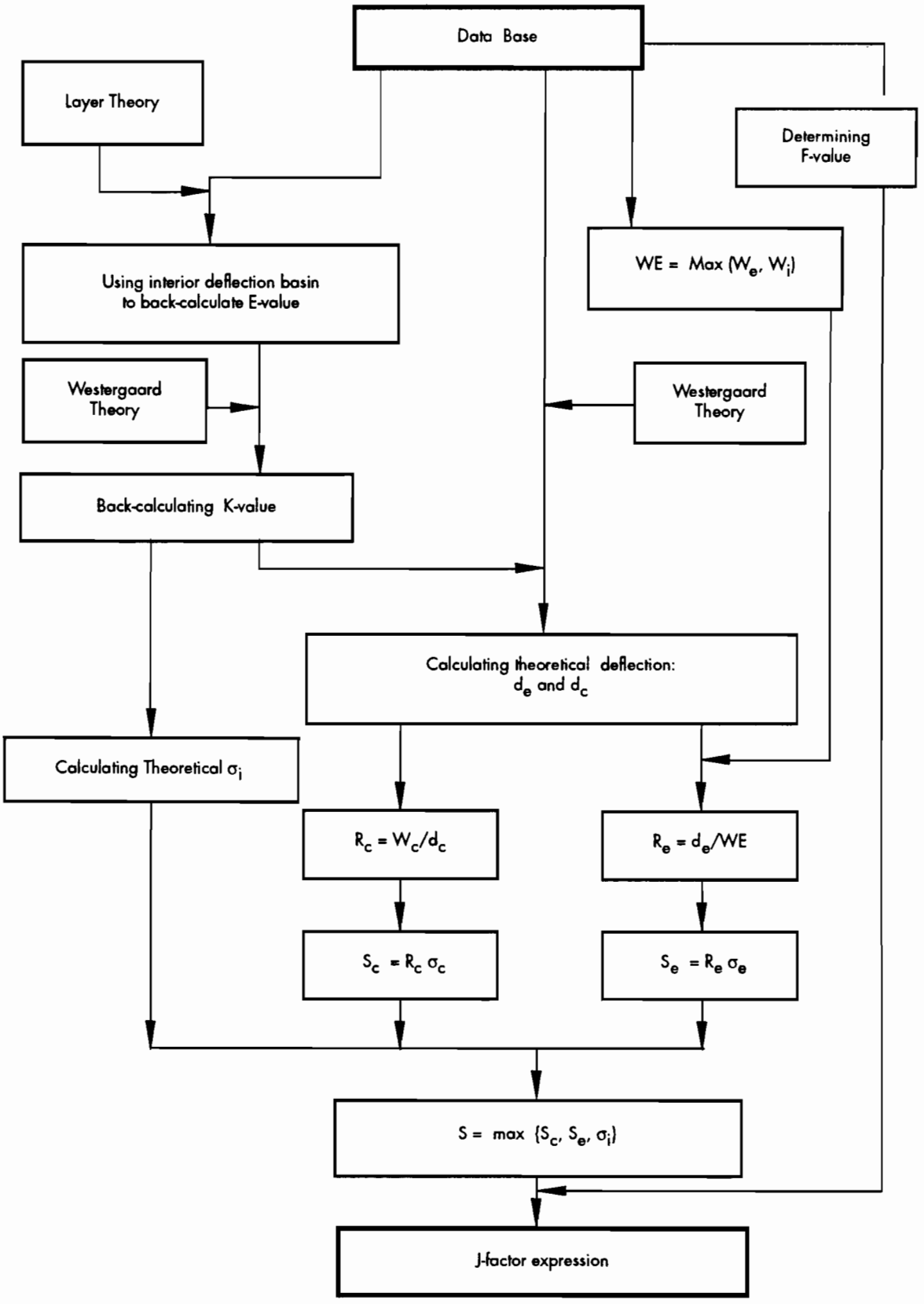

Figure 4.8 A flowchart of the J-factor model for jointed concrete pavements

CHAPTER 5. APPLICATION OF THE J-FACTOR MODEL

In Chapter 4, a rational J-factor model for estimating load transfer coefficients for CRC pavements based on field deflection measurements was developed. The objective of this chapter is to obtain the load transfer coefficient values (J-values) by applying the J-factor model to the FWD measurements taken from Texas in-service CRC pavements. This objective can be achieved by:

(1) developing a procedure for correcting the effect of temperature differential on FWD measurements;
(2) setting up a database for the J-factor model utilizing information available in the rigid pavement database; and
(3) developing a computer program to calculate the load transfer coefficient values.

5.1 TEMPERATURE DIFFERENTIAL CORRECTION ON DEFLECTION MEASUREMENTS

Many studies have shown that temperature differential (DT) has a significant effect on pavement deflection measurements, especially those near the pavement edge (Refs 5, 10, 25, 32, and 33). For example, when the temperature at the top of a pavement slab is higher than the temperature at the bottom, the temperature differential of the pavement is positive, causing the pavement edge to warp downward. Conversely, the pavement warps upward when the temperature at its top is lower than that at the bottom. If the temperature at the top is the same as that at the bottom (i.e., the temperature differential is zero), the pavement slab flattens. For downwardly warped pavements, the measured deflections would be less than those of an unwarped pavement; and, in the case of upward warping, the measured deflections would be larger than without warping.

The 1988 summer deflection measurements were taken at various times over several days. Figure 5.1 shows the frequencies of pavement surface temperatures taken at each deflection measurement. As seen from the figure, more than 70 percent of the deflections were measured when pavement surface temperature was greater than 100 degrees Fahrenheit. This high temperature condition usually causes the pavement edge to warp downward. Therefore, it is necessary to correct the temperature differential effects on the deflection measurements so that a meaningful comparison of different types of pavement can be made.

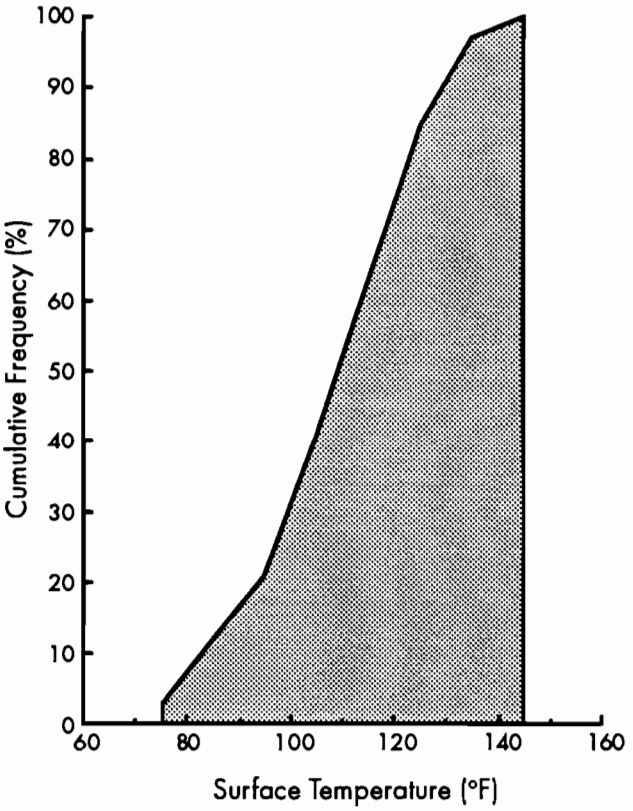

Figure 5.1 Frequency of pavement surface temperature data

Research studies have shown that the effect of temperature differentials on interior deflection measurements (Refs 25 and 33) and on edge deflections of CRCP with tied PCC shoulders (Ref 25) can be disregarded. Figure 5.2 shows the influence

of a tied PCC shoulder on CRC pavement edge deflections. Therefore, only the edge deflections of pavement without a tied PCC shoulder need to be corrected for the temperature differential effect. Commonly, deflection measurements are corrected back to a standard condition of zero temperature differential. In other words, a flat pavement slab condition is used as the basis for comparison.

Generally speaking, the effect of temperature differentials on deflection measurements may vary with slab properties, slab thickness, subbase conditions, moisture conditions, and shoulder type. It is difficult to account for the effects of all these variables because of the complexity and variety of conditions. However, the *AASHO Road Test Report* (Ref 5) indicates that there is a good relationship between the measured deflections and the corresponding temperature differentials at the Road Test. Therefore, if such a relationship between the measured deflections and the corresponding temperature differentials for Texas conditions can be obtained, corrections of the temperature differential effect on the statewide deflection measurements can be carried out. However, field measurement data are not available in the rigid pavement database for developing such a relationship. Therefore, we sought other resources for a suitable temperature differential correction model.

5.1.1 Selection of a Temperature Differential Correction Model

Table 5.1 presents a list of the available temperature differential correction models from the literature review. In that table, FT is the temperature differential correction factor. Thus, if DT is the temperature differential of an in-service pavement, and the measured deflection is W, then the deflection at the zero temperature differential condition would be equal to (FT) × (W).

Models 1 and 2 were developed at the AASHO Road Test (Ref 5). They are from corner deflection measurements and edge deflection measurements, respectively. Model 3 was developed by McCullough in a statewide study of CRCP deflections in Texas (Ref 10). Model 3 was developed from corner deflections of the crack. It can be considered, however, the same as a model developed from the edge deflection measurements between the cracks, since there was no significant difference in deflections between the corner of the crack and at the edge between the cracks (Ref 10). Models 4 and 5 were developed from data collected at the BRC slab. Model 4 is from corner deflection measurements; Model 5, from edge deflection measurements.

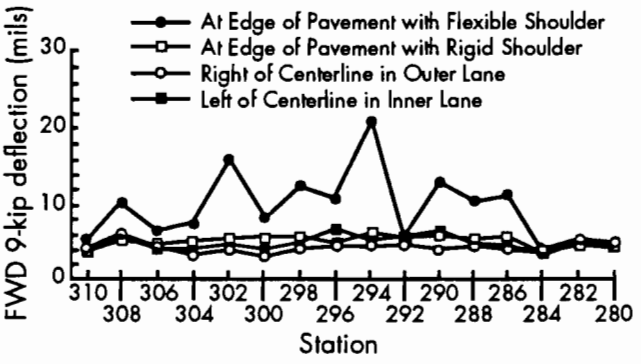

a) Low temperature differential – AM period

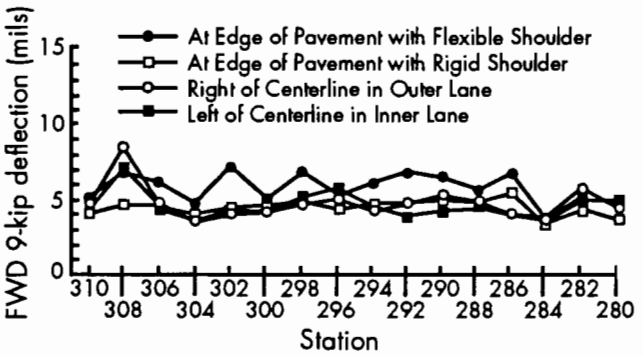

b) High temperature differential – PM period

Figure 5.2 Influence of tied PCC shoulder on CRCP edge deflections (Ref 25)

Figure 5.3 presents a plot of FT versus temperature differential for five models. As seen from the figure, Models 1, 3, and 4 each have a higher FT value, which implies that temperature differential has an effect on deflections. Models 2 and 5 have lower FT values. Therefore, Models 1, 3, and 4 can be classified into one group for corner deflections; Models 2 and 5 into a second group for edge deflections. In the second group, Model 2 has a higher FT value than Model 5 and was derived from the AASHO Road Test. Therefore, Model 2 was selected for temperature differential corrections on the statewide edge deflection measurements.

Table 5.1 Temperature differential correction models

Model Number	Loading Condition	Temperature Differential Influencing Factor	Source
1	Corner	$FT = 10^{0.015DT}$	AASHO Road Test
2	Edge	$FT = 10^{0.0075DT}$	AASHO Road Test
3	Crack	$FT = 10^{0.0147DT}$	McCullough
4	Corner	$FT = 10^{0.0114DT}$	Chapter 3
5	Edge	$FT = 10^{0.0053DT}$	Chapter 3

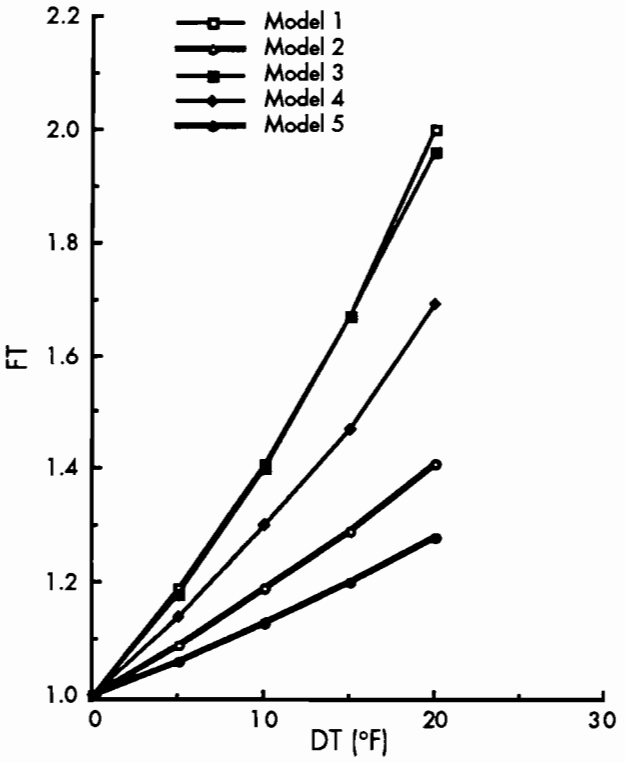

Figure 5.3 Comparison of different temperature correction models

5.1.2 Development of a Temperature Differential Estimating Model

A temperature correction model—Model 2—was selected in the above section. The use of this model requires a knowledge of the temperature differential in pavement. A portable slab was used in the summer 1988 deflection measurements to estimate the temperature differentials for the in-service CRC pavements (Ref 42, in which relationships between the temperature differentials at the portable slab and those in a test pavement were also investigated). The two models derived from Weissmann (Ref 42) are described below.

Model 1:

$$DTpvt_t = 0.315 \times (DT_{LSt-0}) - 0.051 \times (DT_{LSt-1}) + 0.0292 \times (DT_{LSt-2}) + 0.557 \times (DT_{LSt-3}) - 0.018 \times (D) \quad (5.1)$$

Model 2:

$$DTpvt_t = 0.35 \times (DT_{LSt-0}) - 0.026 \times (DT_{LSt-1}) + 0.015 \times (DT_{LSt-2}) + 0.473 \times (DT_{LSt-3}) - 0.037 \times (D) \quad (5.2)$$

where

$DTpvt_t$ = temperature differential in the pavement at instant t,
LS = portable slab coarse aggregate (limestone),
DT_{LSt-i} = portable slab temperature differential at instant t-i, and
D = pavement thickness (inch).

Model 1 predicts temperature differentials for the in-service pavement from the portable slab when aggregate types of the portable slab and the in-service pavement are the same. Model 2 predicts temperature differentials for the in-service pavement from the portable slab when aggregate types of the portable slab and the in-service pavement are not the same.

The use of these two models requires that temperatures be known at three instances before the desired temperature differential is estimated. However, such temperature data are presently not fully available at the rigid pavement database. Therefore, we sought other alternatives for estimating temperature differentials for in-service pavements.

Theoretical temperature prediction models were the first alternatives sought. Barber's mathematical model (Ref 43) is typical, and can be used for asphalt and concrete pavements. Shahin modified

Barber's model to simulate both maximum and minimum temperatures of asphalt pavements (Ref 44). Uddin later modified Shahin's model to predict the temperature differential in concrete pavements (Ref 33). The use of this latter model requires a knowledge of the ambient air temperature, solar radiation, wind speed, thermal properties of concrete, and other temperature data. Figure 5.4 shows a comparison of the predicted and measured temperature differentials from Uddin (Ref 33). Deviations are noted.

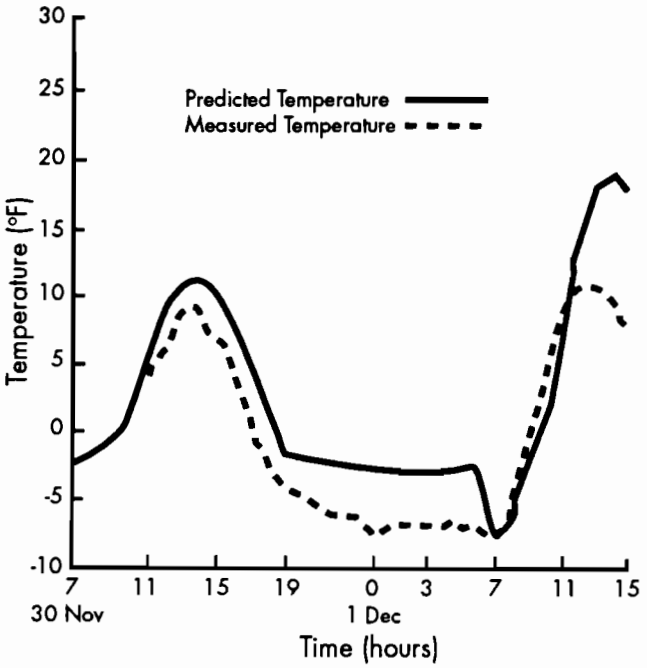

Figure 5.4 Comparison of predicted and measured temperature differentials (Ref 33)

A second alternative model was sought to define a relationship between pavement surface temperatures and temperature differentials. It was found that a linear relationship exists between the measured pavement surface temperature and the measured temperature differential. Pavement surface temperature data are available, but since Barber's model requires additional data collection, this alternative for estimating temperature differentials of in-service CRC pavements was selected.

The relationship between pavement surface temperatures and temperature differentials was developed using data from Morales-Valentin (Ref 32). Figures 5.5 and 5.6 show temperature differential versus surface temperature from data collected on jointed pavement test sections placed in June and August, respectively. Figure 5.7 shows a similar plot from data collected on an in-service jointed pavement in September. Regression equations for each of these three plots are derived below.

(1) Regression equation for June data:

$$DT = -50.061 + 0.6285\ (STEMP) \qquad (5.3)$$
$$R^2 = 0.88$$

(2) Regression equation for August data:

$$DT = -49.609 + 0.604\ (STEMP) \qquad (5.4)$$
$$R^2 = 0.91$$

(3) Regression equation for September data:

$$DT = -49.096 + 0.612\ (STEMP) \qquad (5.5)$$
$$R^2 = 0.93$$

where

DT = temperature differential, and
STEMP = pavement surface temperature.

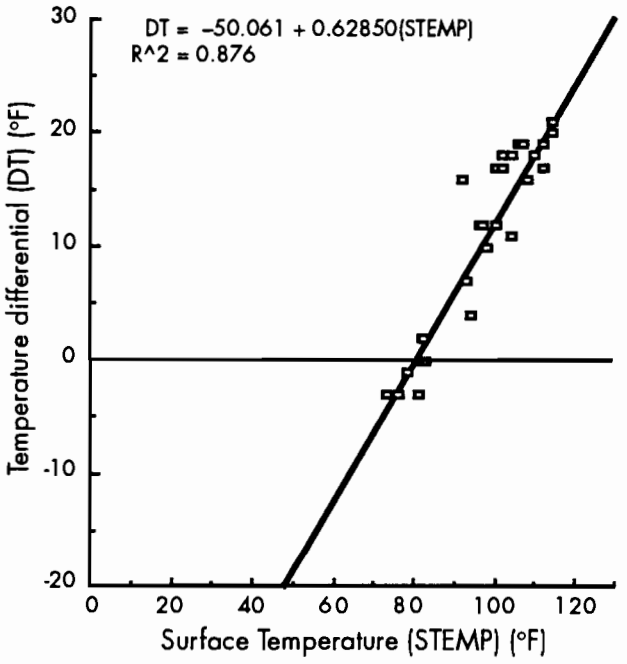

Figure 5.5 Temperature differential versus surface temperature for a 10-inch PCC test slab (June data)

The R^2 is approximately 90 percent for all three regression equations, which indicates a strong linear relationship between surface temperature and temperature differential. It is interesting to note that Equations 5.3, 5.4, and 5.5 have almost the same intercept and slope. The simplest form was chosen to represent Equations 5.3, 5.4, and 5.5, and is listed below.

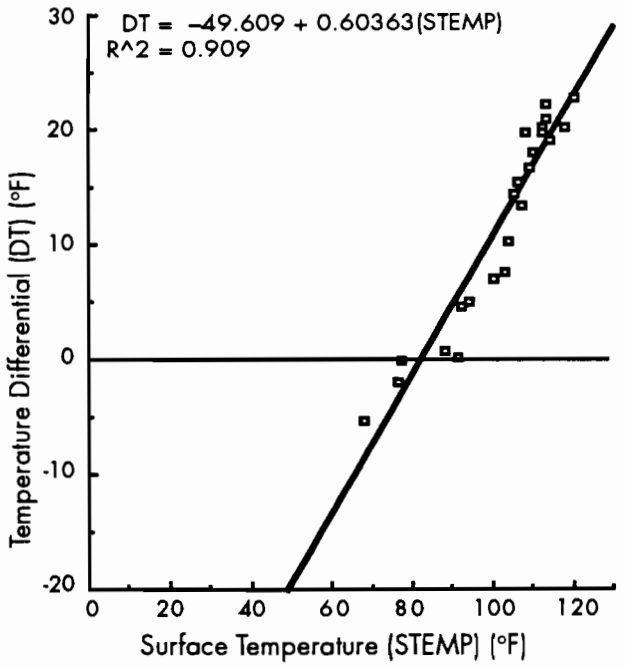

Figure 5.6 Temperature differential versus surface temperature for a 10-inch PCC test slab (August data)

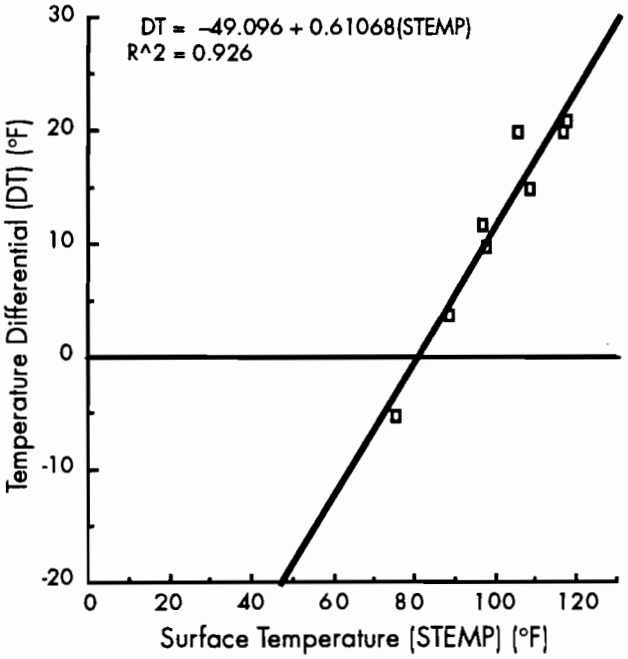

Figure 5.7 Temperature differential versus surface temperature for a 10-inch in-service PCC slab (September data)

$$DT = -50.0 + 0.60\ (STEMP) \qquad (5.6)$$

Further, a linear relationship between the temperature differential and slab thickness is assumed, resulting in the following normalized model:

$$DT_D = -5.0 + 0.060\ (STEMP) \times D \qquad (5.7)$$

where

D = slab thickness (inch), and
DT_D = temperature differential in the pavement with a D-inch slab.

The 1988 deflection measurements were collected only in July and August. Equation 5.7 is derived from measurements taken in June, August, and September; therefore, it is assumed that Equation 5.7 can be applied to temperature differential estimations for those CRC pavements whose deflections were collected in July and August.

5.2 SETTING UP A DATABASE FOR THE J-FACTOR MODEL FOR CRCP

This section describes the variables and the corresponding data needed for calculating load transfer coefficients for CRC pavements in Texas. These variables are referred to as primary variables. A brief description is also provided for variables that may also affect the load transfer coefficient, but which are not included in the J-factor model. These variables are referred to as secondary variables, and will be included in the statistical analysis in Chapter 6. The database set-up is based on FWD measurements taken on the Texas in-service CRC pavements in 1988.

5.2.1 Primary Variables

Primary variables include (1) slab thickness, (2) coarse aggregate type, (3) elastic modulus of concrete, (4) subbase type, (5) modulus of subgrade reaction, (6) Poisson's ratio, (7) deflections and loading positions, (8) radius of contact, and (9) AASHO Road Test information. These variables are described in the following sections.

Slab Thickness (D): Slab thickness is the thickness of the top layer of a concrete pavement structure. The top layer normally consists of portland cement concrete and reinforcing steel. Basically, there is a design thickness value and an existing pavement thickness value. Design slab thickness data are available in the rigid pavement database. However, since the data on existing pavement thickness are not available, the two types of thickness are assumed to be the same. In the 1988 FWD measurements, three levels of thickness slabs are included: 8, 9, and 13 inches.

Coarse Aggregate Type (CAT): Past study and current research show that the type of coarse aggregate used in concrete mix has significant effects on pavement performance, especially in the early

development of crack patterns (Ref 45). Although this variable is not directly used in the J-factor model, it is used to estimate the design value of concrete modulus of elasticity. In this sense, it is classified as a primary variable. Pavement sections selected for the 1988 FWD measurements contain three types of coarse aggregates: (1) crushed limestone (LS), (2) siliceous river gravel (SRG), and (3) a combination of crushed limestone and siliceous river gravel (SRG/LS).

Elastic Modulus of Concrete (E): The elastic modulus of concrete is classified into two categories for the J-factor model: (1) design value of concrete elastic modulus (ED), and (2) in situ concrete pavement elastic modulus (EF).

Design values of concrete elastic modulus were not available at the rigid pavement database, and were assigned according to a report released by TxDOT (Ref 46). In this report, an elastic modulus of 4,000,000 psi for crushed limestone and 5,000,000 psi for siliceous river gravel concrete pavements was recommended (Ref 46). It was assumed that the elastic modulus of concrete, composed of a combination of limestone and siliceous river gravel, has a value of 4,500,000 psi.

The back-calculated values of in-service concrete pavement elastic modulus are available in the rigid pavement database. (Detailed information on these values can be found in Ref 24.)

Subbase Type (SBT): The subbase in pavement structures is also an important factor in pavement performance. Subbase type not only affects strength under the concrete layer, but also affects drainage conditions and friction between concrete and subbase. Subbase type is not directly used in the J-factor model, but is used to estimate the design value for the modulus of subgrade reaction (K-value). Four different subbase types were included in the study: (1) portland cement-stabilized, (2) asphalt cement-stabilized, (3) lime-treated, and (4) crushed-stone.

Modulus of Subgrade Reaction (K): The modulus of subgrade reaction design value (KD) is the only value needed in the calculation of the load transfer coefficient. The existing modulus of subgrade reaction can be obtained using interior deflection data.

Design values for the modulus of subgrade reaction are not currently available from the database. Therefore, based on the report released by the TxDOT (Ref 46), an assumed value of 300 pci is used for cement-treated subbase; 250 pci for asphalt-treated subbase; 225 pci for lime-treated subbase; and 200 pci for crushed-stone subbase. These values are also in accordance with those used in a previous study for this research project (Ref 47).

Poisson's Ratio (μ): Poisson's ratio is also a basic property of the concrete materials. Data on this ratio are not available at the rigid pavement database; therefore, a value of 0.2 is assumed for all calculations in this report.

Deflection Data and Loading Positions: Deflection data used to calculate the load transfer coefficient include deflections measured in the interior (W_i) and those measured at the edge of the pavement (W_e) between cracks (Figure 3.2). Again, deflection data were transformed to a load of 9,000 pounds, and deflections measured at drop-height 4 were used for the calculation. (For detailed information about the deflection measurement procedure, see Ref 24.)

Radius of Contact (a): The radius of contact uses a value of 5.9 inches, which is the same as the loading plate radius in the falling weight deflectometer.

AASHO Road Test Information: The following values are used to represent the AASHO Road Test condition.

(1) $E = 4.2 \times 10^6$ psi, and
(2) $K = 100$ pci.

5.2.2 Secondary Variables

Secondary variables include pavement shoulder type, environmental variables (e.g., rainfall and temperature), roadbed soil type, pavement age, and traffic or load applications.

Shoulder Type: Studies show that the provision of a tied concrete shoulder could significantly reduce edge deflections and, thus, improve pavement performance (Refs 25 and 48). This study considers two pavement shoulder types:

(1) tied portland cement concrete shoulder (tied PCC shoulder), and
(2) asphalt concrete shoulder (AC shoulder).

Rainfall: Rainfall has a significant effect on pavement performance, especially when it interacts with swelling clay in the surface layer. Average annual rainfall data ranging from 21 to 42 inches across Texas are available in the rigid pavement database.

Temperature: The effect of temperature on CRC pavement performance has been widely recognized for its direct effect on the development of cracks and on pavement edge response. Average annual low temperatures are available in the rigid pavement database. The average annual low temperature data range from 8 to 54 degrees Fahrenheit.

Roadbed Soil: The swelling characteristics of subgrade soil play a significant role in potential

layer movement within pavement structures. Generally, the prime surface soil characteristic is affected by the presence of swelling clay in the surface layer. Two categories of roadbed soil characteristics are classified in the rigid pavement database: swelling soil (H) and non-swelling soil (L).

Pavement Age: Pavement age plays an important part among the environmental factors that influence pavement performance. Pavement age is determined by subtracting the construction date from a value of 1988.5. The pavement age ranges from 2 to 37 years.

Traffic Data: As traffic load increases, pavement serviceability decreases. Traffic has a direct effect on pavement structural condition, and is the main cause of pavement failure. For example, heavy vehicles may produce permanent damage on the pavement after only one pass. Unfortunately, detailed traffic data are not available for the pavement sections studied; thus, available average daily traffic collected in 1985 and pavement age are used to assess traffic load on the pavement sections studied.

In addition to the primary and secondary variables described above, some other variables were used to identify the surveyed pavement sections, including:

(1) CFTR – section ID variable,
(2) DIR – direction surveyed,
(3) SECT – section surveyed within a CFTR, and
(4) SS – subsection within a SECT.

(For more detailed information about the rigid pavement database, see Refs 21, 24, and 49.)

5.3 COMPUTER PROGRAM

Figure 5.8 graphically outlines the computer program used for calculating the J-values for CRC pavements. Two main steps are used in the calculation: (1) establish a database that contains the primary variables, and (2) calculate the J-values using the developed J-factor model.

In step one, deflection data that form the SAS data file (FWD.SDS) are obtained. Then deflection data collected at drop height 4 are selected and normalized to a load of 9,000 lbs. The MASTER data file (MASTER.SDS) provides information about slab thickness, coarse aggregate type, and subbase type. With this information, design values for the elastic modulus of concrete and for the modulus of subgrade reaction can be assigned. The ELMOD data file (ELMOD.SDS) provides the in-service pavement elastic modulus of concrete as back-calculated from FWD measurements. Next, temperature differential corrections on deflection measurements are performed. Deflections are corrected back to the condition of zero temperature differential. Step one is accomplished by Program A.

In step two, Program B calculates the modulus of subgrade reaction using measured interior deflections and the Westergaard interior deflection equation. The program then calculates edge stresses and deflections from the Westergaard edge equations, and calculates interior stress from the Westergaard interior stress equation. The F-value can then be determined, using the interior condition along with the design values. The edge stress calculated from the Westergaard edge equation is modified by multiplying it by the ratio of measured deflection to deflection calculated from the Westergaard deflection equation. The modified edge stress is referred to as field edge stress. After comparing field edge stress and interior stress, the maximum stress is used to calculate the J-value.

Computer Program A is written in SAS language; Program B, in FORTRAN language. Both programs are presented in Appendix A, and the derived load transfer coefficients are given in Appendix B.

Direct measurement of the temperature differential of in-service CRC pavements seems infeasible, especially regarding statewide deflection measurements and considering the other information available in the rigid pavement database.

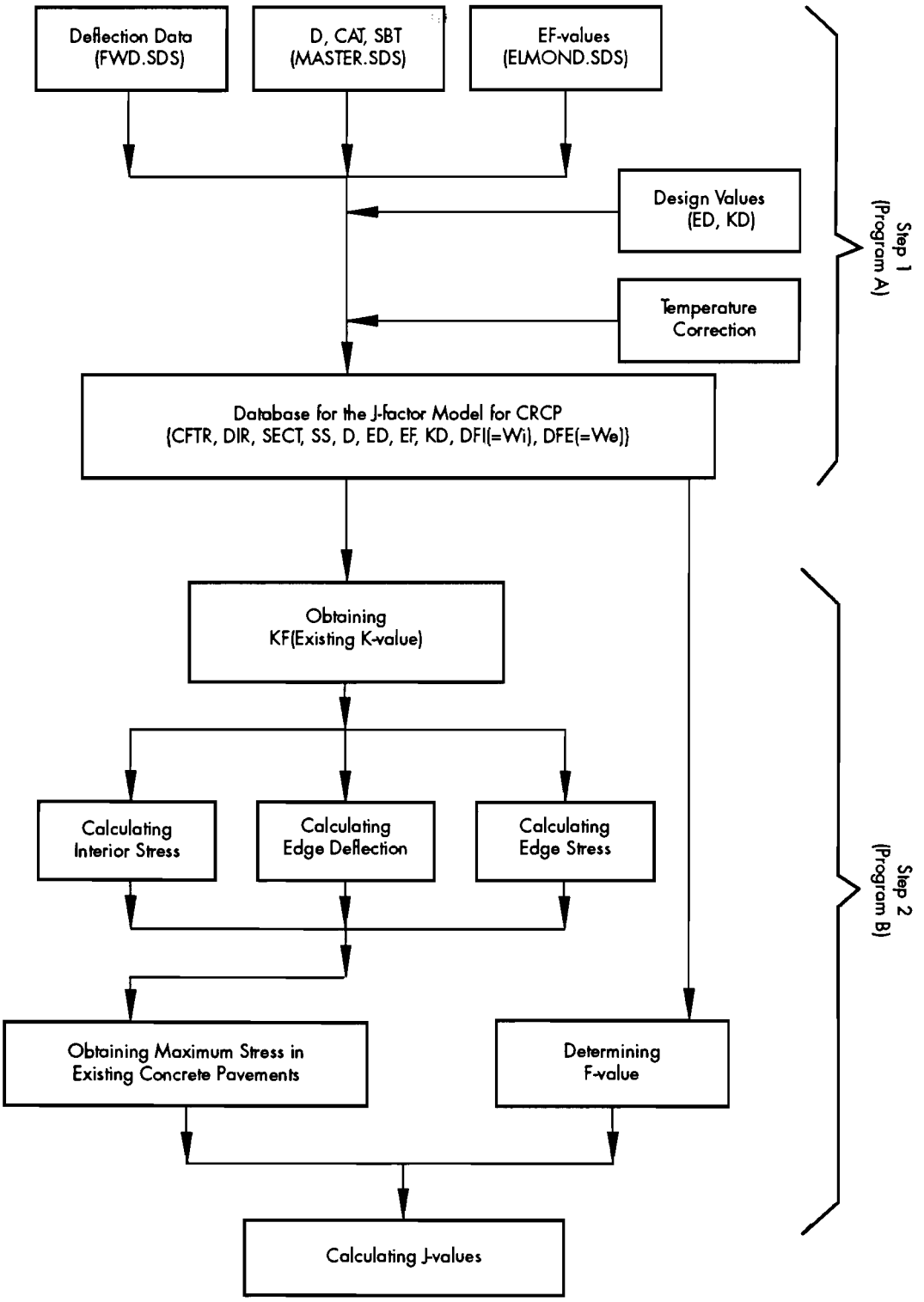

Figure 5.8 Flowchart of the computer program for calculation of the J-value

CHAPTER 6. ANALYSIS OF FIELD J-VALUES

In Chapter 5, field values of the load transfer coefficient (field J-values) were obtained. This chapter presents statistics for the field J-values obtained and a multiple regression analysis of these field J-values. The purpose of the multiple regression analysis is to identify those factors that may have the most important influence on the J-value. For this purpose, a stepwise regression procedure is used in the statistical analysis. A brief description of the stepwise regression procedure is provided before application of the procedure.

6.1 STATISTICS OF FIELD J-VALUES

The primary objective of this study was to provide suitable values of load transfer coefficients for use with the AASHTO guide for the design of CRC pavements in Texas based on field measurements. For this purpose, an analysis of statistics for the field J-values is performed in this section.

Statistics for the field J-values were obtained at each of the following three levels:

(1) Level 1: Each subsection represents an observation;
(2) Level 2: Each section represents an observation; and
(3) Level 3: Each CFTR section represents an observation.

The statistics obtained for each level of the calculation include frequency (for Levels 1 and 2 only), mean, standard deviation, coefficient of variation, 5th and 95th percentiles, and minimum and maximum J-values. The number of observations for each level of calculations is also presented.

6.1.1 Level 1

Each subsection has only one observation of the J-value at Level 1. In other words, each subsection has only one data point for the J-value. Statistics at this level tend to provide general information about J-values across Texas. Total data points are classified into two groups in terms of shoulder type, in accordance with the classification used in the AASHTO guide. Figure 6.1 depicts the frequencies of J-values for pavements with AC shoulders, while Figure 6.2 shows the frequencies of J-values for pavements with tied PCC shoulders. Table 6.1 summarizes the statistics of J-values at Level 1.

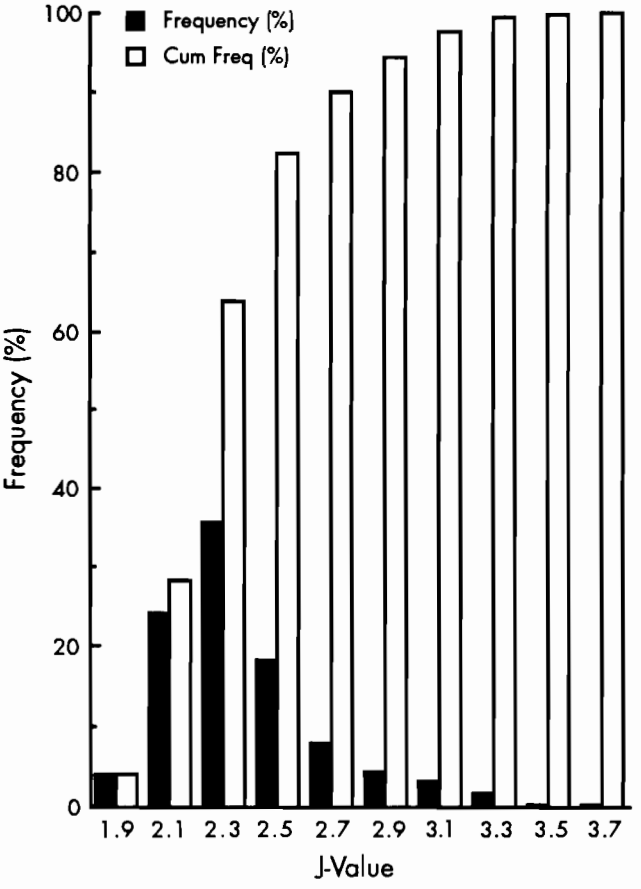

Figure 6.1 Frequencies of J-values at Level 1, AC shoulder

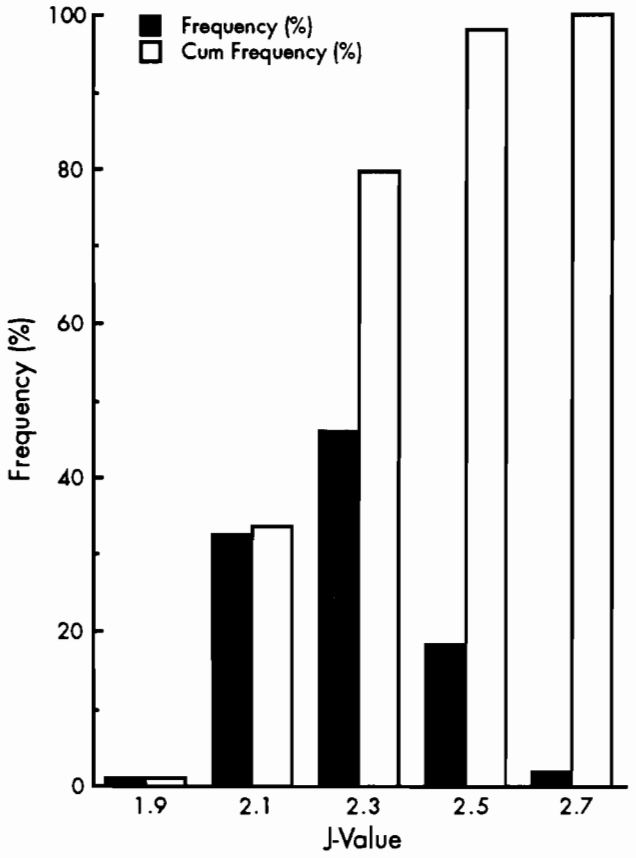

Figure 6.2 Frequencies of J-values at Level 1, PCC shoulder

As shown in Table 6.1, the mean J-values for pavements with an AC shoulder and with a tied PCC shoulder are 2.4 and 2.3, respectively; the standard deviations of the J-values for pavements with an AC shoulder and with a tied PCC shoulder are 0.30 and 0.14, respectively. The 5th percentile of the J-values for pavements with an AC shoulder and with a tied PCC shoulder are almost the same. However, the maximum J-value for pavements with an AC shoulder is 3.7, a value higher than the maximum J-value of 2.7 for pavements with a tied PCC shoulder. Pavements with an AC shoulder have a larger deviation for the J-values, as can be observed in Figures 6.1 and 6.2. Such deviation is perhaps the result of the effects of tied PCC shoulders on reducing pavement edge deflections and erosion near the edge, so that deviation of edge deflections is reduced. Figures 6.1 and 6.2 also show that a J-value of 2.3 has the highest frequency. These data might support the use of 2-inch reductions in thickness in the early stage of CRC pavement design in Texas.

Theoretically, for the best condition (interior loading) the lowest J-value would be 2.3. However, because field values are not always the same as those used for design (i.e., actual slab thickness may be thicker than design thickness and field K-value may also be higher), J-values lower than 2.3 are noted in Figures 6.1 and 6.2. A thicker slab and a higher K-value in the field will result in an obtained J-value lower than the theoretically predicted J-value. After checking the K-values for observations having J-values lower than 2.3, it was found that field K-values corresponding to observations are very high. Some K-values reach 2,000 pci. Figure 6.3 shows the frequencies of the field K-values back-calculated from field measurements on the CRC pavements with an AC shoulder. As the figure shows, more than 30 percent of the observations have a K-value higher than the maximum design K-value, 300 pci.

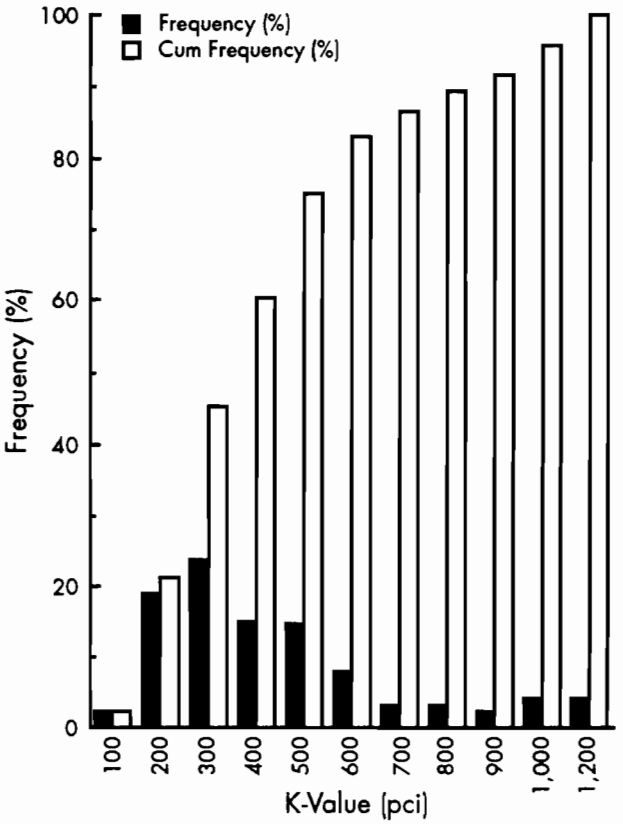

Figure 6.3 Frequencies of modulus of subgrade reactions obtained from field measurements

Table 6.1 Summary of statistics for J-values at Level 1

Shoulder	Mean	STD	COV (%)	Min	Max	5%	95%	OBS
AC	2.4	0.30	12	1.7	3.7	2.0	3.0	483
PCC	2.3	0.14	6	2.0	2.7	2.1	2.5	98

6.1.2 Level 2

At Level 2, J-values for each section were obtained by averaging the J-values in each subsection within the section. The average J-value for the section was treated as an observation, since each subsection within a section has the same structural conditions, namely, the same thickness, the same subgrade condition (e.g., cut and fill), and the same materials (Ref 23). The average J-values for the section would better represent the actual J-value in the pavement section than each subsection J-value. Figures 6.4 and 6.5 show the frequencies of J-values for each section of pavements with an AC shoulder and with a tied PCC shoulder, respectively. A summary of the statistics for the averaged section J-value is presented in Table 6.2.

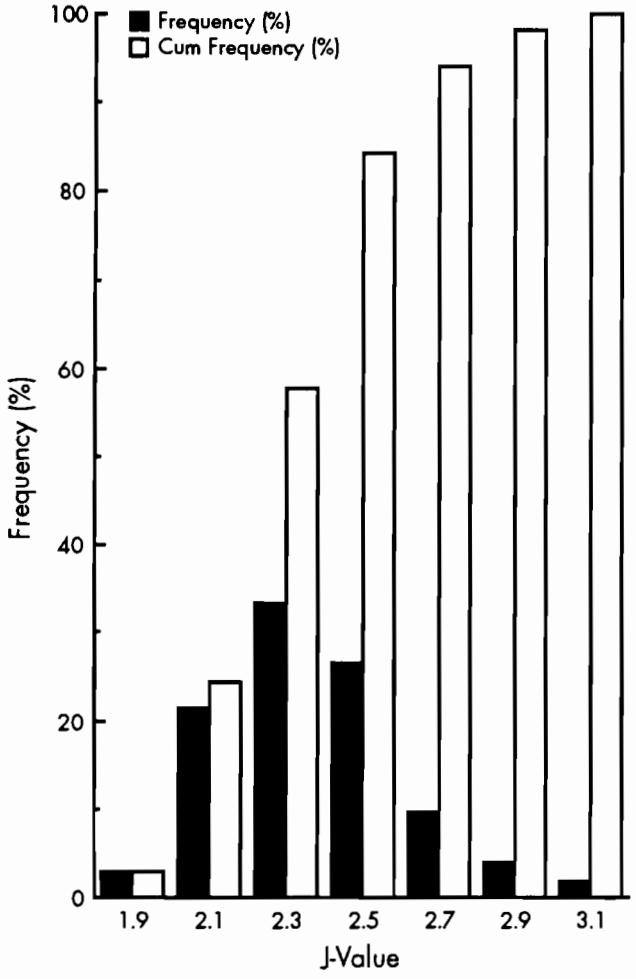

Figure 6.4 Frequencies of J-values at Level 2, AC shoulder

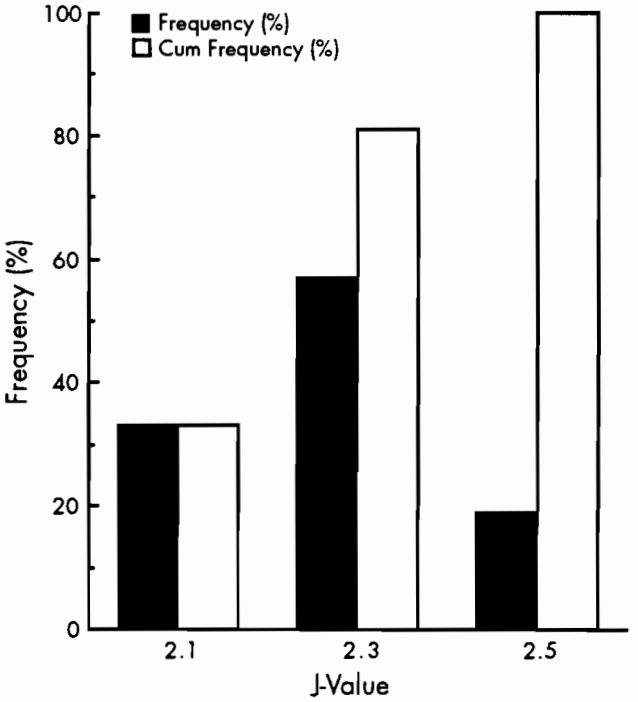

Figure 6.5 Frequencies of J-values at Level 2, PCC shoulder

The mean J-values at Level 2 are the same as those at Level 1. However, standard deviations for the J-values at Level 2 are lower than those at Level 1. The ranges between the minimum J-values and maximum J-values at Level 2 are also narrower than those at Level 1. Again, at Level 2, pavements with a tied PCC shoulder have a lower mean J-value, lower standard deviation, lower coefficient of variation, and a narrower range between minimum and maximum J-values than pavements with an AC shoulder.

6.1.3 Level 3

At Level 3, the J-values for each CFTR section were obtained by averaging the J-values for each subsection within the CFTR section. The average J-values are referred to as CFTR-J for this CFTR section. The standard deviations obtained are referred to as CFTR-STD.

If the effects of roadbed grading and other contract elements are ignored, pavement structures, traffic loads, and environmental conditions within a CFTR section are seen as invariant (Ref 23). Accordingly, the statistics for CFTR-J and CFTR-STD tend to provide information about how much the

Table 6.2 Summary of statistics for J-values at Level 2

Shoulder	Mean	STD	COV (%)	Min	Max	5%	95%	OBS
AC	2.4	0.24	10	2.0	3.2	2.0	2.9	102
PCC	2.3	0.13	6	2.1	2.5	2.1	2.5	21

J-value and standard deviation may vary from this pavement to other pavements and from this location to other locations. Tables 6.3 and 6.4 present a summary of the statistics for CFTR-J and a summary of the statistics for CFTR-STD.

As seen in Table 6.3, the maximum CFTR-J is 3.0, and the minimum is 2.2 for pavements without a tied PCC shoulder. For pavements with a tied PCC shoulder, the minimum is also 2.2, but the maximum is 2.4. As shown in Table 6.4, the mean value of CFTR-STD for pavements with an AC shoulder is 0.21, whereas the mean value of CFTR-STD for pavements with a tied PCC shoulder is 0.08.

6.2 MULTIPLE REGRESSION ANALYSIS OF FIELD J-VALUES

6.2.1 *Stepwise Regression Procedure*

The stepwise regression procedure is one of the most suitable multiple regression procedures available for identifying those independent variables that may have an important influence on the dependent variable. In this study, the forward stepwise regression procedure of the SAS computer package (Ref 50) was used in all multiple linear regression analyses.

6.2.1.1 Regression Model

Supposing that Y is the dependent variable, and X_i (i = 1, 2, 3, ···, K) represents the *ith* independent variable, K is the number of potential independent variables that may influence the dependent variable Y. If a linear relationship is assumed to exist between the independent variables and the dependent variable, the regression model can be written in the following form:

$$Y = b_0 + b_1 X_1 + b_2 X_2 + b_3 X_3 + \cdots + b_k X_k + E \quad (6.1)$$

where

b_0, b_1, b_2, b_3, ···, b_k = estimated regression coefficients, and
E = error term.

In the forward stepwise regression procedure, one independent variable at a time is included in the regression equation. In step 1, the variable most strongly related to the dependent variable is included in the model. In step 2, the next most strongly related variable among the remaining variables is included. This process continues until only variables that are not linearly related to Y, given other variables in the model, remain out of the equation; that is, for each independent variable, the following model is estimated at step 1.

$$Y = b_0 + b_1 X_i + E \quad (6.2)$$

The independent variable (say X_1) having the largest F-statistic becomes the first variable included in the model, if that F-statistic has a significance level greater than a specified value (say 5 percent). In step 2, the remaining K–1 independent variables are tested to determine which, when combined with X_1, provides the best two-variable model of the form

$$Y = b_0 + b_1 X_1 + b_2 X_i + E \quad (6.3)$$

This is accomplished by calculating the F-statistic for b_2 for all the remaining K–1 independent variables and then selecting the independent variable with the largest absolute value of F-statistics to be included in the model, given that the F-statistic

Table 6.3 Summary of statistics for CFTR-J at Level 3

Shoulder	Mean	STD	COV (%)	Min	Max	5%	95%	OBS
AC	2.4	0.21	9	2.2	3.0	2.2	2.8	29
PCC	2.3	0.09	4	2.2	2.4	2.2	2.4	7

Table 6.4 Summary of statistics for CFTR-STD at Level 3

Shoulder	Mean	STD	COV (%)	Min	Max	5%	95%	OBS
AC	0.21	0.11	53	0.04	0.45	0.04	0.40	29
PCC	0.08	0.06	71	0.02	0.19	0.02	0.19	7

also has a significance level greater than a specified level. This process continues until no variable has a significance level greater than the specified level.

6.2.1.2 Definitions and Interpretation of Statistical Terms

The following gives the definition and interpretation of some statistical terms that are used in the analysis, along with the criteria used in the analysis.

Model Fitting Method: The least-squares method is used in the stepwise regression to determine the coefficients of the independent variables in the model. The sum of squares of the deviations from the mean value of observed Y values (SSM) in the model can be expressed in terms of the sum of squares due to regression (SSR) and the sum of squares for error (SSE). These have the following relationship:

$$SSM = SSR + SSE \tag{6.4}$$

where

SSM = Sum of squares for the mean,
SSR = Sum of squares due to regression, and
SSE = Sum of squares for error about the mean.

The SSM, SSR, and SSE, their degrees of freedom (df), and the resulting mean squares (MS) are summarized in the SAS regression output. The MS is determined by dividing the sum of squares by the corresponding degrees of freedom.

F-statistic: If df1 is the degree of freedom associated with SSR, and df2 is the degree of freedom associated with SSE, the F-statistic can be defined as

$$F = \frac{SSR / df1}{SSE / df2} \tag{6.5}$$

or

$$F = \frac{MS \text{ due to regression}}{MS \text{ due to error}} \tag{6.5a}$$

This F-statistic has an F distribution with df1 and df2 degrees of freedom.

Given the following test:

Null hypothesis H_0: $b_1 = b_2 = b_3 = \ldots = b_k = 0$
Alternative hypothesis H_1: Not all b_i $(i > 0)$ equal to zero.

If the calculated F-statistic is greater than the given critical F-value, the null hypothesis is rejected and the alternative hypothesis is accepted. In other words, not all the coefficients are equal to zero.

In the stepwise regression, a partial F-statistic for each included variable is also given. The partial F-statistic for each included variable is obtained by testing the null hypothesis, H_0: $b_i = 0$, against the alternative hypothesis, H_1: $b_i \neq 0$, for the variable X_i only.

Coefficient of Multiple Determination: The coefficient of multiple determination is the ratio of SSR to SSM and is designated by the symbol R^2. R^2 is a measure of the predictive power of the regression. Obviously, R^2 can approach two extreme values: zero and one. In the case of an R^2 of zero, no linear relationship exists between the independent and dependent variables in the model. In the case of R^2 equal to one, a perfect linear relationship exists. R^2 is also closely related to the F-statistic.

The stepwise procedure in the SAS also gives the partial R^2 in the printout as the proportion of the sum of squares for error removed by adding an independent variable into the regression model. (For detailed information and a rigorous discussion about the stepwise regression procedure and SAS computer package, see Refs 50, 51, and 52.)

6.2.1.3 Criteria for Adding and Excluding Independent Variables

In the SAS computer package, a user can specify the significance level for entry into the model used in the forward stepwise regression procedure. If the largest partial F-statistic for an independent variable has a significance level greater than the specified level, this independent variable is included into the model; otherwise, it is excluded. In this study, the purpose of the statistical analysis of the field J-values is to identify those variables that may have an important influence on the J-value. Therefore, a high significance level of one percent was used in the analysis to guard against including unimportant variables that do not significantly influence the J-value.

6.2.2 Application of Stepwise Regression Procedure

6.2.2.1 Description of Variables

The linear regression model defined in Equation 6.1 was used for all the regression analyses. The dependent variable is the J-factor and is a continuous variable. Independent variables considered in the regression analyses are listed in Table 6.5.

Table 6.5 Independent variables considered in stepwise regression analysis

Continous Variables:

D = slab thickness;
RK = LOG (KF/KD);
RE = EF/ED;
RAIN = average annual rainfall;
TEMP = annual lowest temperature;
LA = LOG (pavement age +1);
LADT = LOG (ADT85); and
LTRAF = LOG (ADT85 x pavement age + 1).

Dichotomous or Dummy Variables:

SRG = 1 SRG – Siliceous River Gravel; 0 Otherwise

LS = 1 LS – Limestone; 0 Otherwise

ACT = 1 ACT – Asphalt Cement Stabilized; 0 Otherwise

CT = 1 CT – Portland Cement Stabilized; 0 Otherwise

LT = 1 LT – Lime treated; 0 Otherwise

SOILH = 1 High Swelling Soil; 0 Otherwise

SH = 1 AC shoulder – Asphalt Concrete Shoulder; 0 Otherwise

These independent variables include most of the variables listed in Chapter 5, with some additional treatments made, including the use of log transformation (preliminary analysis showed that such treatments gave better results). These independent variables can be grouped into two categories: continuous or quantitative variables, and dichotomous or dummy variables.

The continuous variables include the slab thickness (D), log transformation of the ratio (RK) of field K-value (KF) to design K-value (KD), ratio (RE) of field E-value (EF) to design E-value (EF), average annual rainfall (RAIN), annual lowest temperature (TEMP), log transformation of the pavement age (LA), log transformation of the ADT collected in 1985 (LADT), and LTRAF, which is equal to log (pavement age × ADT85 + 1). A log base of 10 was used.

The dichotomous variables have only two values: zero and one. They are used to signify observations that belong to one category or the other. Therefore, m categories can be represented by (m–1) dichotomous variables. It is important to realize that the numerical values of a dichotomous variable do not reflect any quantitative ranking of the categories. The dichotomous variables include SRG, LS (identifying coarse aggregate type); ACT, CT, LT (identifying subbase type); SOILH (identifying soil type); and SH (identifying shoulder type). Altogether, there are 15 continuous and dummy variables considered in the multiple regression analysis.

6.2.2.2 *Data Set-Up for Regression Analysis*

Different data sets were set up for the regression analysis. The first data set was the combined data set, composed of a total of 581 data points. The combined data set was then subdivided into subsets so that some of the independent variables could be controlled by placing a constant value on them. Regression equations developed for each data set were assessed according to the values of the corresponding R^2 statistics. Table 6.6 describes all the data sets used in the regression analysis.

6.2.2.3 *Estimated Regression Equations and Statistics*

The results of the regression analyses on different data sets are summarized in this section. Table 6.7 presents the independent variables in the final regression equations, the estimated parameters, and the model R^2 value. The independent variables in the final regression equations are presented in order of decreasing importance as determined by the partial R^2 value.

Combined Data Sets (Data Set T): Five variables, which include RK, LS, RAIN, CT, and SH, are significant at the given significance level of 1 percent in this data set. The most influential variable in the regression equation is RK, whose coefficient is negative. This finding indicates that the higher the value of RK, the lower the J-value. In other words, a high K-value in the field will result in a lower J-value. The inclusion of variable SH in the regression equation indicates that there is a difference in the J-value between pavements with a tied PCC shoulder and those without a tied PCC shoulder. The positive sign of the coefficient of SH shows that pavements with an AC shoulder have a higher J-value than those with a tied PCC shoulder. As expected, rainfall has a negative effect on pavement performance and results in a higher J-value, as shown by the positive coefficient in the variable RAIN.

It is noted that limestone pavements have a higher J-value compared with other aggregate pavements. In addition, pavements with a

portland-cement-stabilized subbase have a higher J-value. These results seem contrary to expectations. One cause could be the use of a low E-value (4 million psi) as a design value for limestone pavements and a high K-value (300 pci) as a design value for portland-cement-stabilized subbases.

As seen in Table 6.8, the field E-values that are back-calculated from the in-service pavements with limestone aggregate type are higher than those used for the design. The difference between the E-value in the field and that used in the design for limestone pavements is the largest compared with the other two aggregate pavements.

Table 6.6 Data sets used in the regression analysis

Data Set Designation	Data Points	Description	Independent Variables (fixed)
T	581	All data points	
AC	483	Data points from pavements with an AC shoulder	SH
PC	98	Data points from pavements with a tied PCC shoulder	SH
AC-H	172	Data points from pavements with an AC shoulder and high swelling soil	SH, SOILH
AC-L	311	Data points from pavements with an AC shoulder and low swelling soil	SH, SOILH
AC-H-SRG	73	Data points from SRG pavements with an AC shoulder and high swelling soil	SH, SOILH, SRG
AC-H-LS	99	Data points from LS pavements with an AC shoulder and high swelling soil	SH, SOILH, LS
AC-L-SRG	97	Data points from SRG pavements with an AC shoulder and low swelling soil	SH, SOILH, SRG
AC-L-LS	73	Data points from LS pavements with an AC shoulder and low swelling soil	SH, SOILH, LS
AC-H-ACT	88	Data points from pavements with an AC shoulder, ACT subbase and high swelling soil	SH, SOILH, ACT
AC-H-LT	64	Data points from pavements with an AC shoulder, LT subbase and high swelling soil	SH, SOILH, LT
AC-L-ACT	69	Data points from pavements with an AC shoulder, ACT subbase and low swelling soil	SH, SOILH, ACT
AC-L-LT	48	Data points from pavements with an AC shoulder, LT subbase and low swelling soil	SH, SOILH, LT

Portland-cement-stabilized subbase was expected to have a higher K-value; however, it had the lowest field K-value (which was back-calculated from the in-service pavements with portland-cement-stabilized subbase) compared to the other three types of subbase.

Also note that, because the R^2 for the model is only 0.47, the combined data sets were further subdivided. The following is a discussion of the results of this data-set subdivision.

Table 6.7 Summary of regression analysis results

Data Set	Ranking of Independent Variable	Coefficient of Independent Variable	Model R^2
T	RK	-0.63	0.34
	LS	0.15	0.42
	RAIN	0.003	0.44
	CT	0.08	0.46
	SH	0.1	0.47
	constant	2.2	
AC	RK	-0.63	0.35
	LS	0.17	0.41
	CT	0.12	0.44
	constant	2.4	
PC	RK	-0.56	.97
	RE	0.2	0.997
	TEMP	0.0003	0.998
	ACT	-0.004	0.998
	constant	2.1	
AC-H	RK	-0.71	0.36
	RE	0.24	0.38
	TEMP	0.01	0.43
	LADT	0.3	0.45
	ACT	-0.13	0.48
	constant	0.6	
AC-L	RK	-0.5	0.32
	LS	0.2	0.45
	CT	0.1	0.48
	constant	2.3	
AC-H-SRG	RK	-0.8	0.4
	RAIN	0.096	0.5
	constant	-1.33	
AC-H-LS	RK	-0.7	0.34
	LS	0.3	0.39
	constant	2.5	
AC-L-SRG	RK	-0.6	0.85
	constant	2.3	
AC-L-LS	RK	0.6	0.38
	CT	0.3	0.46
	constant	2.5	
AC-H-ACT	RK	-0.7	0.52
	RE	0.3	0.56
	constant	2.1	
AC-H-CT	RK	-1	0.36
	constant	2.6	
AC-L-ACT	RK	-0.6	0.19
	LS	0.2	0.26
	constant	2.3	
AC-L-CT	LS	0.5	0.4
	RK	-0.8	0.7
	constant	2.3	

Table 6.8 Comparison of field and design values

	E-Value (million psi)			K-Value (pci)			
	SRG	LS	SRG/LS	ACT	CT	LT	CRS
Design	5.0	4	4.5	250	300	225	200
Field	5.6	5.6	5.0	376	376	405	509
Percent Difference	12	40	13	25	25	80	55

$$\text{Percent Difference} = \frac{\text{Field} - \text{Design}}{\text{Design}} \times 100\%$$

Effect of Temperature: In data sets PC and AC-H, TEMP is included in the regression equations for both data sets. The positive coefficient indicates that the higher the temperature, the higher the J-value. The effect of annual low temperatures on pavements that have an AC shoulder and that are constructed over high swelling soil is larger than that on pavements having a tied PCC shoulder, as can be seen from the difference in the absolute value of the coefficients in the two data sets. A high annual low temperature implies a large variation of temperature; and a larger variation of temperature has a higher J-value.

Effect of Rainfall: The effect of rainfall on the J-value has been discussed above. We might note in addition that the effect of rainfall on the J-value for pavements over low swelling soil may not be the same as for pavements over high swelling soil. This difference can be seen by comparing the regression equations from data set AC-H-SRG with data set AC-L-SRG. This comparison indicates that rainfall has a significant effect on the J-value for pavements over high swelling soil, while the effect of rainfall is not significant for pavements over low swelling soil.

Effect of Traffic: The effect of average daily traffic (ADT) on the J-value can be found in the regression equation on data set AC-H. The positive coefficient indicates that a higher J-value is needed for higher ADT. It is noted that the log transformation of the product of ADT and pavement age is not significant in all the data sets. If a higher ADT implies heavier traffic, then this result may imply that CRC pavements can have a very long service life when the pavement is not subjected to heavy traffic.

Effect of Slab Thickness: Slab thickness does not appear to be significant for all the regression analyses on different data sets. However, it should be realized that more than 80 percent of the data points are from 8-inch pavements, and the results may be subject to this limitation. Further investigation is recommended.

Effect of Coarse Aggregate Type: The effect of coarse aggregate type on the J-value is observed from the analysis results. No conclusion is made here because of the reasons explained in this section.

Effect of Subbase Treatment Type: While the effect of different subbase treatments on the J-value is evident, no conclusion is made here because of the reasons explained in this section.

In summary, the analysis shows that a higher J-value relates to conditions with a lower K-value, a higher E-value, a higher annual minimum temperature, a higher rainfall, and heavier traffic. Commonly, a low K-value is often related to a high swelling soil and a large rainfall, and a high E-value may be related to high thermal coefficient coarse aggregates used in the concrete. Therefore, heavier traffic, higher annual low temperatures, pavements made with higher thermal coefficient coarse aggregates, and higher rainfall will all require a higher J-value for the design of CRC pavements.

6.3 SUMMARY

In the first part of this chapter, three different levels of statistics for the field J-values obtained in Chapter 5 were determined. A multiple regression analysis of each J-value was performed in order to identify those variables that may have an important influence on the J-value. A stepwise regression procedure was employed in all regression analyses. The multiple regression analysis results show that modulus of subgrade reaction, concrete modulus of elasticity, annual lowest temperature, average annual rainfall, and average daily traffic all appear to be significant variables. The most influential variable is the modulus of subgrade reaction. A higher modulus of subgrade reaction results in a lower J-value. However, a higher concrete modulus of elasticity results in a higher J-value.

CHAPTER 7. DISCUSSION OF THE RESULTS

Following a discussion of the statistical results of the J-values obtained in Chapter 6, this chapter recommends final load transfer coefficients for the design of CRC pavements in Texas. In addition, a comparison is made between the final load transfer coefficients and those previously developed.

7.1 DETERMINATION OF FINAL LOAD TRANSFER COEFFICIENTS

A summary of the statistics for the J-values determined at three different levels for CRC pavements with an AC shoulder is presented in Table 7.1. The summary of the statistics for the J-values at three different levels for CRC pavements with a tied PCC shoulder is presented in Table 7.2.

Table 7.1 Summary of statistics for the J-values, AC shoulder

Level	Mean	STD	Min	Max	5%	95%
1	2.4	0.30	1.7	3.7	2.0	3.0
2	2.4	0.24	2.0	3.2	2.1	2.9
3	2.4	0.21	2.2	3.0	2.2	2.8

Table 7.2 Summary of statistics for the J-values, PCC shoulder

Level	Mean	STD	Min	Max	5%	95%
1	2.3	0.14	2.0	2.7	2.1	2.5
2	2.3	0.13	2.1	2.5	2.1	2.5
3	2.3	0.10	2.2	2.4	2.2	2.4

As seen in Table 7.1, the mean J-value for CRC pavements with an AC shoulder is 2.4 at all three levels. This value can be used as a lower boundary for the J-value used in the design of CRC pavements in Texas. The 95th percentile of the J-value obtained at Level 1—3.0—can be used as an upper boundary for the J-value. This value is also the maximum J-value at Level 3. In other words, there is a 95 percent confidence level in using this value in Texas. A J-value of 2.9 (the 95th percentile for the J-value at Level 2) is recommended for the design. The recommended standard deviation for the J-values of CRC pavements with an AC shoulder is 0.21 (from the mean value of CFTR-STD, as shown in Table 6.4).

Regarding the design of CRC pavements with a tied PCC shoulder, a J-value of 2.3 (the mean J-value determined at all three levels, as shown in Table 7.2, and the minimum J-value recommended by the AASHTO Guide for the design of this type of pavement) can be used as a lower boundary. The 95th percentile of the J-value determined at Level 1 is 2.5, which is recommended for the design of CRC pavements with a tied PCC shoulder. The selected standard deviation of the J-value for CRC pavements with a tied PCC shoulder is 0.08 (from the mean value of CFTR-STD in Table 6.4). This is a significantly lower standard deviation than that for CRC pavements with an AC shoulder, indicating the effects of tied PCC shoulders on reducing deflections and variations at the pavement edge. Considering the standard deviation of 0.08 for the J-value and a mean J-value of 2.3, a J-value of 2.6 is recommended for the design of CRC pavements with a tied PCC shoulder. This upper boundary J-value is a little higher than the maximum J-value of 2.4 at Level 3 and the maximum J-value of 2.5 at Level 2, but is lower than the maximum J-value of 2.7 at Level 1. Again, considering the J-value range of 2.3 to 2.6 for CRC pavements with a tied PCC shoulder, we selected a J-value range of 2.6 to 3.0 for CRC pavements with an AC shoulder (to minimize overlap).

7.2 COMPARISON OF THE J-VALUES DEVELOPED IN THIS STUDY WITH THOSE PREVIOUSLY DEVELOPED

Table 7.3 compares the recommended J-values and standard deviations derived from this study with those developed in the past. Standard deviations are presented in parentheses near the corresponding J-values. The present study is referred to in the table as Project 1169.

It is noted that the range of J-values for CRC pavements with tied PCC shoulders recommended

in this study is the same as that in Volume 2 of the AASHTO guide. However, the range of J-values recommended in this study for CRC pavements with AC shoulders is somewhat different from that found in Volume 2 of the AASHTO guide. Treybig presented an estimate of the standard deviation of J-values for CRC pavements with an AC shoulder; his estimate was based on experience (Ref 11). This estimated standard deviation is almost the same as that obtained in this study. Volume 1 of the AASHTO guide uses J-values that are somewhat higher than those obtained in this study.

Overall, this study shows, for the first time using field deflection measurements, that the ranges of J-values recommended by the AASHTO guide are reasonable. Furthermore, the standard deviations of J-values for CRC pavements for two types of pavement shoulders were obtained in this study.

On the other hand, it should be kept in mind that the recommended J-values in this study were obtained from deflections taken in the summer. If pavement deflections vary greatly from season to season, the J-values may need to be adjusted. Further research under other seasonal conditions, including winter conditions, is recommended. In addition, these J-values are also based on good load transfer conditions of in-service CRC pavements in Texas; that is, appropriate reinforcements are required to keep the cracks held tightly so that the loss of load transfer is not significant enough to cause critical stress to occur at the cracks. Accordingly, it would be useful to establish some relationship between load transfer and crack width (or crack spacing). Crack width and crack spacing can be predicted from some theoretical models, such as CRCP7, developed at the Center for Transportation Research. Load transfer can then be predicted from given construction conditions, pavement structure, material properties, and load applications. This would result in a significant improvement in pavement performance predictions.

Table 7.3 Comparison of the J-values derived from this study with those previously developed

		Load Transfer Coefficient	
Year	Procedure/Author	CRCP with an AC shoulder	CRCP with a tied PCC shoulder
1963	Hudson and McCullough (Ref 9)	2.2	/
1969	Trebig (Ref 11)	2.33 (0.19)	/
1972	NCHRP Report 128 (Ref 14)	2.2	/
1972	ACI (Ref 15)	2.2	/
1981	ARBP (Ref 20)	3.2	2.56
1986	AASHTO, Vol. 2 (Ref 7)	2.6 - 3.1	2.3 - 2.6
1986	AASHTO, Vol. 1 (Ref 6)	2.9 - 3.2	2.3 - 2.9
1990	Project 1169	2.6 - 3.0 (0.21)	2.3 - 2.6 (0.08)

CHAPTER 8. IMPLEMENTATION

Because proper implementation of the research findings in the design process is one of the most effective ways to improve pavement design, reduce the cost of pavement construction, and, thus, maximize benefits, this chapter describes and discusses procedures for implementing the findings of this study. The first part of the chapter discusses the implementation of the J-factor model for obtaining load transfer coefficients (J-values) from field deflection measurements for the design of CRC pavements at the project level. The remainder of the chapter describes the implications of implementing the load transfer coefficient developed in this study for designing CRC pavements in Texas (for use with the AASHTO guide).

8.1 IMPLEMENTATION OF THE J-FACTOR MODEL

Implementation of the J-factor model includes the following steps or elements: rigid pavement type identification, section information, sample size determination, deflection measurements, temperature gradient measurements, load transfer efficiency analysis, calculation of load transfer coefficients, and determination of design J-values. These steps, outlined in Figure 8.1, are discussed in more detail below.

8.1.1 Rigid Pavement Type Identification

While the J-factor model developed in this study (see Chapter 4) can be applied to two types of rigid pavement (continuously reinforced concrete pavements, or CRC pavements, and jointed concrete pavements), only CRC pavements are discussed with respect to the procedure for obtaining load transfer coefficients. It is necessary to identify pavement type so that the proper procedure can be used.

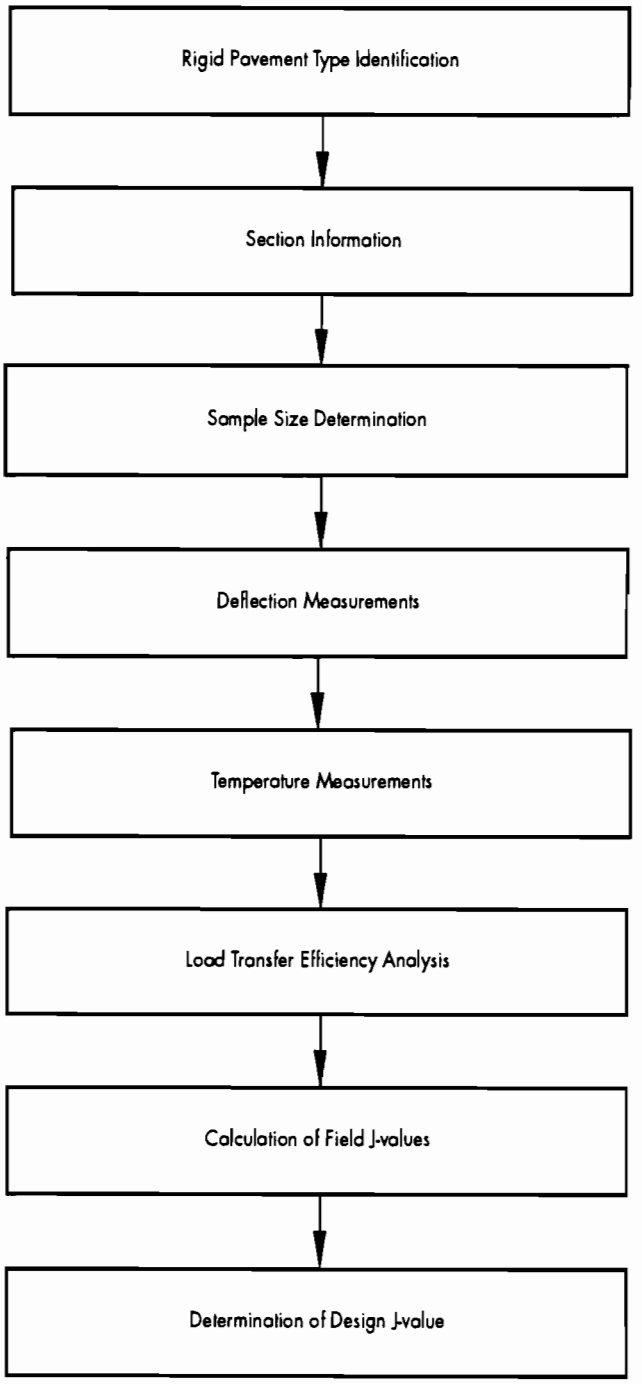

Figure 8.1 Steps for implementation of the J-factor model

8.1.2 Section Information

Section information may include the following items:

(1) Pavement structures: thickness (D), coarse aggregate type, subbase type, soil condition, shoulder type, and original design values (i.e., D, E-value, and K-value) for the pavement structure.
(2) Pavement conditions: distress types, such as the number of transverse cracks in the section.
(3) Traffic: percent of trucks, ADT, number of load applications, and pavement age.
(4) Environmental conditions: rainfall and temperature variations.

This information can be used for both short-term and long-term analysis. (More information about procedures for obtaining the above information can be found in Ref 23.)

8.1.3 Sample Size Determination

For continuously reinforced concrete pavements (given a section length, L in feet), the sample size can be determined as follows:

$$N = \frac{1}{\left(\frac{a}{(Z_\alpha)C}\right)^2 + \frac{1}{M}} \qquad (8.1)$$

where

a = allowable error, percentage of the mean;
C = correlation coefficient;
Z_α = number of standard deviations from the mean (of the J-value) for a normal distribution with a confidence level of α;
M = L/X; and
X = mean crack spacing for a selected section (feet).

For a given set of conditions, that is, L = 1,000 feet, X = 5 feet, a = 5 percent, C = 0.2/2.4, and α = 0.05, the required sample size is N = 7. This result gives an approximate 200-foot interval between the two consecutive measurement sets (see Section 8.1.4 for the definition of a measurement set). As a rule of thumb, five measurement sets can be used for a 1,000-foot section. (For more information, see Refs 54, 55, and 56.)

8.1.4 Deflection Measurement Procedures

A falling weight deflectometer (FWD) was used to show the procedure for deflection measurements; however, the principle can be applied to other types of deflection measurement tools. A conventional FWD has seven sensors that can measure deflections at seven different positions under an applied load. Two types of sensor arrangements, called geophone configurations, are recommended to collect deflection data. The Type 1 geophone configuration is shown in Figure 8.2, while Type 2 is shown in Figure 8.3. The Type 1 geophone configuration can be used for back-calculating pavement layer properties; Type 2 can be used for the analysis of load transfer at joints/cracks.

Deflection measurements for CRC pavements are outlined in Figure 8.4. The measurements include two paths: (1) interior path, 6 feet from the edge, and (2) edge path, 6 inches from the edge. The allowable measurement path error (away from the path) should be less than 3 inches (to reduce the measurement error). As shown in Figure 8.4, four measurement points related to the transverse cracks in the crack slab (Points 1, 2, 3, and 4) are counted as a measurement set. Point 1 is on an interior path; Points 2, 3, and 4 are on the edge path. It is recommended that at least one selected location have a crack spacing of no less than 8 feet, in order to minimize the effects of cracks on back-calculated pavement properties.

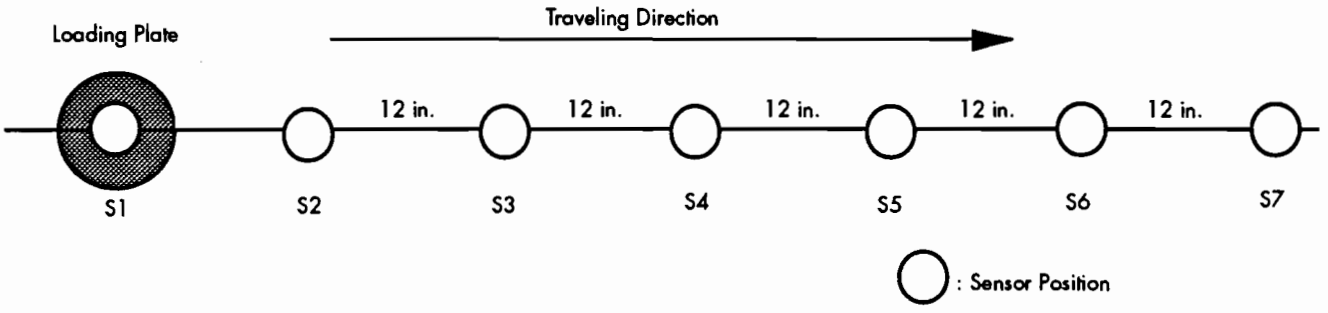

Figure 8.2 Type 1 geophone configuration

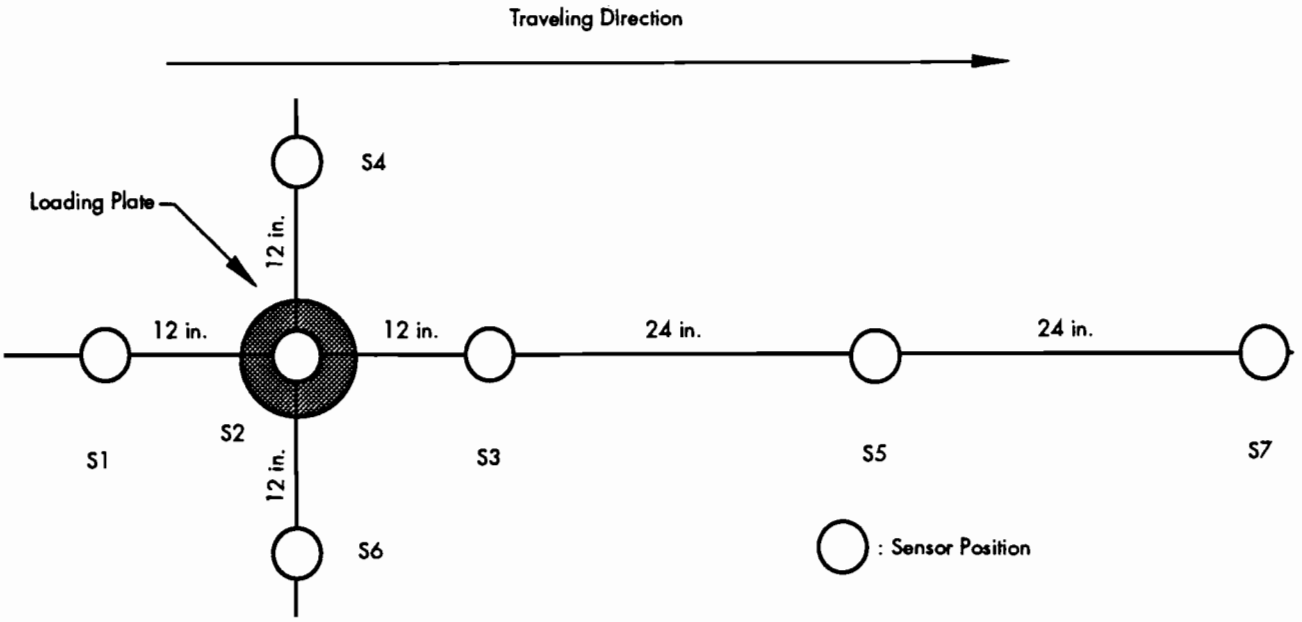

Figure 8.3 Type 2 geophone configuration

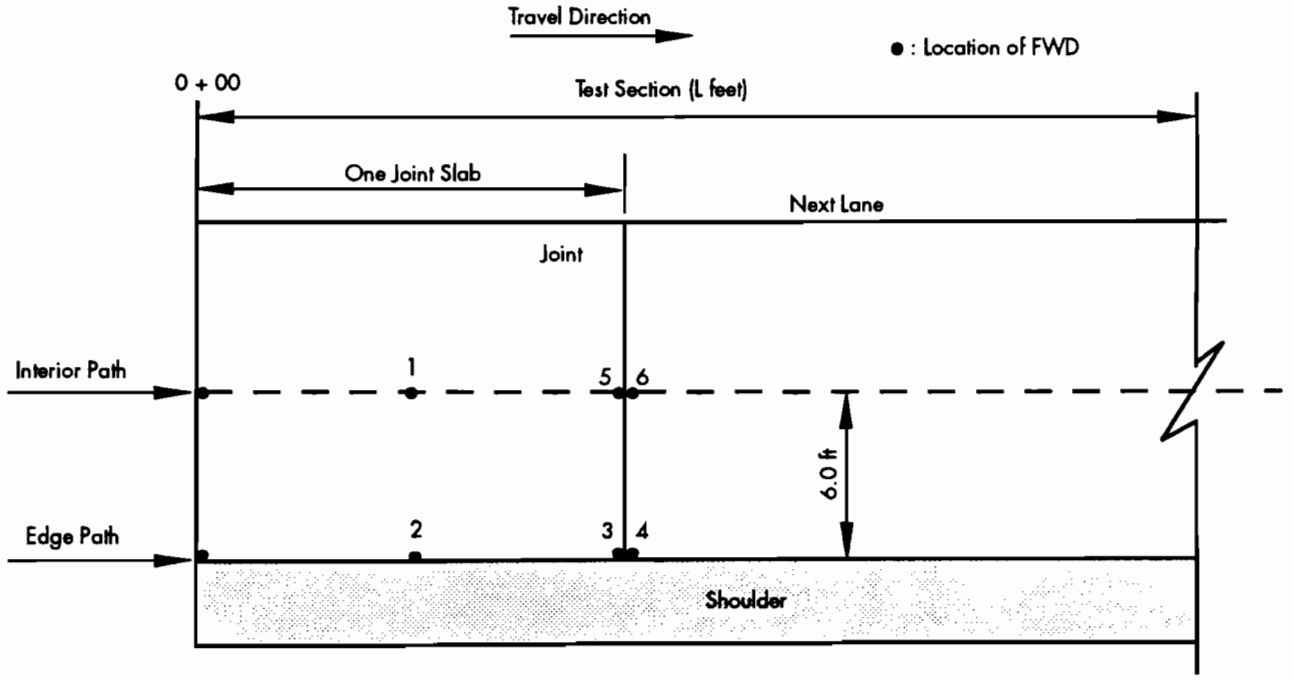

Figure 8.4 Deflection measurements of CRC pavement

8.1.5 Temperature Gradient Measurements

Actual temperature gradient measurements are recommended during deflection measurements. These measurements may be taken by drilling three holes of differing depths in the pavement section just beyond the selected section. The three depths can be at 1 inch from the surface, at half depth of the slab thickness, and at 1 inch above the bottom of the slab bottom, as shown in Figure 8.5. After clearing the dust from the hole, a small amount of mineral oil (or similar heat transfer agent) should be placed in the bottom of the hole (to a depth of 1 inch or less) in order to provide thermal conduction. A hand-held thermometer with electronic readout can then be used to record temperatures at the three different slab depths. After drilling the hole, a 15-minute delay in temperature measurement is expected. The temperature measurements should be collected hourly for the duration of the deflection testing for a given section. The time at

which temperature readings were taken should also be recorded. (More information about this method can be found in Ref 57.) On the other hand, if it is not feasible to measure directly the temperature gradient of the in-service pavement, a portable slab can be used to estimate the temperature gradient of the in-service pavement (Ref 59).

Once temperature differentials are known for a given deflection measurement, the correction of temperature differential effects on the deflection measurement can be accomplished using the procedure described in Chapter 5.

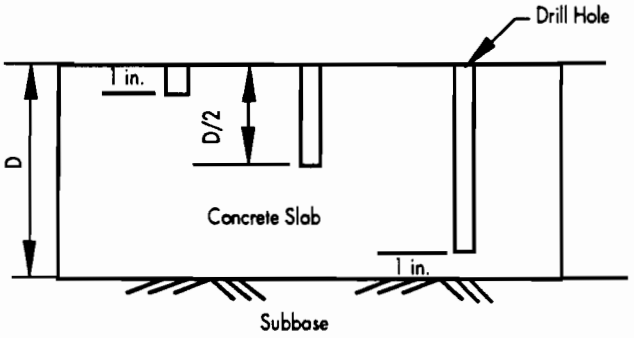

Figure 8.5 Illustration of temperature gradient measurements

8.1.6 Load Transfer Efficiency Analysis

The procedure developed in Chapter 3 can be used to evaluate load transfer efficiencies of crack/joints and corner/edge conditions. The procedure may also include use of Equations 3.1, 3.10, and 3.11.

8.1.7 Calculation of J-Values from Measurements

For CRC pavements, if the load transfer efficiency evaluation in Section 8.1.6 shows that the load transfer efficiencies at the cracks are higher than 90 percent, and the ratio of corner deflections to edge deflections is around 1.0, then the J-factor model developed for CRC pavements in Chapter 4 can be used directly. In the case of poor load transfer efficiencies at the cracks, that is, when the ratio of corner deflections to edge deflections is greater than 1.1, finite-element models should be used to estimate field stresses. Equation 4.6 can then be used to calculate the J-values.

8.1.8 Determination of Design J-Values

The procedure described in Chapter 6 can be used to determine the design J-values. Users can select a desired confidence level for choosing a design J-value.

8.2 IMPLEMENTATION OF LOAD TRANSFER COEFFICIENTS DEVELOPED IN THIS STUDY

Table 8.1 shows the load transfer coefficients developed in this study. For the design of CRC pavements with a tied PCC shoulder, the J-value ranges from 2.3 to 2.6, with a recommended value of 2.5. For the design of CRC pavements with an AC shoulder, the J-value ranges from 2.6 to 3.0, with a recommended value of 2.9. The low J-values can be used for those conditions associated with low rainfall, minimum temperature variation, and a low percentage of heavy trucks. Table 8.2 presents the recommended design J-values for different design conditions (e.g., percent of heavy trucks of ADT, average annual rainfall).

Table 8.1 Load transfer coefficients for CRCP in Texas

CRCP Group	Load Transfer Type	Load Transfer Coefficient
1	Load transfer devices at the cracks with a tied PCC shoulder	2.3 - 2.6
2	Load transfer devices at the cracks with an AC shoulder	2.6 - 3.0

Table 8.2 J-values for different design conditions

Shoulder Type	% Trucks of ADT	Average Annual Rainfall (in.)	J-value
Tied PCC	< 10	< 30	2.3
		≥ 30	2.4
	≥ 10	< 30	2.5
		≥ 30	2.6
AC	< 10	< 30	2.6
		≥ 30	2.7
	≥ 10	< 30	2.8
		≥ 30	3.0

Figure 8.6 shows the effect of load transfer coefficients on slab thickness for an example design condition given in Table 8.3, based on the AASHTO guide procedure. Ranges of J-values recommended in this study and those in the AASHTO guide are also indicated in the figure.

Table 8.4 presents the standard deviations of the J-values for CRC pavements with two types of pavement shoulder. For CRC pavements with a tied PCC shoulder, the standard deviation of the J-value is 0.08, while for CRC pavements with an AC

shoulder, the standard deviation of the J-value is 0.21. The use of these standard deviations results in the combined standard errors for traffic and performance predictions (S_0) (Ref 6) of 0.39 and 0.42 for CRC pavements with a tied PCC shoulder and for CRC pavements with an AC shoulder, respectively (see Ref 7). Table 8.5 shows the standard deviations of the traffic and performance predictions (S_0) for the design of CRC pavements with the two types of pavement shoulders.

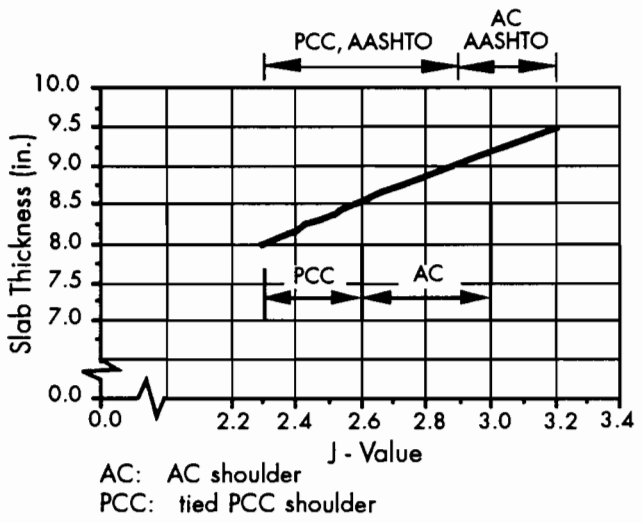

Figure 8.6 Effect of J-value on slab thickness

Table 8.3 Example design conditions

K = 100 psi	E = 4,00,00 psi
S_c = 800 psi	C_d = 1.0
S_0 = 0.39	R = 90 percent
ΔPSI = 4.5 – 3.0 = 1.5	$W_{18} = 6.50 \times 10^6$

Supposing that a load transfer coefficient of 2.5 is used for the design of a CRC pavement with a tied PCC shoulder and that a load transfer coefficient of 2.9 is used for a CRC pavement with an AC shoulder, Figure 8.7 shows the effect of reliability and the standard deviation for the traffic and performance predictions (S_0) on slab thickness for the two types of pavement shoulders for the design conditions given in Table 8.3.

As can be seen from Figure 8.7, the effect of reliability on slab thickness for a CRC pavement with an AC shoulder is greater than that for a CRC pavement with a tied PCC shoulder. In other words, when considering higher levels of reliability, the thickness for a CRC pavement with an AC shoulder increases faster than that for a CRC pavement with a tied PCC shoulder. This effect shows one of the advantages of using tied PCC shoulders for CRC pavements: less thickness is required for higher reliability.

Table 8.4 Standard deviation of J-value

CRCP Group	Load Transfer Type	Standard Deviation
1	Load transfer devices at the cracks with a tied PCC shoulder	0.08
2	Load transfer devices at the cracks with an AC shoulder	0.21

Table 8.5 Standard deviation of traffic and performance predictions

CRCP Group	Load Transfer Type	Standard Deviation of Reliability S_0
1	Load transfer devices at the cracks with a tied PCC shoulder	0.39
2	Load transfer devices at the cracks with an AC shoulder	0.42

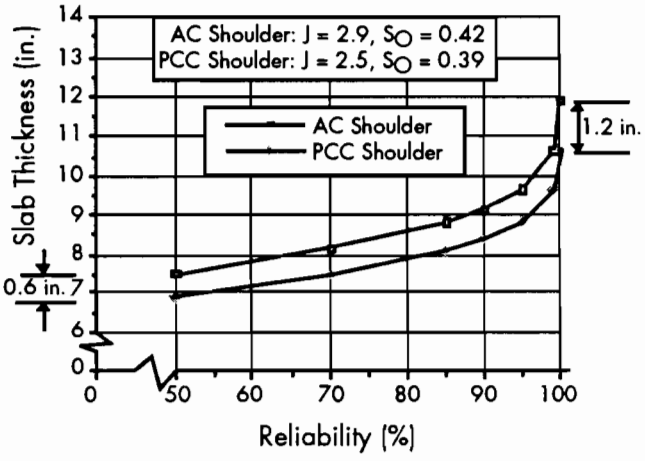

Figure 8.7 Effect of reliability on slab thickness

CHAPTER 9. SUMMARY, CONCLUSIONS, AND RECOMMENDATIONS

9.1 SUMMARY

The main objective of this study was to develop load transfer coefficients for use with the AASHTO guide for the design of CRC pavements in Texas based on field measurements. In conjunction with this objective, an evaluation of structural conditions of in-service CRC pavements in Texas was performed to assess the abilities of in-service CRC pavements to transfer load across cracks and joints. A rational procedure was developed for obtaining load transfer coefficients for rigid pavements based on field deflection measurements, and field load transfer coefficients were determined using information available in the rigid pavement database at the Center for Transportation Research of The University of Texas at Austin.

9.2 CONCLUSIONS

The following conclusions are based on the analyses presented in previous chapters and on the results obtained in this study:

(1) The J-value for CRC pavements with an asphaltic concrete shoulder in Texas ranges from 2.6 to 3.0. A J-value of 2.9 can be used in the design of this type of pavement. The standard deviation of the J-value for this type of pavement is 0.21 (refer to Tables 8.1 and 8.4).
(2) The J-value for CRC pavements with a tied portland cement concrete shoulder ranges from 2.3 to 2.6. A J-value of 2.5 can be used in the design of this type of pavement. The standard deviation of the J-value for this type of pavement is 0.08 (refer to Tables 8.1 and 8.4).
(3) Low J-value is related to subbases with a high modulus of subgrade reaction, low rainfall, concrete with low thermal-coefficient coarse aggregates, and light traffic conditions.
(4) Texas CRC pavement design practice provides good load transfer at the cracks. Average load transfer efficiencies at the cracks are about 95 percent for in-service CRC pavements, as determined using the Teller procedure based on the summer deflection measurements.
(5) The difference between edge and interior deflections is significant. The average ratio of edge deflection to interior deflection varies with slab thickness and shoulder type. Pavements with a tied shoulder have a lower average ratio, indicating the effect of the pavement shoulder on reducing pavement edge deflections. The average ratio decreases with an increase in slab thickness.

9.3 RECOMMENDATIONS FOR USE OF LOAD TRANSFER COEFFICIENT

The following recommendations are based on the results and findings of this study:

(1) Different load transfer coefficients should be used in the design of CRC pavements with an AC shoulder (as opposed to those with a tied PCC shoulder). For the design of CRC pavements with an AC shoulder, the range of J-values is between 2.6 and 3.0, with a recommended value of 2.9. For the design of CRC pavements with a tied PCC shoulder, the range of J-values is between 2.3 and 2.6, with a recommended value of 2.5.
(2) Different standard deviations of load transfer coefficients should be used for the reliability design of CRC pavements with an AC shoulder (as opposed to those with a tied PCC shoulder). For the design of CRC pavements with an AC shoulder, a value of 0.21 is recommended. For the design of CRC pavements with a tied PCC shoulder, a value of 0.08 is recommended.
(3) The following guidelines are also recommended: a higher J-value should be used when there are large variations of temperature in the region, or when the coarse aggregates have a high thermal coefficient. Regions with more rainfall should also use a higher J-value. Pavements designed for a high percentage of heavy truck loads and high equivalent load

applications should also use a higher J-value. If a stiffer subbase having a high modulus of subgrade reaction is used, a lower J-value may be acceptable.

9.4 RECOMMENDATIONS FOR FUTURE STUDY

Because the conclusions presented above are based on limited data collected during the summer, they are subject to seasonal limitations. To develop more reliable load transfer coefficients for the design of CRC pavements in Texas, the following areas are recommended for future study:

(1) Analyze the seasonal variation of load transfer at the cracks in CRC pavements.
(2) Monitor the deterioration of load transfer at discontinuities in the pavements from construction phase to failure.
(3) Study the possibility of establishing an empirical-mechanistic model to predict the loss of load transfer considering environmental effects, construction variation, material properties, and load applications.
(4) Incorporate the effects of temperature differentials and the lateral distribution of traffic into the J-factor model for future study.
(5) Perform a comparison study of the responses of jointed concrete pavements and CRC pavements based on field measurements.
(6) Incorporate a wider range of CRCP thicknesses in future studies.

REFERENCES

1. *The AASHO Road Test: Proceedings of a Conference*, HRB Special Report 73, 1962.

2. Spangler, M. G., "Stresses in the Corner Region of Concrete Pavements," Iowa Engineering Experiment Station Bulletin 157, 1942.

3. Kelley, E. F., "Application of the Results of Research to the Structural Design of Concrete Pavements," *Public Roads*, July 1939.

4. Westergaard, H. M., "Stresses in Concrete Pavements Computed by Theoretical Analysis," *Public Roads*, April 1926.

5. "The AASHO Road Test Report 5 - Pavement Research," HRB Special Report 61E, 1962.

6. "AASHTO Guide for Design of Pavement Structures," Vol 1, American Association of State Highway and Transportation Officials, 1986.

7. "AASHTO Guide for Design of Pavement Structures," Vol 2, American Association of State Highway and Transportation Officials, 1986.

8. Hudson, W. R., "Comparison of Concrete Pavement Load Stress at AASHO Road Test with Previous Work," Highway Research Record, No. 42, 1963.

9. Hudson, W. R., and B. F. McCullough, "An Extension of Rigid Pavement Design Methods," Highway Research Record, No. 60, 1964.

10. McCullough, B. F., and H. J. Treybig, "A Statewide Deflection Study of Continuously Reinforced Concrete Pavement in Texas," Highway Research Record No. 239, 1968.

11. Treybig, H. J., "Sensitivity Analysis of the Extended AASHO Rigid Pavement Design Equation," Master's thesis, The University of Texas at Austin, 1969.

12. "AASHO Interim Guide for the Design of Pavement Structures," American Association of State Highway Officials, 1963.

13. Continuously Reinforced Pavement Group, "Design and Construction: Continuously Reinforced Concrete Pavement," Chicago, 1968.

14. McCullough, B. F., C. J. Van Til, and R. G. Hicks, "Evaluation of AASHO Interim Guides for Design of Pavement Structures," NCHRP 128, Highway Research Record, 1972.

15. "A Design Procedure for Continuously Reinforced Concrete Pavements for Highways," *ACI Journal*, June 1972.

16. Faiz, Asif, "Evaluation of Continuously Reinforced Concrete Pavements in India," Purdue University, October 1975.

17. La Coursiere, S. A., M. I. Darter, and S. A. Smiley, "Performance of Continuously Reinforced Concrete Pavement in Illinois," Civil Engineering Studies, Transportation Engineering, Series No. 10, University of Illinois, Urbana, Illinois, 1978.

18. Colly, B. E., and H. A. Humphrey, "Aggregate Interlock at Joints in Concrete Pavements," Highway Research Board, Washington, D.C., 1967.

19. "AASHTO Interim Guide for Design of Pavement Structures," American Association of State Highway and Transportation Officials, 1981.

20. "Design of Continuously Reinforced Concrete Pavement for Highways," Associated Reinforced Bar Producers, 1981.

21. Dossey, T., and A. J. Weissmann, "A Continuously Reinforced Concrete Pavement Database," Research Report 472-6, Center for Transportation Research, The University of Texas at Austin, November 1989.

22. Weissmann, A. J., and K. Hankins, "A State-Wide Diagnostic Survey of Continuously Reinforced Concrete Pavements in Texas," Research Report 472-5, Center for Transportation Research, The University of Texas at Austin, November 1989.

23. Chou, Chia-pei, B. F. McCullough, and W. R. Hudson, "Development of a Long-Term Monitoring System for the Texas CRC Pavement Network," Research Report 472-2, Center for Transportation Research, The University of Texas at Austin, October 1988.

24. Weissmann, A. J., "Development of Procedures for Monitoring and Predicting the Long-Term Performance of Continuously Reinforced Concrete Pavements," Doctoral dissertation, The University of Texas at Austin, May 1990.

25. Owusu-Antwi, E., "Assessment of the Load Transfer Efficiency of Joints and Cracks in Rigid Pavements Using the FWD," Doctoral dissertation, The University of Texas at Austin, May 1990.

26. Bush, A. J., III, and Y. B. Gilbert, "Nondestructive Testing of Pavements and Back-calculation of Moduli," ASTM Special Technical Publication, pp 369-386, 1989.

27. Westergaard, H. M., "New Formulas for Stresses in Concrete Pavements of Airfields," Proceedings, American Society of Civil Engineers, Vol 73, No. 1, January 1947.

28. Teller, L. W., and E. C. Sutherland, "The Structural Design of Concrete Pavements: Part 4 — The Study of the Structural Action of Several Types of Transverse and Longitudinal Joint Designs," Public Roads, Vol 17, Nos. 7 and 8, September and October 1936.

29. Friberg, B., "Load and Deflection Characteristics of Dowels in Transverse Joints of Concrete Pavements," Proceedings of 18th Annual Meeting, Highway Research Board, Washington, D.C., November 1938.

30. Darter, M. I., and E. J. Barenberg, "Zero-Maintenance Design for Plain Jointed Concrete Pavements," Proceedings of International Conference on Concrete Pavement Design, Purdue University, West Lafayette, 1977.

31. Ricci, E. A., A. H. Meyer, W. R. Hudson, and K. H. Stokoe, II, "The Falling Weight Deflectometer for Nondestructive Evaluation of Rigid Pavements," Research Report 387-3F, Center for Transportation Research, The University of Texas at Austin, November 1985.

32. Morales-Valetin, G. E., A. H. Meyer, and W. R. Hudson, "Temperature Differential Effect on Falling Weight Deflectometer Deflections Used for Structural Evaluation of Rigid Pavements," Research Report 460-1, Center for Transportation Research, The University of Texas at Austin, February 1987.

33. Uddin, W., S. Nazarian, W. R. Hudson, A. H. Meyer, and K. H. Stokoe, II, "Investigation into Location/Temperature Parameters and In Situ Material Characterization of Rigid Pavements," Research Report 256-5, Center for Transportation Research, The University of Texas at Austin, December 1983.

34. Owusu-Antwi, E., A. H. Meyer, and W. R. Hudson, "Preliminary Evaluation of Procedures for Assessment of Load Transfer Across Joints and Cracks in Rigid Pavements Using the Falling Weight Deflectometer," Proceedings of Fourth International Conference on Concrete Pavement Design and Rehabilitation, Purdue University, West Lafayette, 1989.

35. Ioannides, A. M., M. R. Thompson, and E. J. Barenberg, "Westergaard Solutions Reconsidered," TRR 1043, 1985.

36. Hudson, W. R., and F. H. Scrivner, "AASHO Road Test Principle Relationships: Performance with Stress, Rigid Pavements," HRB Special Report 73, 1962.

37. Tabatabaie, A. M., and E. J. Barenberg, "Finite Element Analysis of Joined or Cracked Concrete Pavements," paper presented at the 57th Annual Meeting of Transportation Research Board, Washington, D.C., January 1978.

38. Barenberg, E. J., A. M. Tabatabaie, and R. E. Smith, "Longitudinal Joint System in Slip-Formed Rigid Pavements," Vol II, Interim Report, Department of Civil Engineering, University of Illinois, Urbana, 1979.

39. Westergaard, H. M., "Stresses in Concrete Runways of Airports," Proceedings, 19th Annual Meeting, HRB, 1939.

40. Westergaard, H. M., "New Formulas for Stresses in Concrete Pavements of Airfields," Proceedings, American Society of Civil Engineers, Vol 73, No. 1, January 1947.

41. "AASHTO Interim Guide for Design of Pavement Structures," American Association of State Highway and Transportation Officials, 1972.

42. Weissmann, A. J., and K. Hankins, "Development of Procedures for CRCP Diagnostic Survey," Research Report 472-4, Center for Transportation Research, The University of Texas at Austin, November 1989.

43. Baber, E. S., "Calculation of Maximum Pavement Temperatures from Weather Reports," Highway Research Board Bulletin 168, Highway Research Record, Washington, D. C., 1957.

44. Shanin, M. Y., and B. F. McCullough, "Prediction of Low Temperature and Thermal Fatigue Cracking in Flexible Pavements," Research Report 123-4, Center for Highway Research, The University of Texas at Austin, August 1972.

45. Torres-Verdin, V., and B. F. McCullough, "Evaluation of the Effect of Coarse Aggregate Type on CRCP Thickness," Proceedings of Third International Conference on Concrete Pavement Design and Rehabilitation, Purdue University, West Lafayette, 1985.

46. Rigid Pavement Design Based on AASHTO Guide, Draft Released by Texas State Department of Highways and Public Transportation, July 20, 1987.

47. Shyam, V., H. Castedo, W. R. Hudson, and B. F. McCullough, "A Study of Drainage Coefficients for Concrete Pavements in Texas," Research Report 1169-1 (Preliminary), Center for Transportation Research, The University of Texas at Austin, May 1989.

48. Slavis V. C., and C. G. Ball, "Verification of the Structural Benefits of Concrete Shoulders by Field Measurements," Proceedings of Third International Conference on Concrete Pavement Design and Rehabilitation, Purdue University, West Lafayette, 1985.

49. Chou, Chia-pei, "Development of a Long-Term Monitoring System for the Texas CRC Pavement Network," Doctoral dissertation, The University of Texas at Austin, August 1988.

50. "SAS/User's Guide: Statistics," SAS Institute Inc., Carey, NC, 1984.

51. Draper, N., and H. Smith, *Applied Regression Analysis*, 2nd Edition, John Wiley and Sons, Inc., 1980.

52. Mosteller, F., and J. W. Tukey, *Data Analysis and Regression*, Addison-Wesley Publishing Company, 1977.

53. McCullough, B. F., and M. L. Cawley, "CRCP Design Based on Theoretical and Field Performance," Proceedings of Second International Conference on Concrete Pavement Design and Rehabilitation, Purdue University, West Lafayette, 1981.

54. McCullough, B. F., "Development of Equipment and Techniques for a Statewide Rigid Pavement Deflection Study," Departmental Research Report 46-1, Texas Highway Department, January 1965.

55. Torres-Verdin, V., and B. F. McCullough, "Effect of Environmental Factors and Loading Position on Dynaflect Deflections in Rigid Pavements," Research Report 249-4, Center for Transportation Research, The University of Texas at Austin, November 1982.

56. Sullion, T., R. L. Lytton, C. J. Templeton, and Y. J. Chou, "Sample Size Selection," Second North American Conference on Managing Pavements, 1987.

57. "SHRP-LTPP Manual for FWD Testing," Strategic Highway Research Program, January 1989.

58. Uddin, W., A. H. Meyer, W. R. Hudson, and K. H. Stokoe, II, "A Structural Evaluation Methodology for Pavements Based on Dynamic Deflections," Research Report 387-1, Center for Transportation Research, The University of Texas at Austin, August 1985.

59. McCullough, B. F., and H. J. Treybig, "Determining the Relationship of Variables in Deflection of Continuously Reinforced Concrete Pavement," Departmental Research Report 46-4, Texas Highway Department, January 1965.

APPENDIX A

COMPUTER PROGRAM FOR CALCULATION OF THE J-VALUES FOR IN-SERVICE CRCP

```
/*********************************************************************/
/*        COMPUTER GPROGRAM A--DATA BASE SET-UP        */
/*********************************************************************/
/*  E-VALUES   */
CMS FI SDX DISK DUMMY DUMMY A;
DATA A(KEEP=CFTR DIR SECT SS E1); SET SDX.ELMOD;
IF HEIGHT=4;
PROC SORT DATA=A; BY CFTR DIR SECT SS;

/*  D CAT SBT  */
CMS FI SDS DISK DUMMY DUMMY R;
DATA B(KEEP=CFTR D CAT SBT);  SET SDS.MASTER;
PROC SORT DATA=B; BY CFTR;
DATA AB; MERGE A(IN=OK) B; BY CFTR; IF OK;

/*  ST  */
CMS FI SDS DISK DUMMY DUMMY A;
DATA X;  SET SDS.ST;
PROC SORT DATA=X; BY CFTR DIR SECT;
DATA AX; MERGE AB(IN=OK) X; BY CFTR DIR SECT ; IF OK;

/*  DFI, DFE  */
CMS FI SDS DISK DUMMY DUMMY R;
DATA C;   RETAIN;   SET SDS.FWD;
IF OVR ='N';
IF HEIGHT =4;
IF STATION =4 THEN DO;
   DFE=DF1*9000./LBS; END;
IF STATION =5 THEN DO;
   DFI=DF1*9000./LBS; END;
IF STATION =1 OR STATION =2 OR STATION =3 OR STATION =4 THEN DELETE;
PROC SORT DATA=C; BY CFTR DIR SECT SS;
DATA AC; MERGE AX(IN=OK) C; BY CFTR DIR SECT SS; IF OK;
/*  TEMPERATURE DIFFERENTIAL CORRECTION  */
```

```
IF ST='AC' THEN DO;
    DT=(-5.+.06*STEMP)*D;  X=.0075*DT;  FT=10**X;
    DFE=DFE*FT;  END;

/* DESIGN VALUES */
    IF CAT=1 THEN ED=5.0;
    IF CAT=2 THEN ED=4.0;
    IF CAT=3 THEN ED=4.5;
    IF SBT=1 THEN KD=250.0;
    IF SBT=2 THEN KD=300.0;
    IF SBT=3 THEN KD=225.0;
    IF SBT=4 THEN KD=200.0;
    EF=E1/1000000;

/*  OUTPUT */
CMS FI OUT DISK JINP DAT A;
DATA Y;  SET AC;
FILE OUT;
PUT CFTR ',' DIR ',' SECT ',' SS ',' ST ',' D ',' ED 3.1 ',' EF 3.1 ','
  KD 5.0 ',' DFI 5.2 ',' DFE 5.2;
RUN;
```

```
C     ************************************************************************
C     * PROGRAM B--TO FIND THE LOAD TRANSFER COEFFICIENT *
C     *     FROM FIELD MEASUREMENTS ON IN-SERVICE CRCP     *
C     ************************************************************************
      CHARACTER*1 DIR
      CHARACTER*1 SS
      CHARACTER*2 ST
C     ************** INPUT  ***********************************
      OPEN(5,FILE='JINP')
      OPEN(6,FILE='JOUT')
C     **************WRITE OUTPUT *************************
      WRITE(6,10)
C     *************** INPUT ************************************
      DO 100 I =1,581
      READ(5,*)ICFTR,DIR,ISECT,SS,ST,D,ED1,EF1,DK,DFI1,DFE1
C     **** ICFTR=CFTR, ISECT=SECT, DK=KD **************
C     ******* CHANGE UNIT ********
      ED=ED1*1000000.
      EF=EF1*1000000.
      DFI=DFI1/1000.
      DFE=DFE1/1000.
C     ******** CONSTANT ********
      A=5.9
      P=9000.
      U=0.2
C     ********* FIELD K-VALUES*****************************
      CALL FK(D,EF,A,P,U,DFI,FK)
C     ********* EDGE DEFLECTION *************************
      CALL CDFE(D,EF,FK,A,P,U,CDFE)
C     ********* EDGE DEFLECTION RATIO ******************
      R=DFE/FDFE
C     ********* EDGE STRESS ******************************
      CALL CSE(D,EF,FK,A,P,U,CSE)
    ********** FIELD EDGE STRESS ************************
```

```
      SER=R*CSE
C     ********* INTERIOR STRESS **************************
      CALL CSI(D,EF,FK,A,P,U,CSI)
C     ********* INTERIOR STRESS  -- DESIGN CONDITION ********
      CALL DSI(D,DE,FK,A,P,U,DSI)
C     ********* MAXIMUM STRESS AND CALCULATE THE J-VALUE *******
      IF (CSI .GE. SER) THEN
      CALL SPJ(D,A,P,U,ED,FK,DSI,CSI,SPJ)
      ELSE
      CALL SPJ(D,A,P,U,ED,FK,DSI,SER,SPJ)
      END IF
C     ********* WRITE OUTPUT ******************************
   10 FORMAT(2X,'CFTR  DIR  SECT  SS  ST  J')
      WRITE(6,20)ICFTR,DIR,ISECT,SS,ST,SPJ
   20 FORMAT(1X,I5,4X,A2,4X,I2,4X,A2,4X,A2,4X,F4.2)
  100 CONTINUE
      WRITE(*,30)
   30 FORMAT(1X,'END')
      STOP
      END


C     ************************************************
C     * SUBPROGRAM TO FIND THE K-Value     *
C     ************************************************
      SUBROUTINE FK(D,EF,A,P,U,DFI,FK)
      REAL KS,KB
      REAL K
C     ******* INPUT ************************************
      AL1=EF*D*D*D/(12.*(1.-U*U))
      AL=SQRT(AL1)
      B1=P/(8.*AL)
      B2=A*A/(6.28319*AL)
      B3=0.5*A/SQRT(AL)
```

```
      B4=-0.67279
C
      KS=10.
      KB=5000.
      N=0
C
  10  K=0.5*(KS+KB)
      N=N+1
C
      F1=ALOG(B3*(K**0.25))+B4
      F2=B1/SQRT(K)
      F=F2*(1.+B2*SQRT(K)*F1)
C
      XF=DFI-F
      IF(DFI .LE. F) GOTO 200
C     ******** K LT KM ************************************
      IF(ABS(XF) .LE. 0.00001) GOTO 160
      IF(N .GT. 100) GOTO 160
      KB=K
      GOTO 10
C     ******** K GT KM ************************************
 200  IF(ABS(XF) .LE. 0.00001) GOTO 160
      IF(N .GT. 1000) GOTO 160
      KS=K
      GOTO 10
C
 160  RETURN
      END
C     ************************************************************
C     *    SUBPROGRAM TO FIND EDGE DEFLECTION    *
C     ************************************************************
      SUBROUTINE CDFE(D,EF,FK,A,P,U,CDFE)
C     *** SPECIAL THEORY ***********************************
      B=SQRT(1.6*A*A+D*D)-0.675*D
```

```
C    *** FIND RADIUS OF RELATIVE STIFFNESS *********
      SS1=12.0*(1.0-U*U)*FK
      SS2=EF*D*D*D
      AL=(SS2/SS1)**0.25
C    **** FIND EDGE DEFLECTION ************************
      DE1=P*SQRT(2.+1.2*U)
      DE2=SQRT(EF*(D**3)*FK)
      DE3=1.-(0.76+0.4*U)*A/AL
      CDFE=DE1*DE3/DE2
      RETURN
      END


C    ********************************************************
C    * SUBPROGRAM TO FIND THE EGDE STRESS       *
C    ********************************************************
      SUBROUTINE CSE(D,EF,FK,P,U,CSE)
C    **** RADIUS OF RALATIVE STIFFNESS *************
      RR1=12.0*(1.0-U*U)*FK
      RR2=EF*D*D*D
      AL=(RR2/RR1)**0.25
C
      SE11=3.*(1.+U)*P
      SE12=3.14159*(3.+U)*D*D
      SE1=SE11/SE12
      B1=100.*FK*A**4
      BB=E*D*D*D/B1
C
      SE2=ALOG(BB)+1.84-4.*U/3.+(1.-U)/2.+1.18*(1.+2.*U)*A/AL
      CSE=SE1*SE2
      RETURN
      END
```

```
C       ************************************************************
C       * SUBPROGRAM TO FIND THE INTERIOR STRESS      *
C       ************************************************************
C    INTERIOR STRESS (SPECIAL A=5.9 IN.<1.724*D , P=9000 LBS)
        SUBROUTINE CSI(D,EF,FK,A,P,U,CSI)
C    ******** SPECIAL THEORY *******************************
        B=SQRT(1.6*D*D+D*D)-0.675*D
C
        SS1=12.0*(1.0-U*U)*FK
        SS2=E*FD*D*D
        AL=(SS2/SS1)**0.25
C
        SI1=3.*P*(1.+U)/(2.*3.14159*D*D)
        SI2=ALOG(2.*AL/B)+0.5-0.577215
        SI3=3.*P*(1.+U)*B*B/(AL*AL*64.*D*D)
        CSI=SI1*SI2+SI3
        RETURN
        END
```

```
C       ********************************************************
C       *    SUBPROGRAM TO FIND J-VALUE              *
C       ********************************************************
        SUBROUTINE SPJ(D,A,P,U,ED,FK,DSI,S,SPJ)
C    ******** FIND SPANGLER STRESS --DESIGN  CONDITION *******
        CALL SSP(D,ED,DK,A,P,U,TXSPS)
C    ****AASHO ROAD TEST CONDITIONS**********************
C     --- SPANGLER STRESS --AASHO ROAD TEST
        CALL  SSP(D,4200000.,100.,7.,P,0.2,ASPS)
C     ---LOOP 1 STRESS  --AASHO ROAD TEST ---
```

```
      SLP=0.32*P/(D**1.33333)
C     ******** DETERMINE F-FACTOR *******
      GJ=2.3
      F=3.2*ASPS*DSI/(SPL*TXSPS*GJ)
C     ***** DETERMINE J-VALUE ***************************
      AJ=3.2*ASPS*S/(SLP*TXSPS*F)
      RETURN
      END


C     ***************************************************************
C     *  SUBPROGRAM TO FIND SPANGLER EQUATION STRESS   *
C     ***************************************************************
      SUBROUTINE SSP(D,E,AK,A,P,U,SSP)
      SS1=12.0*(1.0-U*U)*AK
      SS2=E*D*D*D
      AL=(SS2/SS1)**0.25
      SP1=1.-1.414*A/AL
      SP2=3.2*P/(D*D)
      SSP=SP1*SP2
      RETURN
      END
```

APPENDIX B

DERIVED J-VALUES FOR IN-SERVICE CRCP IN TEXAS

CFTR	DIR	SECT	SS	ST	J-VALUE
1015	E	1	A	AC	2.49
1015	E	1	B	AC	2.33
1015	E	1	C	AC	2.35
1015	E	1	F	AC	2.39
1015	E	1	G	AC	2.32
1015	E	2	A	AC	2.29
1015	E	2	B	AC	2.33
1015	E	2	C	AC	2.18
1015	E	2	F	AC	2.18
1015	E	2	G	AC	2.16
1015	W	3	A	AC	2.07
1015	W	3	B	AC	2.20
1015	W	3	C	AC	2.16
1015	W	3	F	AC	2.30
1015	W	4	A	AC	2.40
1015	W	4	B	AC	2.38
1015	W	4	C	AC	2.89
1015	W	4	F	AC	2.36
1015	W	4	G	AC	2.36
1015	W	5	A	AC	2.39
1015	W	5	B	AC	2.70
1015	W	5	C	AC	2.41
1015	W	5	F	AC	2.26
2002	E	1	A	AC	2.03
2002	E	1	B	AC	2.29
2002	E	1	C	AC	2.49
2002	E	1	F	AC	2.36
2002	E	1	G	AC	2.25
2002	E	2	A	AC	2.12
2002	E	2	B	AC	2.15
2002	E	2	C	AC	2.20
2002	E	2	F	AC	2.10
2002	E	2	G	AC	2.09
2002	E	3	A	AC	2.10

CFTR	DIR	SECT	SS	ST	J-VALUE
2002	E	3	B	AC	2.11
2002	E	3	C	AC	2.14
2002	E	3	F	AC	2.28
2002	E	3	G	AC	2.17
2002	E	4	A	AC	2.32
2002	E	4	B	AC	2.26
2002	E	4	C	AC	2.26
2002	E	4	F	AC	2.12
2002	E	4	G	AC	1.99
2002	E	5	A	AC	2.39
2002	E	5	B	AC	2.35
2002	E	5	C	AC	2.40
2002	E	5	F	AC	2.36
2002	E	5	G	AC	2.14
2028	N	1	A	AC	2.28
2028	N	1	B	AC	2.19
2028	N	1	C	AC	2.42
2028	N	1	F	AC	2.64
2028	N	1	G	AC	2.72
2028	N	2	A	AC	2.17
2028	N	2	B	AC	2.10
2028	N	2	C	AC	2.31
2028	N	2	F	AC	3.06
2028	N	2	G	AC	2.22
2028	S	1	A	AC	2.30
2028	S	1	B	AC	2.17
2028	S	1	C	AC	2.41
2028	S	1	F	AC	2.11
2028	S	1	G	AC	2.27
2032	E	1	A	PC	2.23
2032	E	1	B	PC	2.35
2032	E	1	C	PC	2.17
2032	E	1	F	PC	2.22
2032	E	1	G	PC	2.17
2032	E	3	A	AC	2.25
2032	E	3	B	AC	2.47

CFTR	DIR	SECT	SS	ST	J-VALUE
2032	E	3	C	AC	2.72
2032	E	3	F	AC	2.54
2032	E	3	G	AC	2.19
2032	W	1	A	AC	1.99
2032	W	1	B	AC	2.25
2032	W	1	C	AC	1.92
2032	W	1	F	AC	1.90
2032	W	1	G	AC	1.82
2032	W	2	A	AC	2.11
2041	N	1	A	AC	2.37
2041	N	1	B	AC	2.30
2041	N	1	C	AC	2.43
2041	N	1	F	AC	2.32
2041	N	1	G	AC	2.15
2041	N	2	A	AC	2.34
2041	N	2	B	AC	2.38
2041	N	2	C	AC	2.46
2041	N	2	F	AC	2.17
2041	N	2	G	AC	2.35
2041	S	1	A	AC	2.33
2041	S	1	B	AC	2.42
2041	S	1	C	AC	2.42
2041	S	1	F	AC	2.41
2041	S	1	G	AC	2.40
2044	S	2	A	AC	1.95
2044	S	2	B	AC	1.84
2044	S	2	C	AC	2.29
2044	S	2	F	AC	2.34
2044	S	2	G	AC	2.49
2044	S	3	A	AC	2.04
2044	S	3	A	AC	2.02
2044	S	3	B	AC	1.74
2044	S	3	C	AC	2.01
2044	S	3	F	AC	2.00
2044	S	3	G	AC	1.88
2044	S	4	A	AC	2.18

CFTR	DIR	SECT	SS	ST	J-VALUE
2044	S	4	B	AC	2.97
2044	S	4	C	AC	2.40
2044	S	4	F	AC	1.92
2044	S	4	G	AC	2.27
2044	S	5	A	AC	2.21
2044	S	5	B	AC	2.17
2044	S	5	C	AC	2.44
2044	S	5	F	AC	2.30
2044	S	5	G	AC	2.57
2049	N	1	A	AC	2.01
2049	N	1	B	AC	2.30
2049	N	1	C	AC	2.01
2049	N	1	F	AC	2.21
2049	N	1	G	AC	2.06
2049	S	1	A	AC	2.13
2049	S	1	B	AC	2.09
2049	S	1	C	AC	2.29
2049	S	1	F	AC	2.36
2049	S	1	G	AC	2.08
2049	S	2	A	AC	2.18
2049	S	2	B	AC	2.06
2049	S	2	C	AC	2.16
2049	S	2	F	AC	2.13
2049	S	2	G	AC	2.60
2049	S	3	A	AC	2.15
2049	S	3	B	AC	2.18
2049	S	3	C	AC	2.20
2049	S	3	F	AC	2.20
2049	S	3	G	AC	2.31
2049	S	4	A	AC	2.44
2049	S	4	B	AC	2.07
2049	S	4	C	AC	1.88
2049	S	4	F	AC	1.99
2049	S	4	G	AC	2.22
2050	N	1	A	AC	2.16
2050	N	1	B	AC	2.04

CFTR	DIR	SECT	SS	ST	J-VALUE
2050	N	1	C	AC	2.16
2050	N	1	F	AC	2.31
2050	N	1	G	AC	2.30
2050	S	1	A	AC	2.18
2050	S	1	B	AC	2.45
2050	S	1	C	AC	2.38
2050	S	1	F	AC	2.31
2050	S	2	A	AC	2.51
2050	S	2	B	AC	2.39
2050	S	2	C	AC	3.09
2050	S	2	F	AC	2.85
2050	S	2	G	AC	2.74
2051	E	1	A	AC	2.27
2051	E	1	B	AC	2.89
2051	E	1	C	AC	3.05
2051	E	1	F	AC	2.54
2051	E	1	G	AC	2.38
2051	E	2	A	AC	2.48
2051	E	2	B	AC	2.55
2051	E	2	C	AC	2.64
2051	E	2	F	AC	2.63
2051	E	2	G	AC	2.60
2051	W	1	A	AC	2.49
2051	W	1	B	AC	2.52
2051	W	1	C	AC	2.81
2051	W	1	F	AC	2.74
2051	W	1	G	AC	2.17
2059	E	1	A	AC	2.93
2059	E	1	B	AC	2.29
2059	E	1	C	AC	2.25
2059	E	1	F	AC	2.63
2059	E	1	G	AC	2.23
2059	E	2	A	AC	2.65
2059	E	2	B	AC	2.80
2059	E	2	C	AC	3.32
2059	E	2	F	AC	2.79

CFTR	DIR	SECT	SS	ST	J-VALUE
2059	E	2	G	AC	2.36
2059	W	1	A	AC	2.32
2059	W	1	B	AC	2.30
2059	W	1	C	AC	2.26
2059	W	1	F	AC	2.36
2059	W	1	G	AC	2.30
2059	W	2	A	AC	2.36
2059	W	2	B	AC	2.26
2059	W	2	C	AC	3.12
2059	W	2	F	AC	3.47
2059	W	2	G	AC	2.53
2060	E	1	A	AC	2.74
2060	E	1	B	AC	2.79
2060	E	1	C	AC	2.44
2060	E	1	F	AC	2.33
2060	E	1	G	AC	2.44
2060	W	1	A	AC	2.26
2060	W	1	B	AC	2.66
2060	W	1	C	AC	2.44
2060	W	1	F	AC	2.76
2060	W	1	G	AC	2.55
2060	W	2	A	AC	2.13
2060	W	2	B	AC	2.35
2060	W	2	C	AC	2.65
2060	W	2	F	AC	2.34
2060	W	2	G	AC	2.57
2075	N	1	A	AC	2.56
2075	N	1	B	AC	2.21
2075	N	1	F	AC	2.46
2075	N	1	G	AC	2.60
2075	S	1	A	AC	2.27
2075	S	1	B	AC	2.73
2075	S	1	C	AC	2.52
2075	S	1	F	AC	2.28
2075	S	1	G	AC	2.25
2075	S	2	A	AC	2.26

CFTR	DIR	SECT	SS	ST	J-VALUE
2075	S	2	B	AC	2.20
2075	S	2	C	AC	2.13
2075	S	2	F	AC	2.62
2075	S	2	G	AC	2.10
2075	S	3	A	AC	2.26
2075	S	3	B	AC	2.00
2075	S	3	C	AC	2.29
2075	S	3	F	AC	1.99
2075	S	3	G	AC	2.04
2075	S	4	A	AC	1.89
2075	S	4	B	AC	1.83
2075	S	4	C	AC	1.97
2075	S	4	F	AC	2.15
2075	S	4	G	AC	2.26
2098	E	1	A	AC	2.13
2098	E	1	B	AC	2.29
2098	E	1	C	AC	2.16
2098	E	1	F	AC	2.16
2098	E	1	G	AC	2.13
2098	E	2	A	AC	2.01
2098	E	2	B	AC	2.04
2098	E	2	C	AC	1.97
2098	E	2	F	AC	1.93
2098	E	2	G	AC	1.89
2098	W	1	A	AC	3.04
2098	W	1	B	AC	2.51
2098	W	1	C	AC	2.18
2098	W	1	F	AC	3.31
2098	W	1	G	AC	2.03
2098	W	2	A	AC	2.22
2098	W	2	B	AC	2.10
2098	W	2	C	AC	2.27
2098	W	2	F	AC	2.97
2098	W	2	G	AC	2.30
3001	N	1	A	AC	3.09
3001	N	1	B	AC	2.93

CFTR	DIR	SECT	SS	ST	J-VALUE
3001	N	1	C	AC	2.47
3001	N	2	A	AC	2.79
3001	N	2	B	AC	2.84
3001	N	2	C	AC	2.66
3001	N	2	F	AC	2.61
3010	S	1	B	AC	2.95
3010	S	1	C	AC	2.54
3010	S	1	F	AC	2.83
3010	S	1	G	AC	2.85
3010	S	2	A	AC	3.01
3010	S	2	B	AC	3.00
3010	S	2	C	AC	3.24
3010	S	2	F	AC	3.20
3010	S	2	G	AC	3.47
3018	S	1	A	AC	2.59
3018	S	1	B	AC	2.41
3018	S	1	C	AC	2.38
3018	S	1	F	AC	2.29
3018	S	1	G	AC	3.09
3018	S	2	A	AC	2.26
3018	S	2	B	AC	2.36
3018	S	2	C	AC	2.28
3018	S	2	F	AC	2.16
4009	W	5	A	AC	2.44
4009	W	5	B	AC	2.45
4009	W	5	C	AC	2.41
4009	W	5	F	AC	2.54
4009	W	5	G	AC	2.62
4011	E	1	A	PC	2.58
4011	E	1	B	PC	2.54
4011	E	1	C	PC	2.49
4011	E	1	F	PC	2.50
4011	E	1	G	PC	2.60
4011	E	2	A	PC	2.34
4011	E	2	B	PC	2.42
4011	E	2	C	PC	2.52

CFTR	DIR	SECT	SS	ST	J-VALUE
4011	E	2	F	PC	2.50
4011	W	1	A	PC	2.35
4011	W	1	B	PC	2.36
4011	W	1	C	PC	2.34
4011	W	1	F	PC	2.35
4011	W	1	G	PC	2.34
4011	W	2	A	PC	2.37
4011	W	2	B	PC	2.44
4011	W	2	C	PC	2.52
4011	W	2	F	PC	2.51
4011	W	3	A	PC	2.35
4011	W	3	B	PC	2.33
4011	W	3	C	PC	2.37
4011	W	3	F	PC	2.38
4011	W	3	G	PC	2.37
4022	E	1	A	PC	2.33
4022	E	1	B	PC	2.33
4022	E	1	C	PC	2.31
4022	E	1	F	PC	2.30
4022	E	1	G	PC	2.40
4022	W	1	A	PC	2.43
4022	W	1	B	PC	2.41
4022	W	1	C	PC	2.36
4022	W	1	F	PC	2.37
4022	W	1	G	PC	2.41
4022	W	2	A	PC	2.31
4022	W	2	B	PC	2.28
4022	W	2	C	PC	2.30
4022	W	2	F	PC	2.33
4022	W	2	G	PC	2.31
4025	W	1	A	PC	2.18
4025	W	1	B	PC	2.02
4025	W	1	C	PC	1.98
4025	W	1	F	PC	2.21
4025	W	1	G	PC	2.19
4025	W	2	A	PC	2.13

CFTR	DIR	SECT	SS	ST	J-VALUE
4025	W	2	B	PC	2.15
4025	W	2	C	PC	2.02
4025	W	2	F	PC	2.05
4025	W	2	G	PC	2.06
4025	W	3	A	PC	2.39
4025	W	3	B	PC	2.69
4025	W	3	C	PC	2.59
4025	W	3	F	PC	2.47
4025	W	3	G	PC	2.41
4025	W	4	A	PC	2.28
4025	W	4	B	PC	2.31
4025	W	4	C	PC	2.32
4025	W	4	F	PC	2.28
4025	W	4	G	PC	2.27
5005	N	1	A	AC	2.10
5005	N	1	B	AC	2.07
5005	N	1	C	AC	2.09
5005	N	1	F	AC	2.15
5005	N	1	G	AC	2.02
5005	N	2	A	AC	2.05
5005	N	2	B	AC	2.14
5005	N	2	C	AC	2.12
5005	N	2	F	AC	2.12
5005	N	2	G	AC	2.12
5005	S	1	A	AC	2.14
5005	S	1	B	AC	2.18
5005	S	1	C	AC	2.13
5005	S	1	F	AC	2.05
5005	S	1	G	AC	2.05
5005	S	2	A	AC	2.04
5005	S	2	B	AC	2.05
5005	S	2	C	AC	2.02
5005	S	2	F	AC	1.96
5005	S	2	G	AC	2.09
5007	S	1	A	AC	2.32
5007	S	1	B	AC	2.29

CFTR	DIR	SECT	SS	ST	J-VALUE
5007	S	1	C	AC	2.24
5007	S	1	F	AC	2.25
5007	S	1	G	AC	2.14
5007	S	2	A	AC	2.23
5007	S	2	B	AC	2.25
5007	S	2	C	AC	2.11
5007	S	2	F	AC	2.15
5007	S	2	G	AC	2.12
5007	S	3	A	AC	2.28
5007	S	3	B	AC	2.28
5007	S	3	C	AC	2.19
5007	S	3	F	AC	2.11
5007	S	3	G	AC	2.33
5008	N	1	A	AC	2.16
5008	N	1	B	AC	2.16
5008	N	1	C	AC	2.19
5008	N	1	F	AC	2.24
5008	N	1	G	AC	2.18
5008	N	2	A	AC	2.17
5008	N	2	B	AC	2.16
5008	N	2	C	AC	2.27
5008	N	2	F	AC	2.18
5008	N	2	G	AC	2.18
5008	S	1	A	AC	2.26
5008	S	1	B	AC	2.18
5008	S	1	C	AC	2.19
5008	S	1	F	AC	2.29
5008	S	1	G	AC	2.26
5008	S	2	A	AC	2.26
5008	S	2	B	AC	2.27
5008	S	2	C	AC	2.29
5008	S	2	F	AC	2.24
5008	S	2	G	AC	2.25
5009	N	1	A	AC	2.22
5009	N	1	B	AC	2.27
5009	N	1	C	AC	2.23

CFTR	DIR	SECT	SS	ST	J-VALUE
5009	N	1	F	AC	2.28
5009	N	1	G	AC	2.28
5009	S	1	A	AC	2.25
5009	S	1	B	AC	2.27
5009	S	1	C	AC	2.35
5009	S	1	F	AC	2.28
5009	S	1	G	AC	2.29
5009	S	2	A	AC	2.26
5009	S	2	B	AC	2.26
5009	S	2	C	AC	2.27
5009	S	2	F	AC	2.33
5009	S	2	G	AC	2.19
12901	E	1	A	PC	2.17
12901	E	1	B	PC	2.14
12901	E	1	C	PC	2.13
12901	E	1	G	PC	2.14
12901	E	2	A	PC	2.19
12901	E	2	B	PC	2.17
12901	E	2	C	PC	2.21
12901	E	2	F	PC	2.14
12901	E	2	G	PC	2.14
12901	W	3	A	PC	2.23
12901	W	3	B	PC	2.22
12901	W	3	C	PC	2.19
12901	W	3	F	PC	2.24
12901	W	3	G	PC	2.24
12901	W	4	A	PC	2.16
12901	W	4	B	PC	2.20
12901	W	4	C	PC	2.21
12901	W	4	F	PC	2.19
12901	W	4	G	PC	2.17
12902	E	1	A	PC	2.14
12902	E	1	B	PC	2.14
12902	E	1	F	PC	2.18
12902	W	2	A	PC	2.17
12902	W	2	B	PC	2.15

CFTR	DIR	SECT	SS	ST	J-VALUE
12902	W	2	C	PC	2.14
12902	W	2	F	PC	2.19
12902	W	2	G	PC	2.18
13013	W	2	A	AC	2.27
13013	W	2	B	AC	2.49
13013	W	2	C	AC	2.25
13013	W	2	F	AC	2.40
13013	W	2	G	AC	2.31
13013	W	3	A	AC	2.17
13013	W	3	B	AC	2.05
13013	W	3	C	AC	2.18
13013	W	3	F	AC	2.12
13013	W	3	G	AC	2.09
13013	W	4	A	AC	2.23
13013	W	4	B	AC	2.32
13013	W	4	C	AC	2.54
13013	W	4	F	AC	2.19
13013	W	4	G	AC	2.88
13013	W	5	A	AC	2.14
13013	W	5	B	AC	2.07
13013	W	5	C	AC	2.14
13013	W	5	F	AC	2.17
13013	W	5	G	AC	2.26
13015	E	4	A	AC	2.80
13015	E	4	B	AC	2.46
13015	E	4	C	AC	2.51
13015	E	4	F	AC	2.52
13015	E	4	G	AC	2.52
13015	W	1	A	AC	2.45
13015	W	1	B	AC	2.38
13015	W	1	C	AC	2.42
13015	W	1	F	AC	2.32
13015	W	1	G	AC	2.27
13015	W	2	A	AC	2.58
13015	W	2	B	AC	2.60
13015	W	2	C	AC	3.66

CFTR	DIR	SECT	SS	ST	J-VALUE
13015	W	2	F	AC	2.66
13015	W	2	G	AC	2.84
13015	W	3	A	AC	2.66
13015	W	3	B	AC	2.51
13015	W	3	C	AC	2.60
13015	W	3	F	AC	2.42
13015	W	3	G	AC	2.29
13015	W	5	A	AC	2.41
13015	W	5	B	AC	2.48
13015	W	5	C	AC	3.28
13015	W	5	F	AC	2.40
13015	W	5	G	AC	2.74
15901	N	1	A	AC	2.42
15901	N	1	B	AC	2.13
15901	N	1	C	AC	3.04
15901	N	1	F	AC	3.06
15901	N	1	G	AC	2.19
17004	S	5	A	AC	2.19
17004	S	5	B	AC	2.06
17004	S	5	C	AC	2.31
17004	S	5	F	AC	2.31
17004	S	5	G	AC	2.29
17007	S	1	A	AC	2.61
17007	S	1	B	AC	2.36
17007	S	1	C	AC	2.25
17007	S	1	F	AC	2.26
17007	S	1	G	AC	2.31
17007	S	2	A	AC	2.36
17007	S	2	B	AC	2.35
17007	S	2	C	AC	2.33
17007	S	2	F	AC	2.31
17007	S	2	G	AC	2.24
17007	S	3	A	AC	2.22
17007	S	3	B	AC	2.24
17007	S	3	C	AC	2.28
17007	S	3	F	AC	2.26

CFTR	DIR	SECT	SS	ST	J-VALUE
17007	S	3	G	AC	2.30
17007	S	4	A	AC	2.29
17007	S	4	B	AC	2.29
17007	S	4	C	AC	2.20
17007	S	4	F	AC	2.22
17007	S	4	G	AC	2.19
17007	S	6	A	AC	2.20
17007	S	6	B	AC	2.49
17007	S	6	C	AC	2.41
17007	S	6	F	AC	2.36
17007	S	6	G	AC	2.31
17011	N	6	A	AC	2.34
17011	N	6	B	AC	2.58
17011	N	6	C	AC	2.67
17011	N	6	F	AC	2.65
17011	N	6	G	AC	3.24
17011	S	1	A	AC	2.50
17011	S	1	B	AC	2.80
17011	S	1	C	AC	2.35
17011	S	1	F	AC	2.53
17011	S	1	G	AC	2.52
17011	S	2	A	AC	2.58
17011	S	2	B	AC	2.46
17011	S	2	C	AC	2.34
17011	S	2	F	AC	2.36
17011	S	2	G	AC	2.37
17011	S	3	A	AC	2.25
17011	S	3	B	AC	2.47
17011	S	3	C	AC	2.55
17011	S	3	F	AC	2.60
17011	S	3	G	AC	2.51
17011	S	4	A	AC	3.21
17011	S	4	B	AC	2.27
17011	S	4	C	AC	2.22
17011	S	4	F	AC	2.37
17011	S	5	A	AC	2.65

CFTR	DIR	SECT	SS	ST	J-VALUE
17011	S	5	B	AC	2.48
17011	S	5	C	AC	2.52
17011	S	5	F	AC	2.37
17011	S	5	G	AC	2.36
20003	E	3	A	AC	2.81
20003	E	3	B	AC	2.56
20003	E	3	C	AC	2.57
20003	E	3	F	AC	2.39
20003	E	5	A	AC	2.55
20003	E	5	B	AC	2.90
20003	E	5	C	AC	3.13
20003	W	1	A	AC	2.54
20003	W	1	B	AC	3.06
20003	W	1	C	AC	2.83
20003	W	1	F	AC	2.60
20003	W	2	A	AC	3.32
20003	W	2	B	AC	2.60
20003	W	2	C	AC	2.79
20003	W	4	A	AC	3.25
20003	W	4	B	AC	3.10
20003	W	4	C	AC	3.04
20003	W	6	A	AC	2.40
20003	W	6	B	AC	2.38
20023	E	4	A	AC	2.53
20023	E	4	B	AC	2.81
20023	E	4	C	AC	2.57
20023	E	4	F	AC	2.43
20023	W	1	A	AC	2.48
20023	W	1	B	AC	2.46
20023	W	1	C	AC	2.41
20023	W	1	F	AC	2.44
20023	W	1	G	AC	2.46
20023	W	2	A	AC	2.52
20023	W	2	B	AC	2.42
20023	W	2	C	AC	2.32
24006	W	1	A	PC	2.06

CFTR	DIR	SECT	SS	ST	J-VALUE
24006	W	1	B	PC	2.24
24006	W	1	C	PC	2.18
24006	W	1	F	PC	2.25
24006	W	1	G	PC	2.52
24006	W	2	A	PC	2.22
24006	W	2	B	PC	2.34
24006	W	2	C	PC	2.25